Master Thesis, Department of Geosciences

Structural Analysis of the Klakk Fault Complex, offshore mid-Norway

Qing He

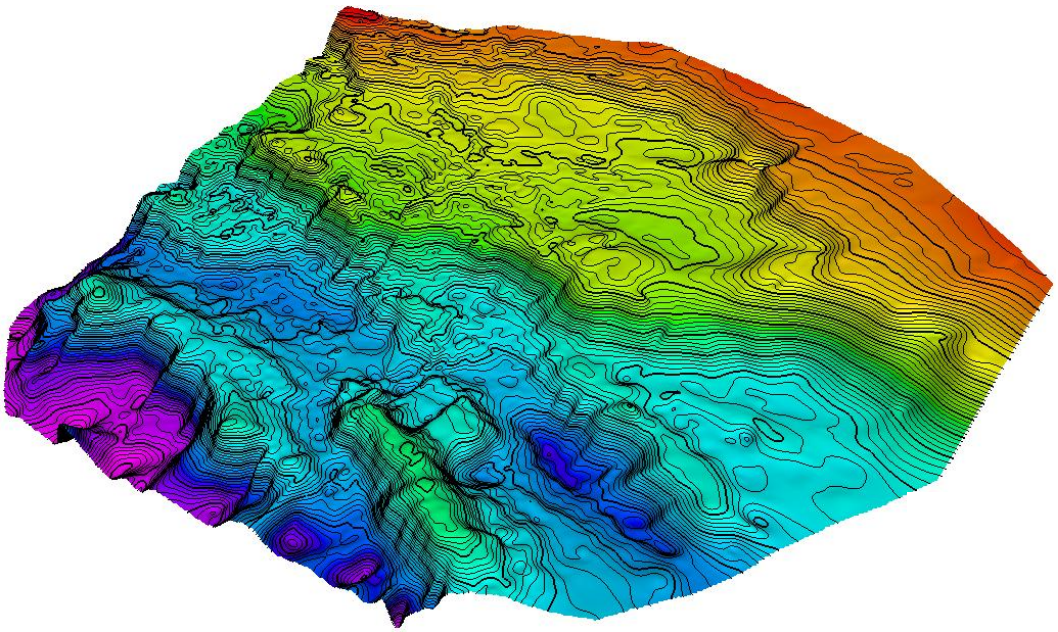

UNIVERSITY OF OSLO

FACULTY OF MATHEMATICS AND NATURAL SCIENCES

STRUCTURAL ANALYSIS OF THE KLAKK FAULT COMPLEX, OFFSHORE MID-NORWAY

QING HE

MASTER THESIS IN GEOSCIENCES

DISCIPLINE: PETROLEUM GEOLOGY AND PETROLEUM GEOPHYSICS

DEPARTMENT OF GEOSCIENCES

FACULTY OF MATHEMATICS AND NATURAL SCIENCES

UNIVERSITY OF OSLO

JUNE 2015

Tutors: Jan Inge Faleide, Roy Helge Gabrielsen and Michael Heeremans
This work is published digitally through DUO – *Digitale Utgivelser ved UiO*
`http://www.duo.uio.no`
It is also catalogued in BIBSYS (`http://www.bibsys.no`)

“東風夜放花千樹，

更吹落，星如雨。

寶馬雕車香滿路。

鳳簫聲動，玉壺光轉，一夜魚龍舞。

娥兒雪柳黃金鏤，

笑語盈盈暗香去。

眾裡尋她千百度，

暮然回首，那人卻在燈火闌珊處。”

Abstract

The Klakk Fault Complex is situated on the mid-Norwegian continental margin separating the Halten Terrace from the Rås Basin at the inner part of the Vøring Basin. Most of the existing interpretations of the Klakk Fault Complex suggest a N-S trend, and the faults are the result of the late Middle Jurasic - earliset Cretaceous and Aptian-Albian rifting events reactivating the N-S trending Permian-Triassic extensional structures. Some previous works suggested that the Klakk Fault Complex from north to south display relative uniform structural pattern with significant displacement which was predominately resulting in the downthrown-side Rås Basin along the fault plane, and they noted that N-S-trending Klakk Fault Complex with the NE-SW lineament on the Halten Terrace led to the rhomboidal geometry of the Halten Terrace. We realized that most of the structures on the mid-Norwegian margin are defined at the base Cretaceous level. We interpreted the Base Cretaceous Unconformity as the transition to the post-rift, and the refined time-structure map of Base Cretaceous Unconformity demonstrates that the Klakk Fault Complex actually comprises of two main strikes (NW-SE and NE-SW). These two trends defining a characteristic pattern within the Klakk Fault Complex and adjacent area on both its western and eastern sides, reflect structural inheritance related to Devonian extension and the post–Devonian fault activities. Moreover, the reactivation of the Klakk Fault Complex during the regional extensional event in Aptian-Albian is not widely manifested in the study area, except the northern part.

Keywords: 2D seismic, mid-Norwegian continental margin, Klakk Fault Complex, structural analysis.

Preface

This master thesis is the result of the two-year master program of Petroleum Geology and Geophysics in Department of Geosciences, University of Oslo (UiO). This master thesis has been supervised by Professor Jan Inge Faleide (UiO & UiT), Professor Roy Helge Gabrielsen (UiO) and Senior Engineer Michael Heeremans (UiO).

Acknowledgements

I would like to express my appreciation for the guidance and help from my supervisors Prof. Jan Inge Faleide and Prof. Roy Helge Gabrielsen. Without your guidance, discussion and patient comments, I could not reach so far and complete this thesis. I also appreciate the help from Dr. Michael Heeremans for preparing the data set and dealing with the technical problems during the interpretation stage. Thanks to PhD candidate Dimitry Zastrozhnov (CEED) for helping on discussion and the reference from Kingdom OMNIS project.

Thanks to TGS and Fugro for providing the seismic data. Thanks to Norwegian Petroleum Directorate (NPD) and Petrobank/Diskos for releasing the information of the exploration wells.

Many thanks to my living partner Preben Jonassen for discussing the thesis and the happy life outside the campus. Thanks to the Jonassen family for supporting us and the happy time we have spent together.

A special thanks to my parents for all-these-years understand, support and faith in me. Thanks to my friends for long-time supporting and encouragement, especially Hui Wang who helped for this thesis.

Last but not the least, thanks to life for all the experience which makes me much stronger.

Qing He
何青

Oslo, Norway. June 1, 2015

Contents

List of Figures

Chapter 1

Introduction

The mid-Norwegian continental margin (62°N - 69°30′N, Blystad et al. (1995)) is a passive margin comprising three main segments (Møre Basin, Vøring Basin and Lofoten-Vesterålen) separated by the Jan Mayen Fracture Zone and Bivrost Lineament/Transfer Zone (Faleide et al., 2008). The main structural elements (Figure 1.1), as defined at the base Cretaceous level, are the Trøndelag Platform, underlying the inner shelf, the Vøring Basin, located beneath the outer shelf. The Halten Terrace and Rås Basin are one part of the Vøring Basin, which are the two most primary structural elements separated by the N-S striking Klakk Fault Complex (Blystad et al., 1995) in this study. The Halten Terrace, as the central part of the mid-Norwegian margin, has originated from multiple Mesozoic and earliest Cenozoic rifting episodes (Tsikalas et al., 2012). The last extension episode preceded and terminated with the opening of the northern part of the North Atlantic ocean during earliest Eocene (Skogseid et al., 1992; Van Balen and Skar, 2000). The Halten Terrace became a separate structural element from the Trøndelag Platform mainly during the extensive late Jurassic-early Cretaceous rifting episode (Skogseid et al., 1992; Blystad et al., 1995; Van Balen and Skar, 2000). The Rås Basin is the result of down-to-the-basin faulting along the Klakk Fault Complex (Blystad et al., 1995), which is covered by more than 10 km thick Cretaceous sediments in the deepest depocenter. The Klakk Fault Complex comprises deep-seated faults striking N-S according to the previous work, e.g., Blystad et al. (1995), and is the main bounding between the terrace area and the Rås Basin in the southeastern Vøring Basin. The fault complex has significant displacements and plays an important role on the Halten Terrace.

The mid-Norwegian continental margin (Figure 1.1) has experienced a long history of the intermittent extension and basin formation, from post-Caledonian orogenic backsliding and collapse in Devonian times (Doré et al., 1999; Roberts et al., 1999; Tsikalas et al., 2012) to post-early Eocene passive margin development dominated by the widening and

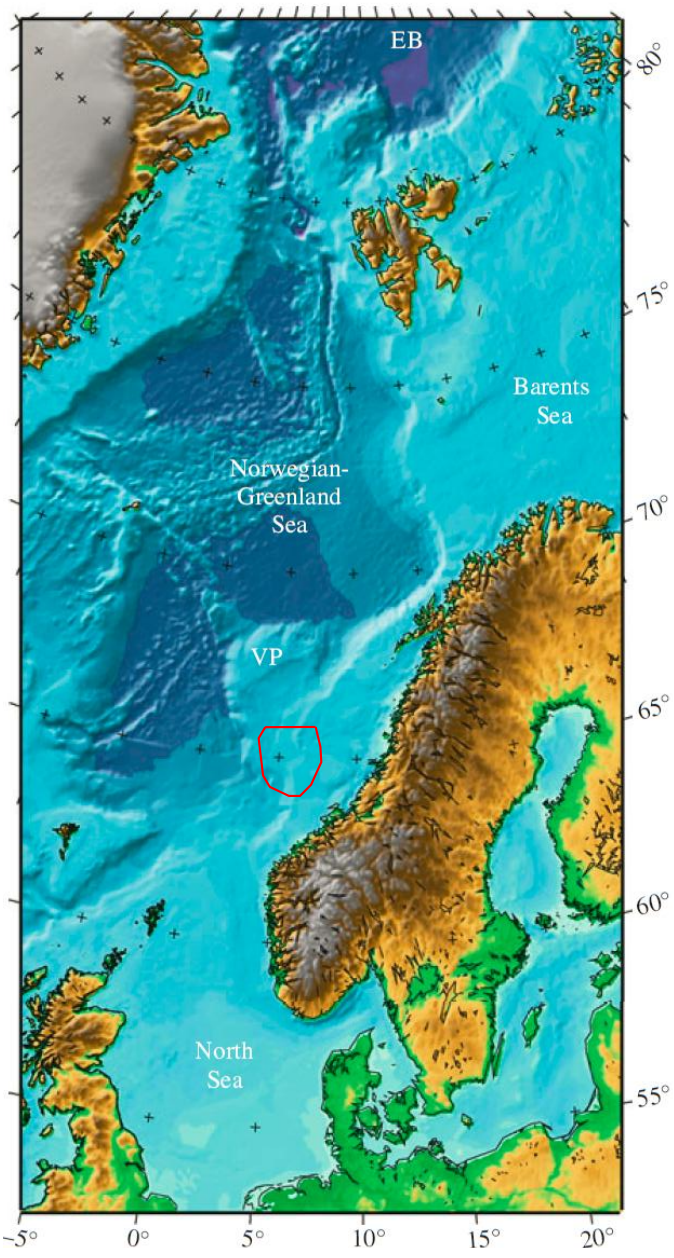

Figure 1.1: Regional setting (bathymetry/topography) of the mid-Norwegian continental shelf and its adjacent area. The study area is marked as the red lasso area. VP=Vøring Plateau, EB=Eurasia Basin. Modified after Faleide et al. (2010).

deepening of the NE Atlantic (Eldholm et al., 2002; Hopper et al., 2003; Tsikalas et al., 2012).

Integrated geophysical and geological studies (e.g., Blystad et al., 1995; Doré et al., 1997b; Brekke, 2000; Færseth and Lien, 2002) have revealed different structural patterns and strikes of the Klakk Fault Complex. The main purpose of this study is to focus on the Klakk Fault Complex and its immediate vicinity, understanding the fault strike, geometry, pattern and displacements. In addition, it is necessary to understand how the Klakk Fault Complex has worked and affected the neighboring structural elements, what is the mechanisms responsible for the structural geometry observed in the study area, how the basement lineaments have influenced the Klakk Fault Complex and the adjoining structures, and what is the relationship between the Base Cretaceous Unconformity and the Klakk Fault Complex illustrating the transition from the Halten Terrace to the deep Rås Basin.

Chapter 2

Geological Setting

The mid-Norwegian continental margin between 62°N and 69°30′N (Blystad et al., 1995) is described as a passive volcanic margin, which has experienced a long history of rifting from Devonian to Early Eocene. The rifting phases took place after the Caledonian orogeny, and end by the time continental break-up (Brekke, 2000; Faleide et al., 2008). During the rifting period, the mid-Norwegian continental margin formed a series of basins and related extensional structures during the late Middle Jurassic - earliest Cretaceous, and initiated the formation of strata related to rifting and subsidence.

The structural elements map in the mid-Norwegian margin (Figure 2.1) demonstrates that the main geological subdivision of the area is the basin area, platform area and the areas west of the escarpment (Bøen et al., 1984). According to Faleide et al. (2008), three segments are dominated in the offshore mid-Norway, which are the Møre Basin, Vøring Basin and Lofoten-Vesterålen. Two dominated NE-SW trending basins (the Møre and Vøring Basins) with a thick Cretaceous fill in central area constitute an overall tectonic framework in the mid-Norwegian continental margin. The basins are flanked by the uplifted mainland and the Cretaceous Trøndelag Platform on the east side, and by the Møre and Vøring Marginal Highs covered by Eocene lavas on the west side (Brekke, 2000). The Møre and Vøring Marginal Highs are cut by the NW-SE Jan Mayen Lineament and Bivrost Lineament.

In Figure 2.1, the blue polygon covering main part of the Halten Terrace and the Rås Basin is the study area in this master thesis. The structural elements involved in the study area are (from east to west, from south to north in order): northern part of the Frøya High, west margin of the Trøndelag Platform, Vingleia Fault Complex, Bremstein Fault Complex, Halten Terrace, Sklinna Ridge, Klakk Fault Complex, Rås Basin, Grip High, Helland-Hansen Arch, Slettringen Ridge and Fles Fault Complex.

Three cross-section (A-A', B-B' and C-C') in the study area cut through the Klakk Fault Complex. An overall cross-sectional geometry of the study area and the mid-Norwegian continental shelf is illustrated by Figure 2.4, Figure 2.5 and Figure 2.6.

2.1 Pre-breakup Tectonic Setting and Evolution

The earliest rift phase took place at the Norwegian Margin after the Caledonian orogeny in the Devonian, subsequently followed by the Permian-Triassic rifting in an intracontinental setting deposited primarily by terrestrial and fluvial clastics. During Jurassic, further rifting led to depositional environment changing of shallow marine, mainly clastic deposits in the Proto-Atlantic sag basin. The rifting phase occurred in the late Middle Jurassic - Early Cretaceous is considered to be of most importance in the previous studies, which result in a Cretaceous sedimentary strata of more than 10 km deposited in the deep Vøring and Møre Basins (Skogseid and Eldholm, 1989; Skogseid et al., 1992; Blystad et al., 1995; Tsikalas et al., 2002; Gernigon et al., 2006). During the Cretaceous time, some small extensional events were recorded in Aptian/Albian time (Blystad et al., 1995; Tsikalas et al., 2005, 2012). The last pre-break up rifting phase took place in the Cretaceous/earliest Tertiary, and then followed by continental break-up and sea-floor spreading in the Early Eocene (Tsikalas et al., 2002; Gernigon et al., 2006).

Late Palaeozoic - Early Mesozoic

The late Caledonian orogenic extension ended during latest Silurian-Early Devonian and the post-orogenic phase initiated the formation of a series of large half-graben basins, which were subsequently filled with thick successions of mainly intracontinenetal deposits (Coward, 1993; Ziegler, 1988b). The rift basins were formed between Norway and Greenland in the western Barent Sea along the NE-SW Caledonian trend in the main Late Palaeozoic rift episodes. According to Gabrielsen et al. (1999), the rift system was recorded as a dominate N-S to NE-SW orientated normal faults with NW-SE striking transfer faults and tectonic activity was concentrated on the Trøndelag Plat form and the Halten Terrace. During this time, the rift system was primarily filled by continental clastics (Brekke et al., 2001).

From Carboniferous to Triassic, mild extension took place in the early Carboniferous by continuing subsidence and sedimentation in the central Greenland (Bütler and Sørensen, 1935). The Norwegian shelf was affected by Permian-early Triassic thinning of a crustal section with variable thickness between 30-35km (Gabrielsen et al., 1999). During this time, significant fault activity was recorded in the Froan Basin and the Vestfjorden Basin. Large volume of sediments was deposited in the Late Triassic. The Triassic faulting in the mid Norwegian shelf took place during the early to mid-Triassic (Jongepier et al.,

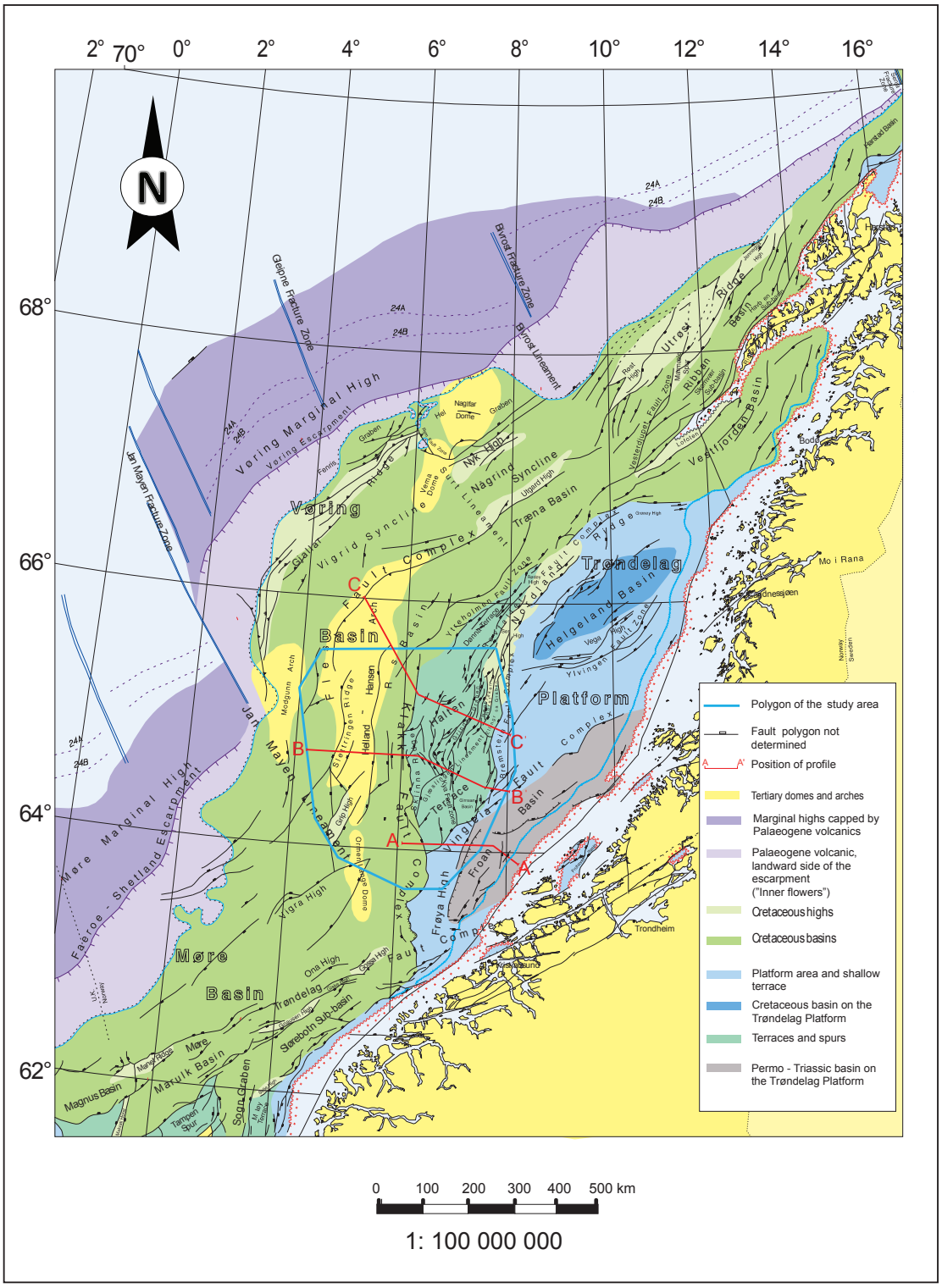

Figure 2.1: Structural elements in the Norwegian continental shelf. It comprises three segments which are the Møre Basin, Vøring Basin and Lofoten-Vesterålen. Two dominated NE-SW trending basins (the Møre and Vøring Basins) with a thick Cretaceous fill in central area. The blue polygon shows the study area. The structural elements involved in the study area are: northern part of the Frøya High, west margin of the Trøndelag Platform, Vingleia Fault Complex, Bremstein Fault Complex, Halten Terrace, Sklinna Ridge, Klakk Fault Complex, Rås Basin, Grip High, Helland-Hansen Arch, Slettringen Ridge and Fles Fault Complex. Modified after Blystad et al. (1995).

1997). This destabilization also affected on the platform areas, such as Halten Terrace (Gabrielsen et al., 1999).

Middle Jurassic - Early Cretaceous

The Middle Jurassic – Early Cretaceous rift phase is of considerable importance due to the consequence of development of major Cretaceous basins (the Møre and Vøring Basins) off mid-Norway and East Greenland. According to Lundin and Doré (1997), the rifting in NE Atlantic propagated northward through the Rockall Trough, West Shetland/Faeroe Trough, central Møre Basin and eastern Vøring Basin coevally with rifting in the Labrador Sea. A shift in extensional stress field vector from W-E to NW-SE in association with the northward propagation in the Early Cretaceous (Doré et al., 1999). This orientation change were explained by Bugge et al. (2002) as a continuation of the Devonian extensional shear zones and detachments, and it is evident by the Cretaceous structures cutting the configuration of Paleozoic structures and basins (Osmundsen et al., 2002).

The Møre and Vøring Basins in mid off-Norway were formed mainly by the rifting in the Late Jurassic-Early Cretaceous. However, no large-scale extension took place in this region contemporaneously with rifting to break-up in Labrador Sea. Based on Surlyk et al. (1981) that coarse clastic submarine fans associated with deep water shales suggest activity along the major boundary faults in central East Greenland persisting into latest Early Cretaceous, and contemporaneous activity has been reported along the flanks of main fault zones in the Møre and Vøring basins (Blystad et al., 1995; Lundin and Doré, 1997). By mid-Cretaceous, most of the structural relief due to the sediments fills in the Møre and Vøring basins.

However, the timing of the Jurassic to early Cretaceous tectonic event is still controversial. Rifting in the late Middle Jurassic to Late Jurassic and the earliest Cretaceous is evident (Blystad et al., 1995; Doré et al., 1999; Brekke, 2000; Faleide et al., 2008), but no consensus can be reached on how far the Early Cretaceous rifting proceeded.

Late Cretaceous-Early Tertiary

The Late Cretaceous was portrayed of the global sea level rising, of which the maximum took place between Norway and Greenland where an epicontinental sea exist (Gabrielsen et al., 1999). Late Cretaceous-Early Tertiary rifting appears to have started in Maastrichtian and subsequently came the break-up in Early Eocene(Lundin and Doré, 1997). The tectonism was characterized by faulting , accelerated basin subsidence and conjugate uplifting, bounding platform basinward-tilting. Erosion occurred during this time on the basin flanks. The rifting resulted in low-angle detachment structures that up-

dome thick Cretaceous sequences and sole out at medium-to-deep intracrustal levels on the Vøring and Lofoten-Vestrålen margins. The rift formed a more than 300 km wide zone associated with lithospheric and post-breakup subsidence (Skogseid, 1994). The opening of the NE Atlantic affected strongly on Møre Basin that lead to the dramatic higher subsidence rate (Bøen et al., 1984; Skogseid and Eldholm, 1989; Olafsson et al., 1992). The Møre Basin was end up by splitting up in the Early Tertiary (Gabrielsen et al., 1999).

2.2 Stratigraphy

From the cross-sections of the study area (Figure 2.4, Figure 2.5 and Figure 2.6), it can be observed that the Upper Triassic and Jurassic sediments can only be confidently mapped on the inner part of the mid-Norwegian continental shelf (on the Halten Terrace area and the eastern part of the Halten Terrace in the study area (Figure 2.1), where the Cretaceous subsidence was low to moderate (Bøen et al., 1984). The west margin of the Halten Terrace is the westernmost area where Jurassic sediments can be found. During the Cretaceous time, the Halten Terrace has been exposed to erosion and the subsequent removal of the Jurassic sediments on the western part of the Halten Terrace took place (Bøen et al., 1984). Before the considerable sediments from the Cretaceous filling the basin to the east of the Halten Terrace, the oldest reflector that can be mapped continuously in the deep basin, which was interpreted as the Base Cretaceous Unconformity (BCU). According to Rønnevik et al. (1983), the BCU was proposed to be in the age of the Mid-Cretaceous. In the deep basin, the Paleozoic and Mesozoic sediments were deposited under the BCU. The cross-sectional profiles also shows that from the south to north, the thickness of the Jurassic sediments varies, and the maximum thickness of the Cretaceous post-rift sediments is located in the basin center in vicinity of the Helland-Hansen Arch.

The definitions of lithostratigraphic units are based on well data from the Halten Terrace and the west margin of the Trøndelag Platform by Dalland et al. (1988). Therefore, the lithostratigraphy (Figure 2.2) was presented by the Halten Terrace area.

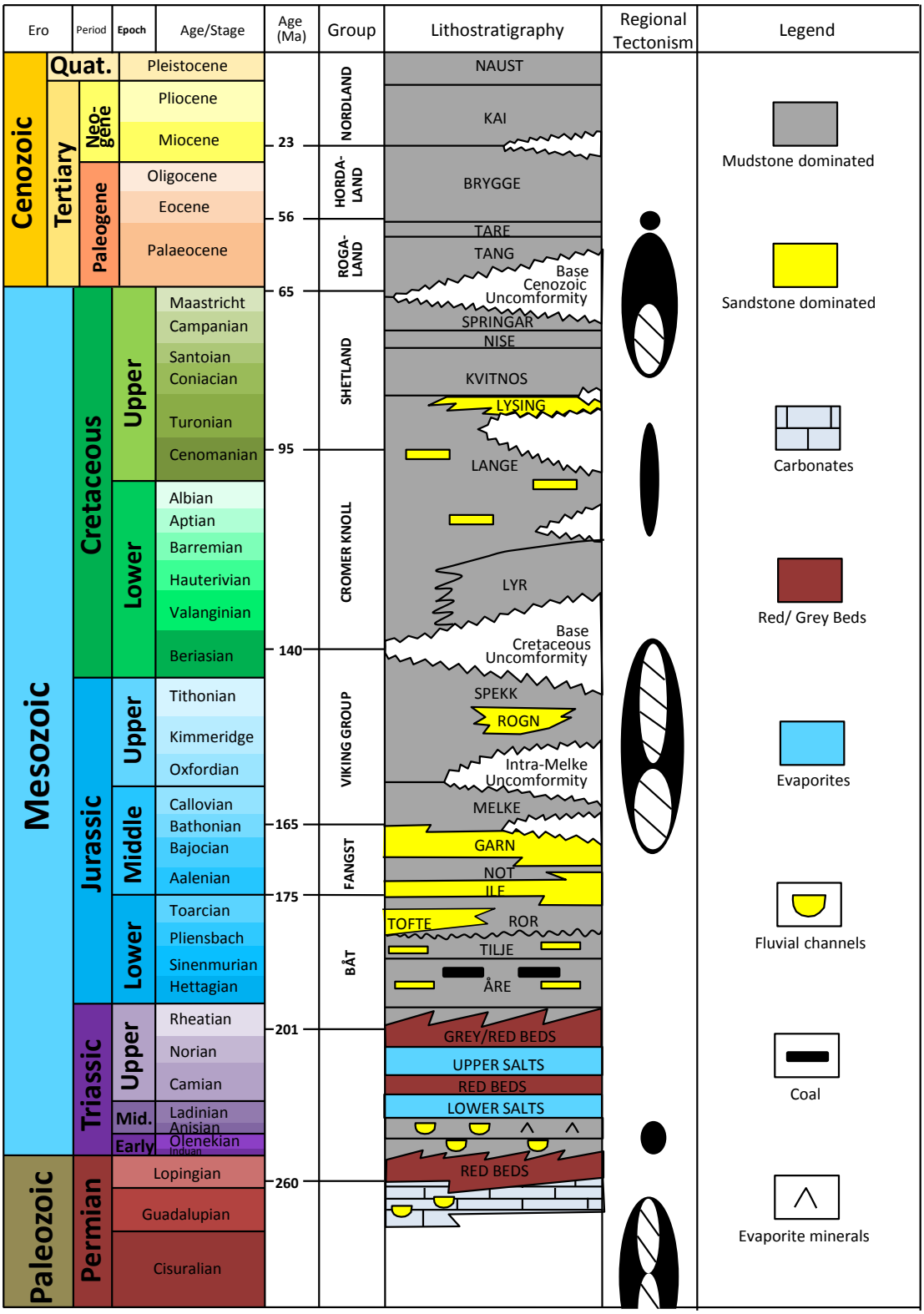

Figure 2.2: Lithostratigraphy of the Halten Terrace area with the regional tectonism in mid-Norwegian continental shelf. Modified after Dalland et al. (1988); Tsikalas et al. (2005); Elliott et al. (2012); Tsikalas et al. (2012) and Bell et al. (2014).

2.3 Structural Elements

The structure elements involved in the study area were refereed in Chapter 2. It is essential to take consideration of the adjoining structural elements of the Klakk Fault Comlex for analyzing the mechanism and tectonism of forming the faults, and how the faults influenced the geometries of the adjacent structural elements. In this section, the main structures (Figure 2.3) will be briefly presented. All the nomenclature of structural elements and the formal definitions are referenced from Blystad et al. (1995). The structural elements are listed in alphabetical order.

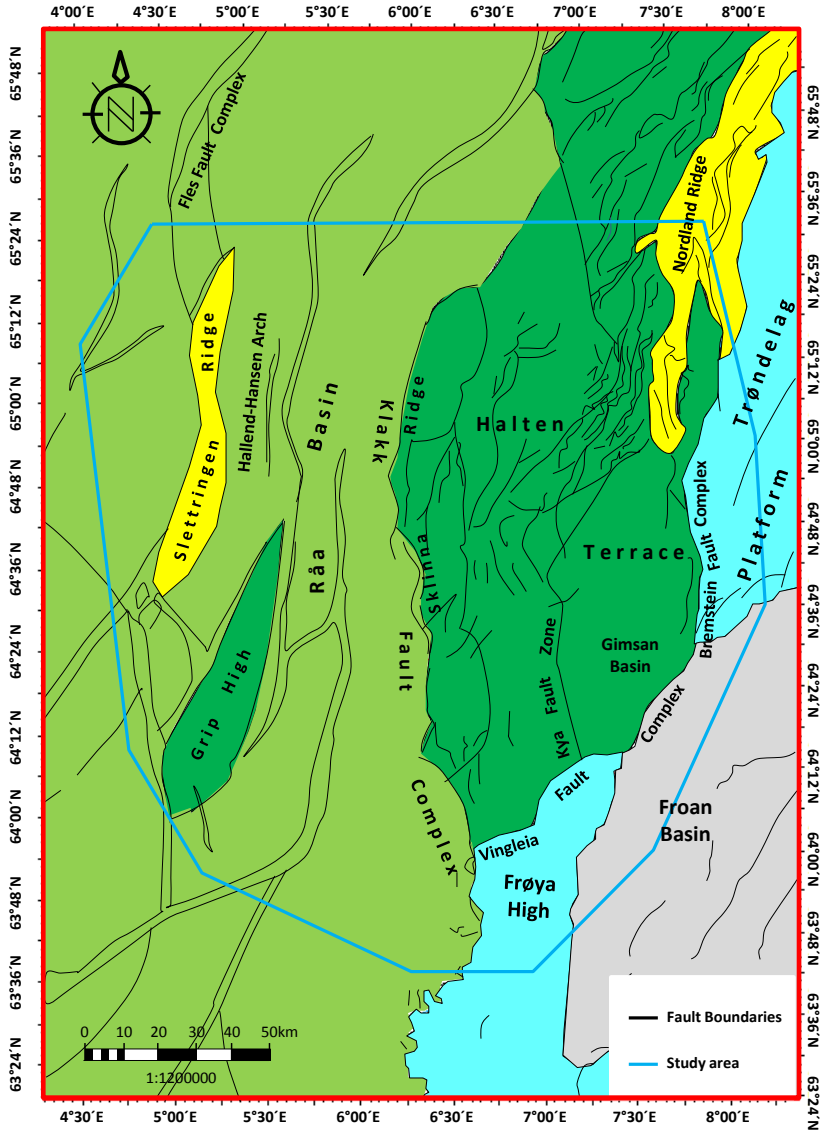

Figure 2.3: Main structural elements in the study area. The blue polygon shows the study area in this master thesis. The southern part (between the Frøya High and Møre Basin) of the Klakk Fault Complex is not involved in this study due to the limitations of seismic data. Modified after Blystad et al. (1995).

2.3.1 Frøya High

The Frøya High is a N-S oriented horst which is *c*a. 120 km long and 30-40 km wide (Blystad et al., 1995). It comprises the most part of southwestern Trøndelag Platform, bounded by the Klakk and Vingleia Fault Complexes from the west and northwest respectively. To the east, the Frøya High is adjacent to the Froan Basin. Internally, it constitutes of a basement rock to the south and becomes narrower northwards. According to (Surlyk et al., 1984) and (Blystad et al., 1995), the Frøya High has been subjected to a long tectonic history and had similarity to East Greenland which may have been block faulted during a supposed Early Permian rifting episode.

2.3.2 Halten Terrace

The Halten Terrace (Figure 2.1, Figure 2.3, Figure 2.4, Figure 2.5 and Figure 2.6) is located between the Trøndelag Platform to the east and the Rås Basin to the west. It is a huge rhomboidal-shaped fault block (Blystad et al., 1995), bounding by the Bremstein Fault Complex to the east, the Klakk Fault Complex to the west, the Vingleia Fault Complex to the southeast and connected to the Dønna Terrace to the north. In the east and northeast, the Halten Terrace is separated by Bremstein Fault Complex from the eastern structural element Trøndelag Platform,in the southeast, by the Vingleia Fault Complex from the Frøya High and in the west by the Klakk Fault Complex from the Møre and Vøring Basin. It contains several low-ranked structural elements, such as the Sklinna Ridge (Figure 2.4, Figure 2.5 and Figure 2.6, Chapter 2.3.7), Gimsan Basin (Figure 2.5), Grinda Graben (Figure 2.6), Kya Fault Zone (Figure 2.5 and Figure 2.6) and etc (Figure 2.3).

Jurassic strata can be found in all parts of the terrace except the western part of the Sklinna Ridge where the Jurassic sediments were eroded in Mid-Cretaceous age, and the older strata is exposure and dip steeply to the east (Blystad et al., 1995). Thin to middle (*c*a. 1200 m) strata of the Cretaceous (with about equal thickness of Lower and Upper Cretaceous) deposited on the terrace.

The Halten Terrace was initiated during the rift event in the late Middle Jurassic-Early Cretaceous and later developed during the Late Cretaceous faulting associated with the Bremstein and Vingleia Fault Complexes (Blystad et al., 1995). During the Callovian, activities took place along the Klakk Fault Complex in the early phase of rifting. While during the latest rifting phase in the Kimmeridgdian, movements acted along the Bremstein Fault Complex. After uplifting and erosion took place, separation from the Trøndelag Platform caused by the faulting of the Bremstein and Vingleia Fault Complexes. In Aptian/Albian age, the Klakk Fault Complex had some weak avtivities again. Final separation occurred in the Cenomian/Turonian by the eastern bounding faults, which

separate the terrace from the platform and linked to a tectonic phase in the Vøring Baisn.

2.3.3 Helland-Hansen Arch

The Tertiary structure Helland-Hansen Arch is elongated in about 280 km long (Blystad et al., 1995). In the south, the arch is narrow and orientated in N-S, while it becomes wider northwards and the orientation changed into NE-SW. In the north, the structure is asymmetrical that is steeper in the northwestern limb and more gentle in the eastern limb.

2.3.4 Grip High

The Grip High is defined at the base Cretaceous and has an orientation of SSW-NNE (Blystad et al., 1995). It is an elongated structure bounding with the west-dipping fault to the west that separates from the Slettringen Ridge. The Grip High was exposure until buried in Turonian time.

2.3.5 Klakk Fault Complex

The Klakk Fault Complex mainly strikes N-S in more than 10-15 km width and *c*a. 270 km length. It dips towards west and some of the escarpment zone was eroded along the western margins of the Sklinna Ridge and Frøya High. Significant displacement happened along the complex, which can reach 2.5 s TWT, separating the Halten Terrace and the Frøya High in the east from the Rås Basin in the west. It is broader in the northern part (along the Sklinna Ridge) than in the southern part (along the Frøya High).

2.3.6 Rås Basin

The Rås Basin was identified at the base of the Cretaceous and by the initial basin infill of the lower Cretaceous (Blystad et al., 1995). It is separated by the Klakk Fault Complex from the Halten Terrace to the east. The southern and the northeastern boundaries of the basin are determined by the Jan Mayen and Surt Lineaments respectively. The whole basin is portrayed of an arch-shape in the plan view, which trending N-S in the south and change to NE-SW in the north. The change also caused the basin infill of the Cretaceous sediments folded, which formed the core of the Hallend-Hansen Arch. The basin floor is *c*a. 6-8 s TWT at the base Cretaceous. In the Cenomanian, the Rås Basin became one part of the Vøring Basin due to the transgressed flanks.

2.3.7 Sklinna Ridge

N-S trending Sklinna Ridge (Figure 2.4, Figure 2.5 and Figure 2.6) is along the westernmost margin of the Halten Terrace with an extension of *c*a. 140 km (Blystad et al., 1995). The Sklinna Ridge was deeply eroded and the pre-Jurassic strata was exposed dipping towards east. The top of the ridge is uneven and can be divided into the flat high and the intervening saddle. The northern part is narrow and the southern part is broader. The ridge was formed in the Late Jurassic as a flank uplift along the Klakk Fault Complex, later it might be movement occurred again during Aptian/Albian time when the Klakk Fault Complex reactivated.

2.3.8 Slettringen Ridge

At a basal Cretaceous unconformity, the Sliettringen Ridge is defined in (Blystad et al., 1995) as a set of N-S trending. It constitutes a set of same trending, rotated fault blocks running from the Møre Basin northwards along the Fles Fault Complex. The ridge is developed below the Helland-Hansen Arch, and it caused by the polarity changing of the Fles Fault Complex in its southern part from west-dipping to east-dipping (Blystad et al., 1995). It developed during the late Middle Jurassic-Early Cretaceous when the rift event proceeded.

2.3.9 Trøndelag Platform

A roughly rhomboidal-shaped Trøndelag Platform is located in off central Norway as one of the major structural elements and includes several subdiviary elements, e.g., Nordland Ridge, Helgeland Basin, Frøya High, Froan Basin, Ylvingen Fault Zone and Vega High. The Møre-Trøndelag Fault Complex is the southeastern boundary and the Revfallet Fault Complex is bounding the north and west of the Trøndelag Platform. In its southwestern corner, it meets the Jan Mayen Lineament and the Møre Basin, from which it is separated by the Klakk Fault Complex (Blystad et al., 1995). The platform is defined at the base Cretaceous level which is underlain by a uniform thickness Jurassic overlying deep basin filled by Triassic and Upper Palaeozoic sediments.

2.3.10 Vøring Basin

The Vøring Basin is one of the three main geological provinces of the Vøring Margin that the main structures and structural unites are defined at the base Cretaceous level (Gabrielsen et al., 1984; Blystad et al., 1995; Skogseid et al., 1992). It is a large sed-

imentary basin province which is constituted of grabens, basins, and structural highs (Blystad et al., 1995). Also, Blystad et al. (1995) and Skogseid et al. (1992) depicted the constituents of the Vøring Basin that, the eastern basin province comprises the Træna Basin and the Rås Basin, eastern flanked by the Halten Terrace and the Dønna Terrace neighboring by the the Nordland Ridge and the Fulla Ridge in east and west respectively, and the western province includes the Vigrid and Någrind Synclines, the Hel and Fenris Grabens, the Nyk and Utgard Highs and the Gjallar Ridge.

The Vøring Basin was initiated by extension in the late Middle Jurassic-Early Cretaceous, so that the basin was divided by three separated basins: the Rås Basin and the Træna Basin to the east and a shallow basin at west of the Fles Fault Complex. In this study, only eastern part (at east of the Fles Fault Complex) is involved, which includes the Halten Terrace, the Rås Bains and the Helland-Hansen Arch.

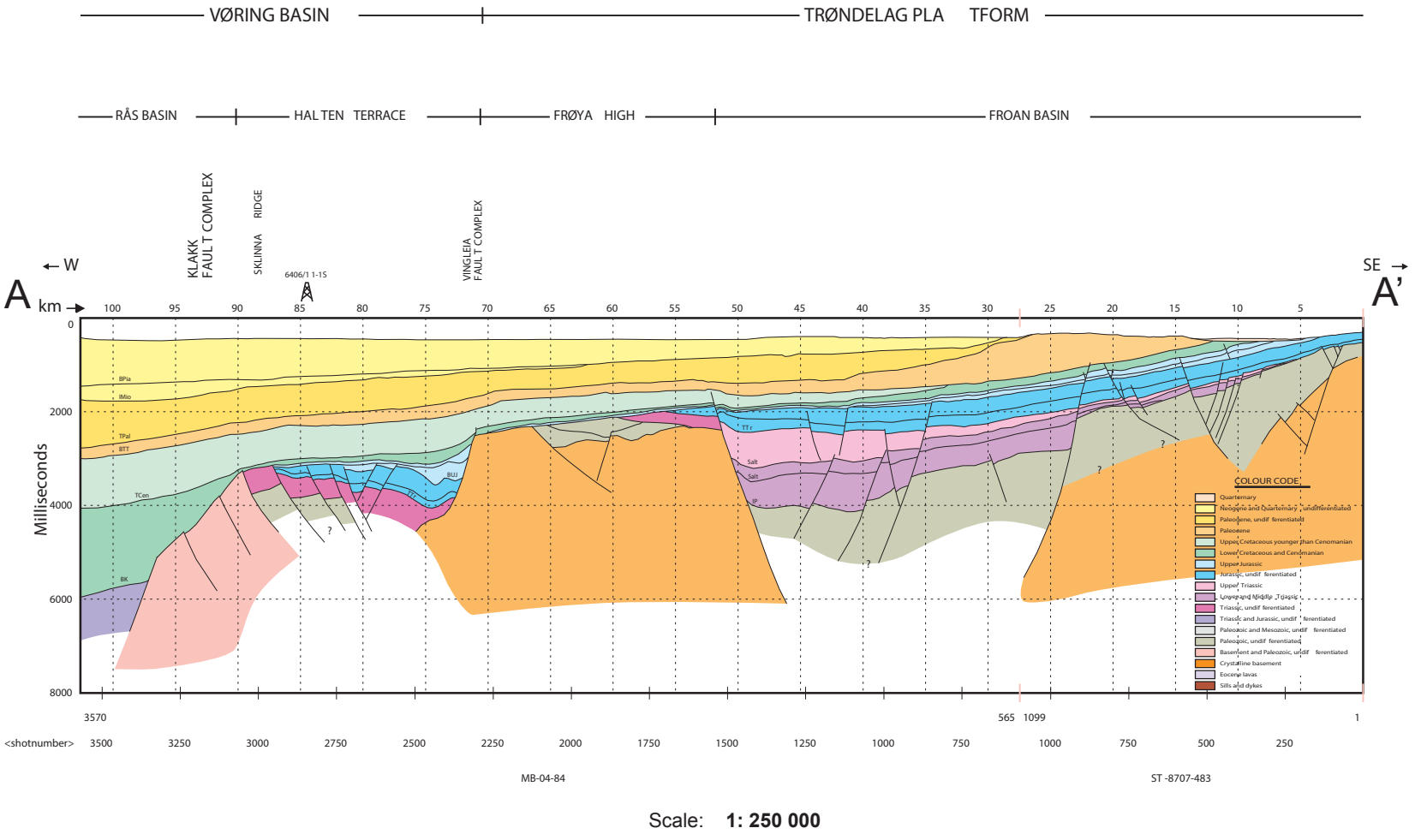

Figure 2.4: A-A' cross-section in Figure 2.1. The structural elements are shown on the top of the cross-section. Modified after Blystad et al. (1995).

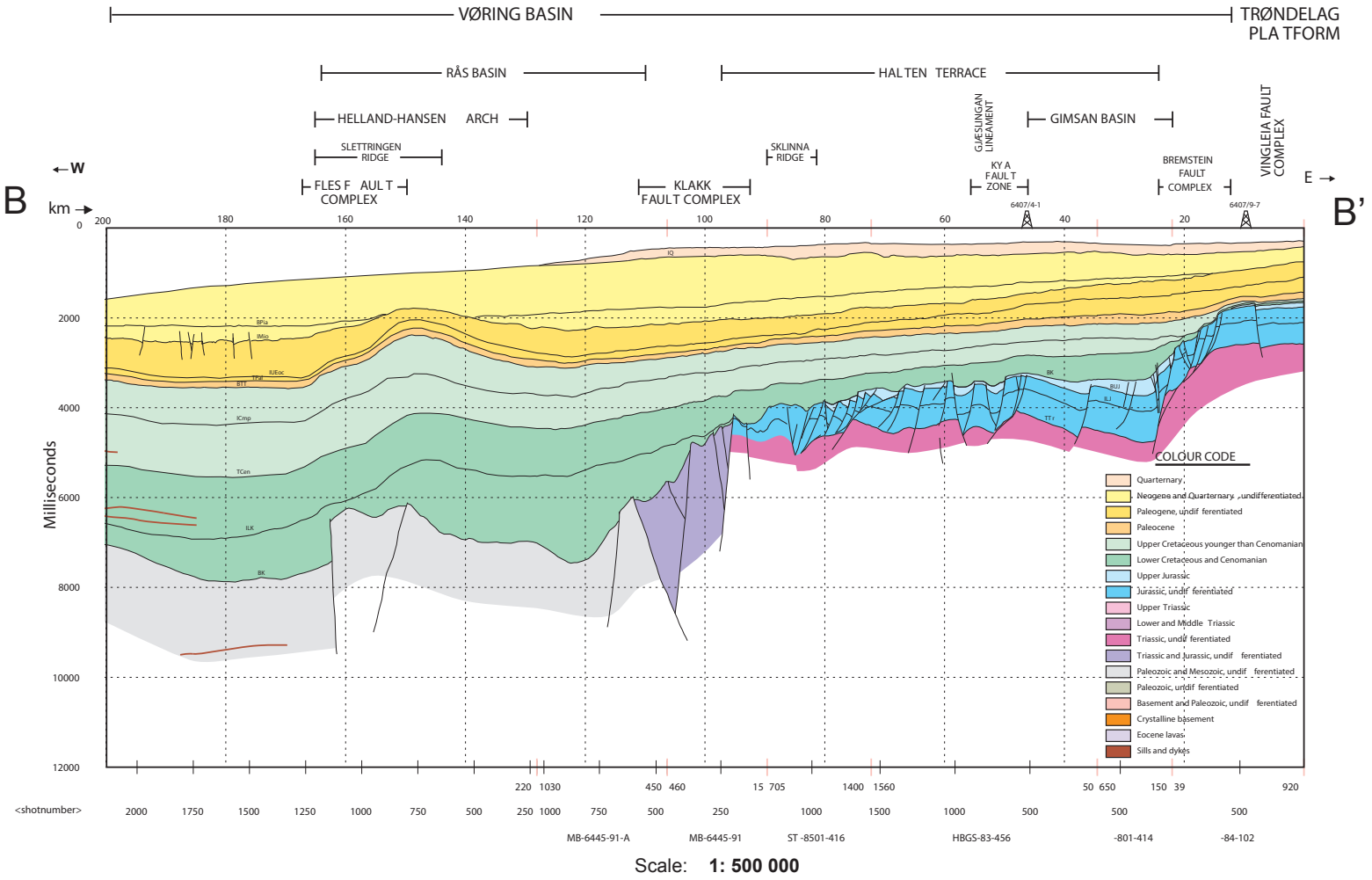

Figure 2.5: B-B' cross-section in Figure 2.1. The structural elements are shown on the top of the cross-section. Modified after Blystad et al. (1995).

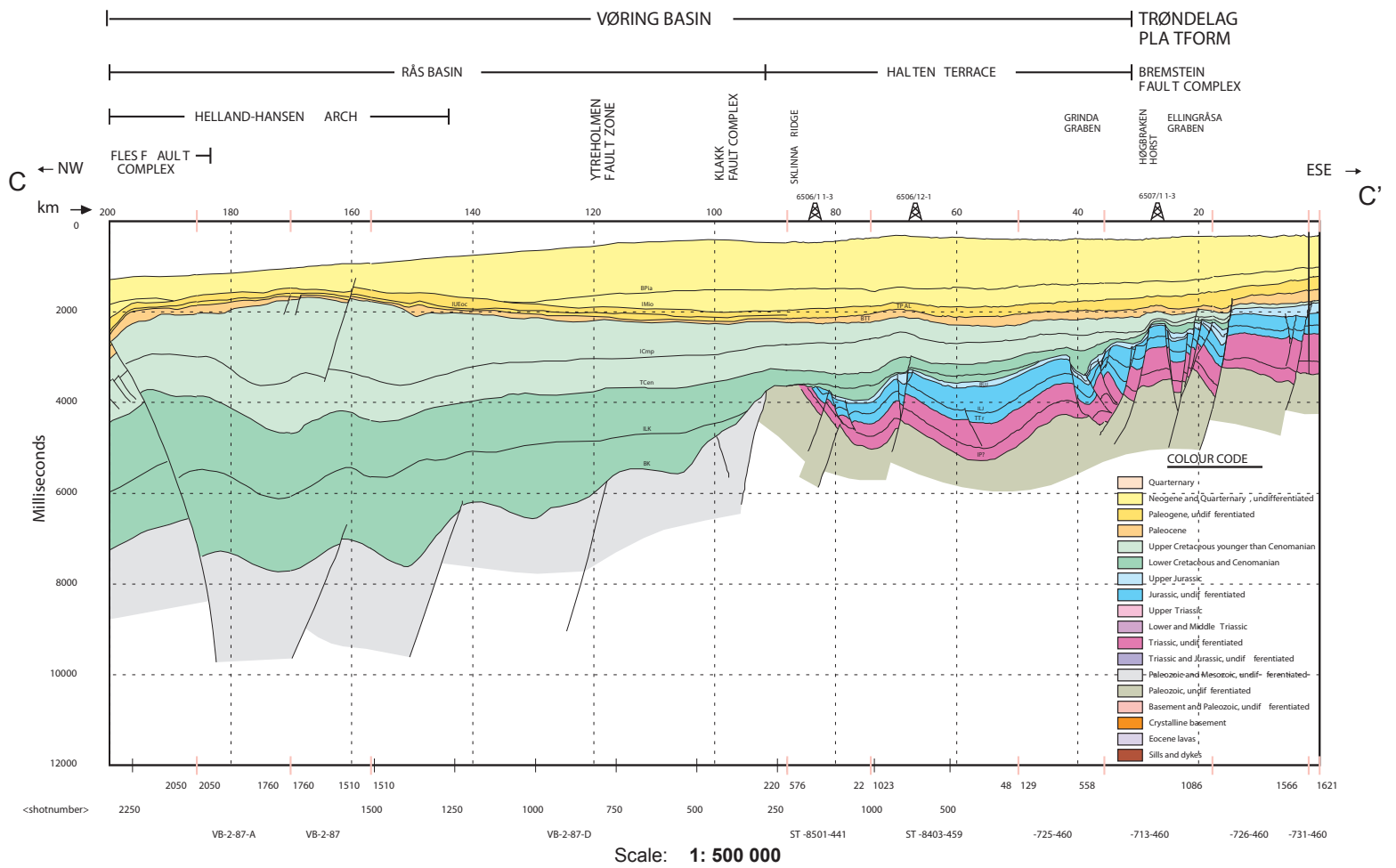

Figure 2.6: C-C' cross-section in Figure 2.1. The structural elements are shown on the top of the cross-section. Modified after Blystad et al. (1995).

Chapter 3

Seismic Interpretation and Results

3.1 Method

The seismic interpretation of the study area is performed utilizing available 2D seismic lines and well data in the software *Petrel 2013* provided by *Schlumberger*. The workflow (Figure 3.1) is mainly comprised of interpretation part and the analysis part.

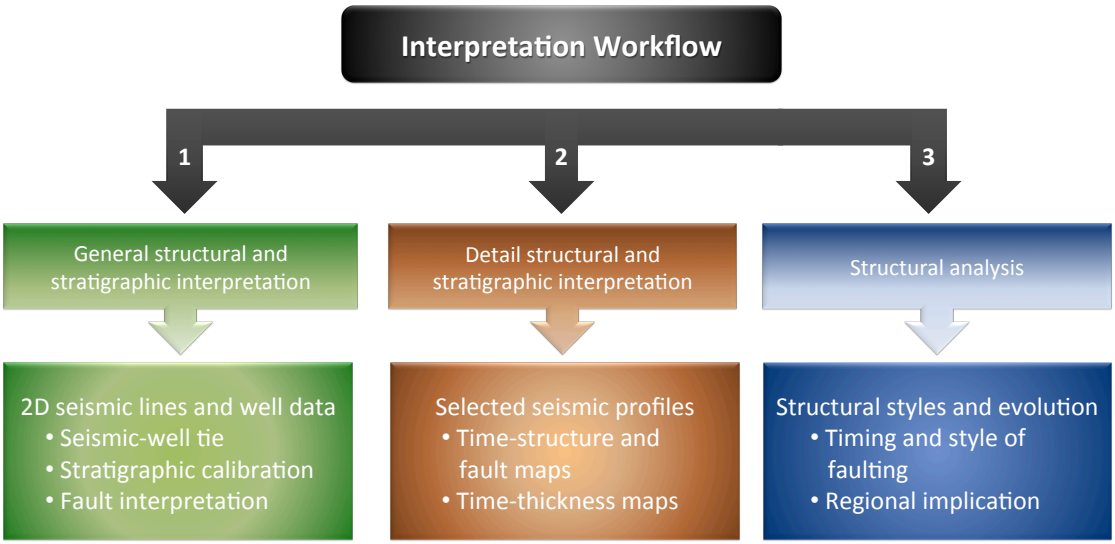

Figure 3.1: Interpretation workflow for this master thesis. Stage 1 and 2 belong to the interpretation part, and stage 3 is the analysis part.

The interpretation procedure is divided into two stages - general structural and stratigraphic interpretation, and detail structural and stratigraphic interpretation. The general structural and stratigraphic interpretation is using 2D seismic lines and well data to interpret horizons and major faults. The detail structural and stratigraphic interpretation is based on the previous work to refine the Base Cretaceous Unconformity,

generating the time-structure maps and time-thickness maps. Fault polygons of the predominate fault complexes and zones can be mapped on the time-structure map of the BCU and selected seismic profiles. The third stage is structural analysis which is trying to identify timing and style of faulting, the interplay of faulting and regional evolution and the regional implications based on the first two stages.

3.2 Data set

The data set (Figure 3.3) comprises regional 2D seismic lines which were acquired by TGS and Fugro and local well data released by Norwegian Petroleum Directorate (NPD), *Factpages* (2015) (`factpages.npd.no/factpages/`).

3.2.1 Seismic Data

The seismic data include high-quality, time-migrated, 2D seismic reflection profiles which have a record length of 0-10 s two-way time (TWT) (some profiles only recorded 0-8 s TWT length) and provide good quality imaging down to the Triassic on the terrace area. The seismic imaging within the deep basin area, however, degrades with depth, and the data quality is generally poor along the west flank of terrace in the study area. The 2D seismic lines have E-W, NW-SE and N-S orientations, covering the Halten Terrace, Sklinna Ridge, Klakk Fault Complex, Rås Basin, Grip High, Helland-Hansen Arch and Slettringen Ridge (Figure 3.3). The E-W oriented seismic profiles are orthogonal to the roughly N-S strike Klakk Fault Complex and traverse the most structures in the Halten Terrace. They provide the best coverage from the Halten Terrace to deeper parts of the Rås Basin. The Klakk Fault Complex is not completely striking N-S and has several segments dipping towards NW. Therefore, the NW-SE seismic profiles are the most precise representation of the cross-sectional view for examining the NW-dipping fault segments. The N-S orientated seismic profiles will not be presented due to the orientation generally parallel to the faults strike, but only are utilized for seismic ties and stratigraphic calibration.

The criterion of the seismic quality was demonstrated in Figure 3.2. Term *seismic reflection* or *reflection* referring to Chapter 3.3 are specified here. A *seismic reflection* of elastic wave at boundaries between different rock formations changes polarity due to the acoustic impedance changes in different mediums. Therefore, we refer *seismic reflection* or *reflection* to a horizon deposited in the same time interval. It can be one bed in a sedimentary sequence.

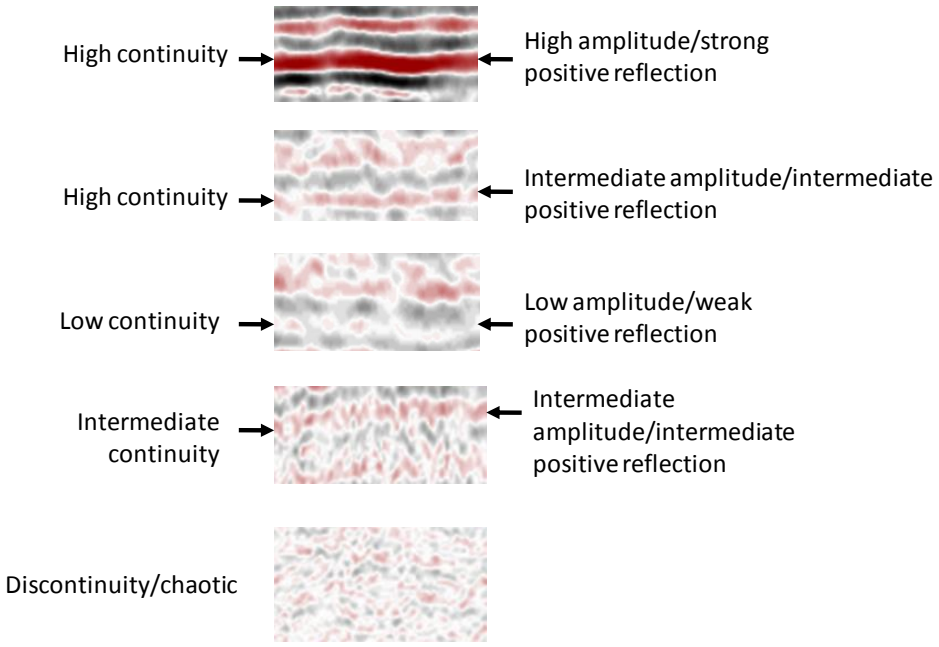

Figure 3.2: The criterion of the reflections in the study area. The reflection continuity is addressed in the left side, and the amplitude is in the right side of the seismic illustrations. The arrows point one seismic reflection. The red represents positive reflections, while the black represents negative.

3.2.2 Well Data

The interpretation of the seismic profiles was aided by seven exploration wells drilled on the Halten Terrace (Figure 3.3) for the available stratigraphic data. These seven exploration wells are integrated with the seismic data for stratigraphic calibration in the study area (Figure 3.3). Detail information of these seven wells are obtained from *Factpages* (2015) (`factpages.npd.no/factpages/`) and Petrobank/Diskos (Table 3.1). All wells are located on the Halten Terrace. The oldest penetrations range from the Upper Triassic (Red Beds and Grey Beds) to the Lower Jurassic (the Åre and Tilje Formations) (Table 3.2).

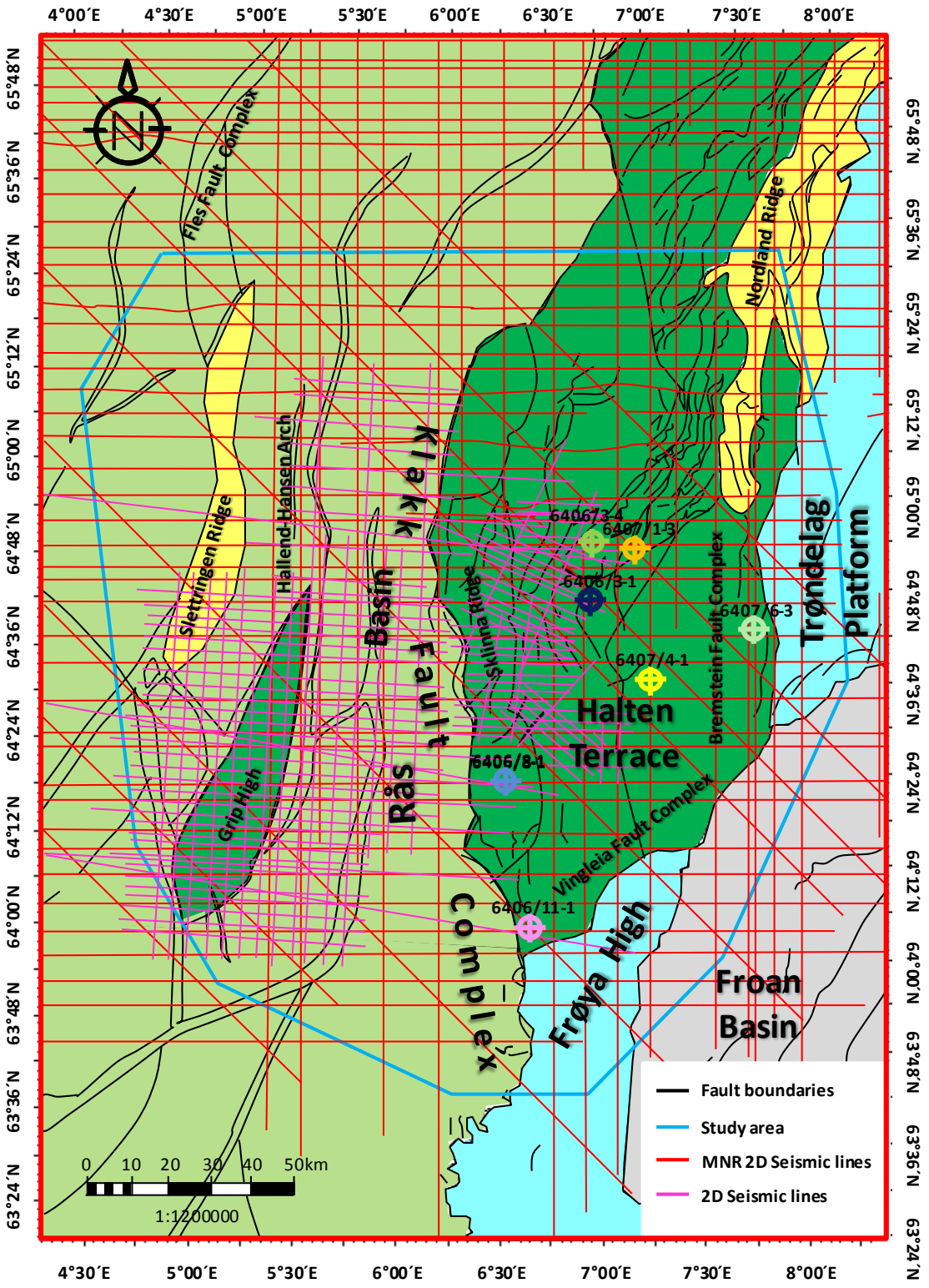

Figure 3.3: 2D seismic lines acquired by TGS and Fugro, and seven local exploration wells drilled on the Halten Terrace. The green 2D seismic lines are the key lines for the interpretation procedure, and the pink 2D seismic lines are the additional line for the detail interpretation of the Base Cretaceous Unconformity. The main area of interest is outlined by the blue polygon. Modified from Blystad et al. (1995).

Table 3.1: Well data from Norwegian Petroleum Directorate (NPD), *Factpages* (2015) (`factpages.npd.no/factpages/`) and Petrobank/Diskos. Seven wells are tied with the regional seismic lines. The well locations can be found in Figure 3.3.

Well names	**6406/11-1**	**6406/3-1**	**6407/1-3**	**6406/8-1**	**6406/3-4**	**6407/6-3**	**6407/4-1**
NS UTM [M]	7104524.70	7183474.26	7195989.53	7140372.60	7197370.60	7176849.07	7164900.01
EW UTM [M]	383011.32	396410.13	407531.49	376765.25	398030.83	436571.55	411212.79
UTM zone	32	32	32	32	32	32	32
Licence number	156	091	073	131	091	092	106
Drilling operator	Saga Petroleum ASA	Den norske stats oljeselskap	Den norske stats oljeselskap	Elf Petroleum Norge AS	Den norske stats oljeselskap	Den norske stats oljeselskap	Den norske stats oljeselskap
Completion date	18.02.1991	14.08.1984	16.01.1984	11.04.1988	29.12.1987	2.16.1987	15.11.1985
Type	Exploration	Exploration	Exploration	Exploration	Exploration	Exploration	Exploration
Discovery	Oil	Gas shows	Oil/Gas	Gas shows	Oil shows	Gas/Condensate	Gas/Condensate
KB [m]	26	22	29	27	29	29	22
Water depth [m]	315	256	286	348	295	222	225
TD(MD)[m RKB]	4185	4902	4469	4914	4414	3220	4835
Oldest penetrated age	Late Triassic	Late Triassic	Late Triassic	Early Jurassic	Early Jurassic	Late Triassic	Middle Jurassic
Oldest penetrated formation	Red Beds	Red Beds	Grey Beds	Åre Fm.	Tilje Fm.	Åre Fm.	Garn Fm.

Table 3.2: Geological tops of the regional seven exploration wells, data are supplied by *Factpages* (2015) (`factpages.npd.no/factpages/`) and Petrobank/Diskos.

Age	Group/ Formation	6406/11-1	6406/3-1	6407/1-3	6406/8-1	6406/3-4	6407/6-3	6407/4-1
		Top depth [m RKB]	Top depth [m RKB]	Top depth [m RKB]	Top depth [m RKB]	Top depth [m RKB]	Top depth [m RKB]	Top depth [m RKB]
Tertiary	Nordland Group	341.0	278.0	315.0	375.0	325.0	251.0	247.0
	Naust Fm.	450.0	616.0		375.0	325.0	251.0	247.0
	Kai Fm.	1191.0	1450.0	1449.0	1363.0	1514.0	1227.0	1264.5
	Hordaland Group	1397.0	1850.0	1762.0		1994.0	1463.0	1656.0
	Brygge Fm.	1397.0	1850.0	1762.0		1994.0	1463.0	1656.0
	Rogaland Group	2143.0	2279.0	2212.5	2597.0	2314.0	1950.0	2097.5
	Tare Fm.	2143.0	2279.0	2212.5	2314.0		1950.0	2097.5
	Tang Fm.	2190.0	2347.0	2281.0	2380.0		1977.5	2174.0
Cretaceous	Shetland Group	2335.0	2410.0	2346.0	2752.0	2437.0	2069.0	2264.0
	Springar Fm.			2346.0		2437.0	2069.0	
	Nise Fm.			2448.0		2655.0	2125.0	
	Kvitnos Fm.			2600.0		2974.0	2322.0	
	Cromer Knoll Group	3205.0	3197.0	3103.0	3963.0	3278.0	2414.0	3010.0
	Lange Fm.				3963.0	3278.0		3012.0
	Lyr Fm.					3884.0	2414.0	
Jurassic	Viking Group	3419.0	3662.0	3521.0	4099.0	3907.5	2444.5	3710.0
	Spekk Fm.		3662.0	3521.0		3907.5	2444.5	3710.0
	Melke Fm.	3419.0	3685.0	3544.0	4099.0	3949.0	2451.0	3772.0
	Fangst Group	3522.0	3782.0	3600.0	4265.0	4025.0	2461.0	3889.5
	Garn Fm.		3782.0	3600.0	4265.0	4025.0	2461.0	3889.5
	Not Fm.	3522.09		3704.0		4120.5	2492.0	3969.0
	Ile Fm.	3599.0	3934.0	3741.0	4368.0	4161.5	2547.5	4021.0
	Båt Group	3722.0	4012.0	3813.0	4494.0	4224.0	2638.5	4106.0
	Ror Fm.	3722.0	4012.0	3813.0	4494.0	4224.0	2638.5	4106.0
	Tofte Fm.	3787.0				4272.0	2691.0	4150.0
	Ror Fm.	3822.0				4299.0	2698.0	4209.0
	Tilje Fm.	3871.0	4177.0	3950.0	4668.0	4372.0	2727.0	4272.5
	Åre Fm.	3985.0	4380.0	4150.0	4894.0		2902.0	4472.0
Triassic	Grey Beds	4134.0	4758.0				3220.0	
	Upper Salts							
	Red Beds	4194.0	4864.0					
	Lower Salts							

3.3 Interpretation Procedure and Methodology

The seismic interpretation started with screening of all the regional MNR 2D seismic lines (Figure 3.3) in the study area and a general picture of stratigraphic framework and structural geometries, thus, can be generated from the initial concepts. After the full assessment of data quality, determination of the horizons were made to describe the geology accurately. The general stratigraphic interpretation was started from two prominent unconformities which are the Base Cretaceous Unconformity (BCU) and the Base Cenozoic, due to their chronostratigraphic significance. In seismic lines, reflections of the unconformities were correlated and mapped in the study area by using the seven available wells and seismic data (Figure 3.3, Table 3.1 and Table 3.2). Horizons in the Jurassic sequence were afterwards selected for the later fault interpretation on the Halten Terrace. Out of the lithostratigraphy in the Halten Terrace, the Top Garn Formation and Top Åre Formation were preferential due to the good quality of seismic reflections. The faults located in the Halten Terrace were interpreted after these four horizons generated. In this contribution, additional seismic lines from the Kingdom OMNIS Project. These additional 2D seismic lines (Figure 3.3) were used in the detail interpretation of the BCU. The refining of the BCU from the Halten Terrace to the Rås Basin did the spadework for generating the time-structure map. In order to analyze reactivation of the Klakk Fault Complex, configuration and variation of the post-rift sediments, seven horizons in the Cretaceous were then selected to interpret along the seismic profiles: Barremian-Aptian (?), Intra-Albian, Near Top Albian, Intra Early Coniacian, Top Early Santonian and Intra Mid-Campanian. The lack of well data in the Rås Basin and obstruction of the tilted fault blocks result in the indeterminacy of the stratigraphy interpretation on the basin side. Hence, seven horizons were tied along one seismic line from a regional study carried out within the Kingdom OMNIS project (Zastrozhnov et al., n.d.).

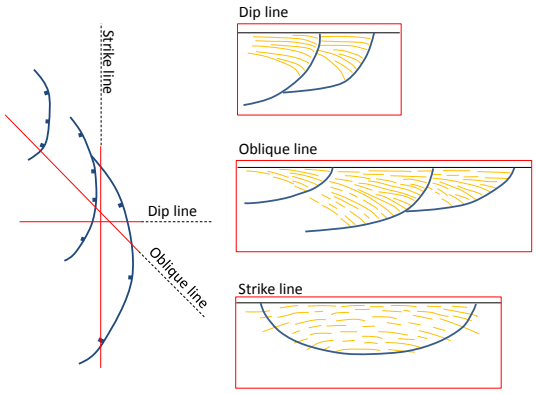

Figure 3.4: The angle between seismic line and fault strike is very important for representing the fault geometry in the cross-sectional geoseismic profiles. The left figure shows the tectonic sketch of the fault strike cutting by different oriented seismic lines. The corresponding morphology of the cross-sections is shown to the right. The more representative geometry is the one recognized on the line that are perpendicular to the strike of fault and sediments, as shown in the dip lines. No scales for figures. Modified after *Basic Principle in Tectonics* (2015)

Attention should be paid that the seismic reflection provides indirect time-domain measurements of the subsurface geology, so that the character and position of the reflections

correlated are the responses to impedance contrasts across real geologic boundaries, and it largely depends on the geometry and properties of the subsurface velocity field (Herron and Latimer, 2011). In addition, the low-angle faults were recognized as the seismic reflections that display the fault planes instead of the stratigraphic sequences. Moreover, the geometry of the reflections largely depends on the angle between the profile and the strike of the faults (Figure 3.4). The more representative geometry is the one recognized on the lines that are perpendicular to the strike of fault and sediments, i.e. NW-SE and E-W orientated seismic lines in the study area. Hence, different seismic lines may display a variant geometry for the same fault.

3.4 Seismic Interpretation Problems and Limitations

The interpretation of the Klakk Fault Complex and the faults in the Rås Basin was difficult to do in the *Petrel* program, due to the lack of 3D seismic data. The 2D seismic data used in this study are widely spaced and do not facilitate mapping of faults accurately. Uncertainty on tracing the same fault in the Klakk Fault Complex also result in the failure in the fault interpretation in Petrel. By observing the faults in the seismic lines, it shows that all the main faults along the western margin of the Halten Terrace and the the faults with large displacement in the Rås Basin appear under the BCU. The refined BCU time-structure map also reveals that, most of these main faults can be shown on the BCU time-structure map, where the big time-elevation change took place. Therefore, the fault polygons (Figure 3.5) were made based on the BCU time-structure map. It should be noted that, the big change on time-elevation in the BCU time-structure map does not always follow the fault displacement between the footwall and hangingwall blocks. Fault types are changing with the variations of the fault strikes so that the BCU time-structure map may not show the heave of fault. The fault polygon, therefore, can not only follow the contour lines in the BCU time-structure map, but also need to be examined in the seismic profiles. Confirmation of whether it is the fault displacement resulting in elevation drop or it is the undulation of the BCU (Figure 3.6). By combining these two, a more precise fault polygon can be generated and represented more accurate on the geometry of the main faults in the plan view.

However, the confidence of the fault polygon remains incomplete. The fault polygon can show the essential strikes and exhibit the heave variation, but it can not precisely represent them, especially on NW-SE strike. In order to reduce the error, the BCU-edge surface map was made to combine with the BCU-time structure map identifying the fault polygon (Figure 3.5).

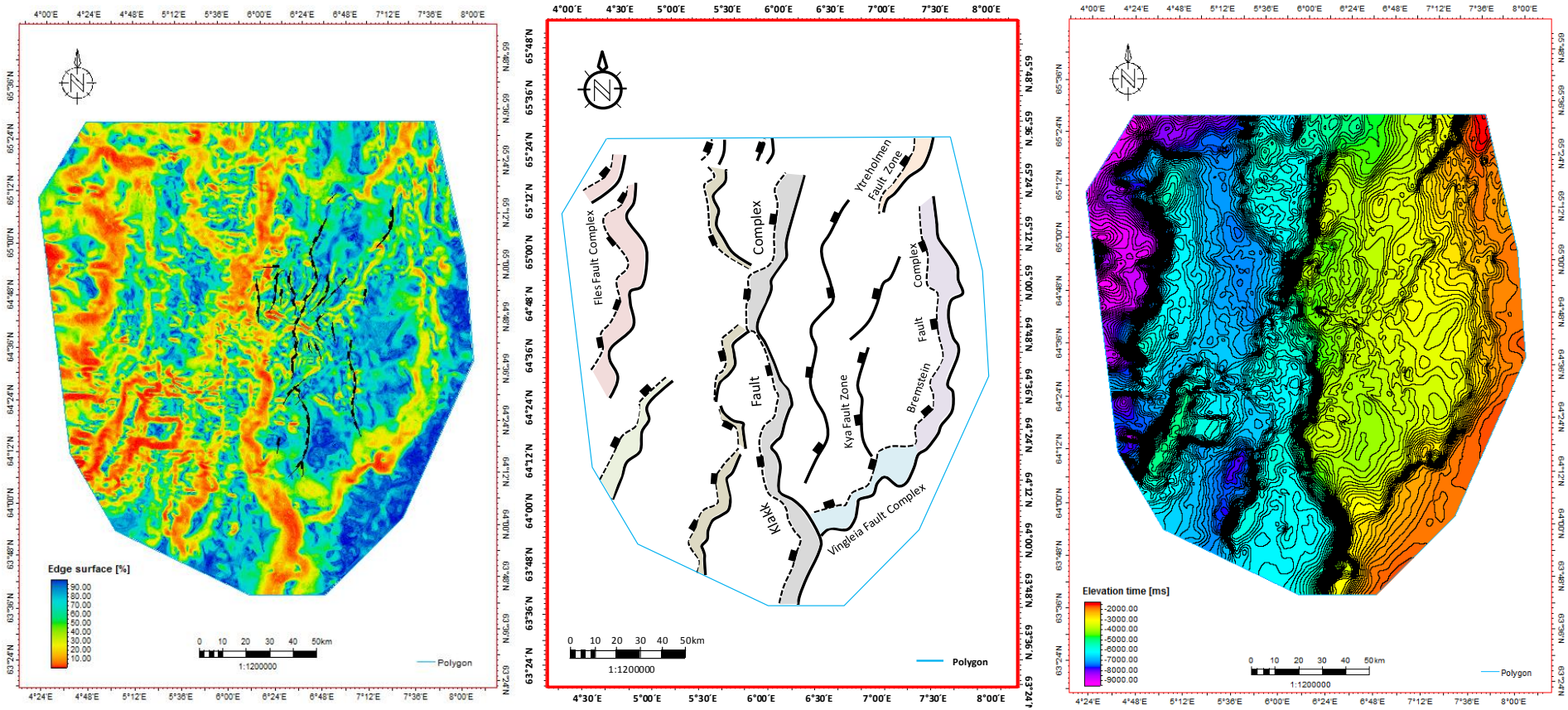

Figure 3.5: Comparison between the fault polygon (middle) with BCU-edge surface map (left) and BCU-time structure map (right). The fault polygon was mainly generated based on the BCU time-structure map to the right side, but a consideration of the cross-sectional geoseismic lines has been taken. The left one illustrates a general morphology of the study area by the bounding faults of the geological structures. The main fault complex are marked in different color and their names. The solid line represents the footwall, and the dotted line represents the hangingwall, the black cube shows the dipping direction. The fault escarpment was filled by the same color means it belongs to the same fault system.

A non-depth-converted seismic line can not represent the truth of the fault heave and throw, depth discrepancies, lithology of sediments, compaction and so on can make differences on the geometry of the faults when depth-conversion achieved.

Because of the poor quality of the seismic in the deep basin, fault interpretation becomes more difficult, uncertainties still remain in the deep part. The length of the deepest geoseismic lines records at 10 s TWT which lead to the limitation to the deep structures in the study area. No wells drilling at the basin side also enlarge the uncertainties in the interpretation and correlation of reflections.

Furthermore, due to the deficiency of stratigraphic correlation in the Rås Basin and limitation of the reference to the Cretaceous horizons Barremian-Aptian and Intra Albian mapping on the Halten Terrace, the time-thickness maps of BCU to Barremian-Aptian and Barremian-Aptian to Intra Albian will not show deposition on the Halten Terrace.

Last but not the least, seismic interpretation alone is not conclusive for the later analysis of the Klakk Fault Complex and its immediate vicinity. Additional methods are essentially necessary. However, special situation along the Klakk Fault Complex is existed. For example, for quantifying the growth history of faults, high vertical resolution of the seismic reflection data set is required. Moreover, depth converted T-z plot (throw-depth plot) has quantity requirement of the corresponding reflections at both hangingwall and footwall fault blocks. In our case, however, the Klakk Fault Complex can only be identified by the Base Cretaceous Unconformity cutoffs at the fault plane. For analyzing the segmentation, linkage and throw of faults, *Traptester* software can approach. It requires at least one horizon cutoff indispensably for the software. Along the Klakk Fault Complex, while, only the erosion surface of the Base Cretaceous Unconformity can be identified. The erosion polygon of graben shoulder along the Klakk Fault Complex mapping based on time-thickness map may helps to do analysis of the rotation and uplift, sediment supply and the isostasy and elastic response to faulting. But in our case, the lack of pre-Cretaceous stratigraphic correlation in the basin side lead to incapable mapping the erosion shoulder in the fault block in the Rås Basin, and widely spacing between the neighboring 2D seismic lines leads to incapability of mapping the erosion area along the Klakk Fault Complex. Comparison of the erosion between the block shoulders of the intrabasin synthetic faults can not be achieved.

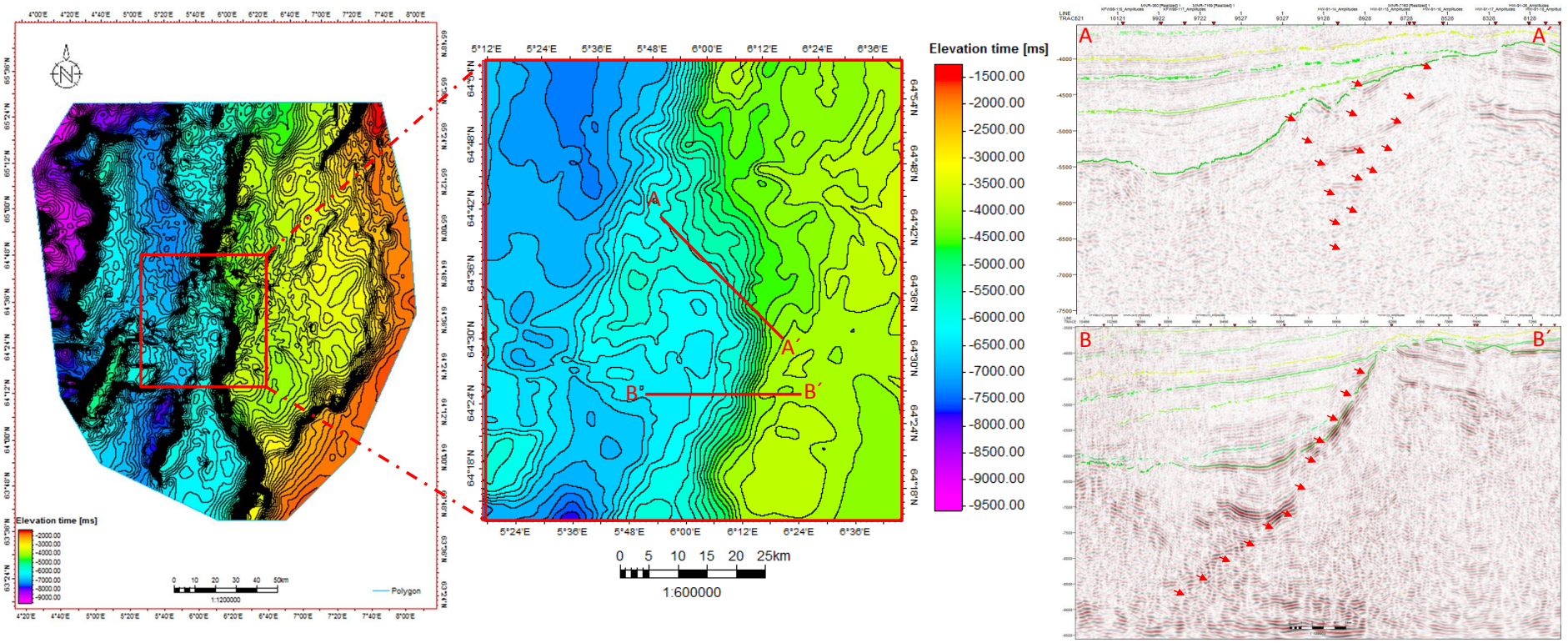

Figure 3.6: Fault dip and geometry are changing with the variations on the fault strike. Seismic lines A-A' and B-B' cut through the fault with two opposite strikes. Seismic line A-A' shows cross-sectional geometry of the NW-SE orientated fault segment, while seismic line B-B' shows cross-section of the NE-SW oriented fault segment. Faults were marked by the red arrows in the seismic profiles, which reveal that fault displacement and undulation of the BCU both can affected on time-elevation change in the time-structure map.

3.5 Seismic Stratigraphy

Eleven horizons were interpreted from the Halten Terrace in the east to the Rås Basin in the west (Figure 3.7). The BCU and Cretaceous horizons can be traced from the Halten Terrace to the Rås Basin, while the Top Åre and Top Garn horizons only can be traced in the Halten Terrace and the seismic reflections stopped at the tilted fault blocks to the west of Halten Terrace and truncated by the BCU. Barremian-Aptian and Intra Albian are obstructed by the the Klakk Fault Complex to the east, but can be mapped to the deep part of the Rås Basin to the west. The lowermost horizon in the Cretaceous crossing over the Klakk Complex from the Rås Basin to the Halten Terrace is the Near Top Albian in the north and the Intra Albian in the south of the study area. However, the continuity of the NTA was also affected by the undulation of the BCU on the Halten Terrace. The Intra Mid-Turonian, Intra Early Coniacian, Top Early Santonian and Intra Mid-Campanian horizons were mapped from the Rås Basin to the Halten Terrace. To the east, these four horizons are stopped at the Trøndelag Platform and the Frøya High.

Two wells tied with key seismic lines which are described in Chapter 3.7. Therefore, these two seismic lines are selected to exhibit the eleven horizons and the seismic stratigraphy, which tied with the well 6407/6-3 and 6407/1-3 on the Halten Terrace respectively (Figure 3.8 and Figure 3.9).

The seven horizons mapped in the Cretaceous were tied by doing reference to Zastrozhnov et al. (n.d.) without the calibration of the well-seismic ties in the Rås Basin. In the basin side, the reflections show relative poorer resolution to the southern part of the study area because of the reflection discontinuity.

The Åre Formation (TÅ) comprises alternating sandstones and claystones interbedded with coals (Dalland et al., 1988). The reflection is *c*a. 4 s TWT across the Halten Terrace. Similar to the other Jurassic reflections, the top of the Åre Formation can be mapped through the Halten Terrace and stopped at the Klakk Fault Complex bounding at west. The reflection of the Top Åre Formation displays medium to high positive amplitude which varies through the Halten Terrace.

The Garn Formation (TG) consists of a series of paralic-shallow-marine sandstones (Dalland et al., 1988; Elliott et al., 2012; Bell et al., 2014). The Top Garn Formation in seismic lines is characterized by a high amplitude positive reflection, which crosses through the Halten Terrace from the Trøndelag Platform in the east and bounded by the Klakk Fault Complex towards west. The reflection is *c*a. 3-4 s TWT underneath the BCU. Six exploration wells penetrated into the Garn Formation in Jurassic.

The Base Cretaceous Uncomformity (BCU) is a prominent seismic reflection for structural analysis, which separates Jurassic from Cretaceous sediments across the Halten

Terrace (Bell et al., 2014). However, the BCU is not correlated with any formation top by stratigraphic calibration in well ties. The uncomformity is displayed as a low-frequency high-amplitude double reflection in the seismic lines (Kyrkjebø et al., 2004)). The occurrence of onlap, downlap and toplap in the seismic lines was paid attention to along this unconformity reflection. According to Dalland et al. (1988); Elliott et al. (2012) and Bell et al. (2014), the Spekk and Melke Formations in the Viking Group are dominated by deep marine mudstone overlain on the sandstone-rich Garn Formation (Figure 3.7). The BCU, thus, was identified by the strong negative reflection above the Garn Formation which is a strong positive reflection. The BCU is mapped between 3-4

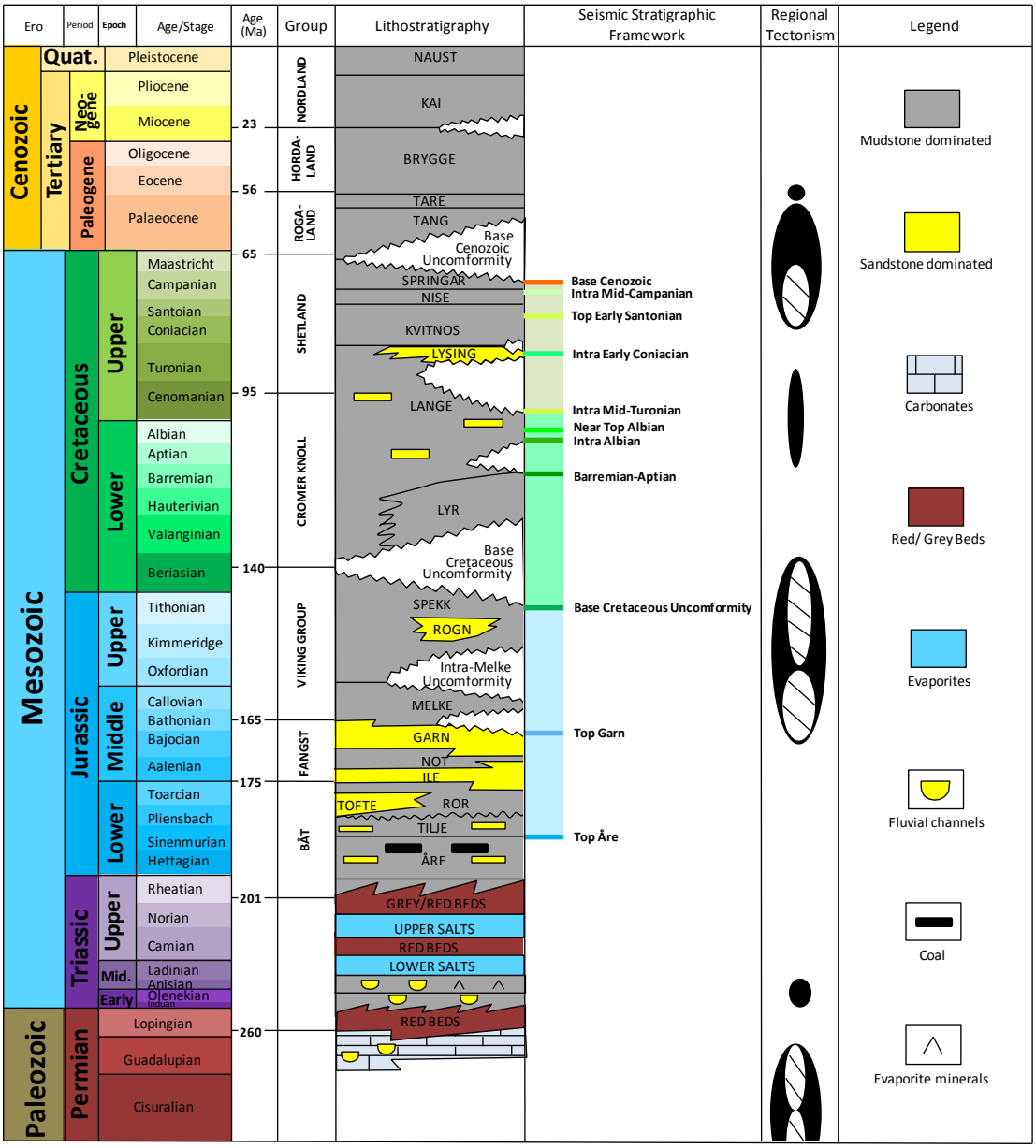

Figure 3.7: Chronostratigraphic column of the Halten Terrace. Color coding of seismic reflections are shown in the Seismic Stratigraphic Framework column, which will be used in all subsequent figures. Modified after Dalland et al. (1988); Tsikalas et al. (2005); Elliott et al. (2012); Tsikalas et al. (2012) and Bell et al. (2014).

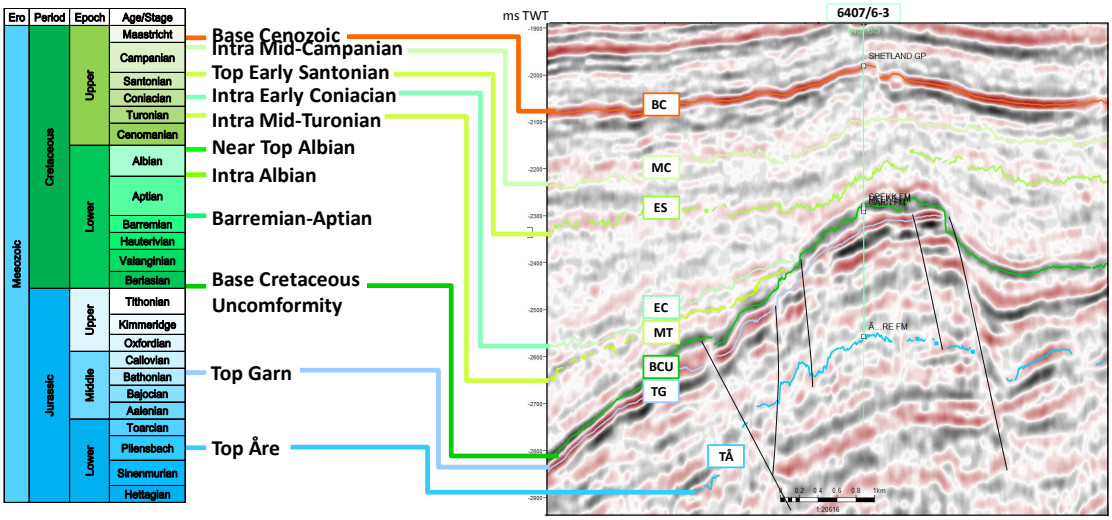

Figure 3.8: Well 6407/6-3 tied with the seismic profile. Location of well 6407/6-3 can be seen in Figure 3.3. The horizons presented in different colors are tied with the lithostratigraphic column (Figure 3.7). Abbreviations are used for representing different horizons in their corresponding ages/stages.

s TWT across the Halten Terrace, and variation upper and lower around 4 s TWT at the Sklinna Ridge. However, the BCU remains undrilled in the Rås Basin, and alternative interpretations for this surface have been presented (Skogseid and Eldholm, 1989; Blystad et al., 1995; Swiecicki et al., 1998; Doré et al., 1999; Brekke, 2000; Reemst and Cloetingh, 2000; Skogseid et al., 2000; Færseth and Lien, 2002). The criteria for interpreting the BCU in the Rås Basin is following Færseth and Lien (2002) and Gómez et al. (2004), which suggest that the lower Cretaceous succession is of post-rift character and thus it favors a Middle to Late Jurassic timing for the main deformation in this region. An onlap surface is obviously observed in the eastern basin flank and on the terrace area. In the Rås Basin, the BCU varies dramatically, which can range from *c*a. 5.5 s TWT to 9 s TWT in the basin center.

The Barremian-Aptian (BA) was interpreted as an intermediate positive reflection, mapped at *c*a. 6.5-7.5 s TWT in deep basin and at 5-6.5 s TWT at the tilted fault blocks. The BA horizon is not continuous at the uplifted footwall fault blocks and the Grip High in the southern part of the Rås Basin, and it is portrayed of onlap on the fault plane of the Klakk Fault Complex and the uncomformity of the base Cretaceous. The late Cretaceous faults cut the reflections in the basin side.

The Intra Albian (IA) is characterized by an intermediate positive reflection. The reflection is 1 s TWT deeper than the BA reflection. Hence, it ranges from 4 s TWT to 5.5 s TWT at the tilted fault blocks, and ranges from 5.5 s TWT to 6.8 s TWT in the deep basin. Similarly, onlap is the significant character at the Klakk Fault Complex to the west margin of the Halten Terrace.

The Near Top Albian (NTA) was correlated to a bed in the Lange Formation. The NTA

is represented by a intermediate positive reflection which is relatively continuous, and is discontinuous at the Grip High at the southern part of the study area. The NTA reflection varies from 4 s TWT to 6 s TWT in the basin side and from 3 s TWT to 4 s TWT in the terrace side.

The Intra Mid-Turonian (MT) can be mapped from the basin side to the terrace side in the study area. It is portrayed of a high amplitude negative reflection. The reflection has the best resolution and continuity among the seven reflections in the Cretaceous post-rift sedimentary sequences at the northern part, but reduces the quality to the south. The reflection is recorded at 3-3.7 s TWT in the seismic lines throughout the Halten Terrace and at the tilted fault blocks in the Rås Basin, but reaches 5.5-6.2 s TWT in the deep basin. The MT horizon separate the Lower Cretaceous from the Upper Cretaceous deposits in the lithostratigraphy.

The Intra Early Coniacian (EC) is characterized by an intermediate positive reflection to the north and a medium to strong positive reflection to the south in the study area. Reflection with a good persistence was cut by the late Cretaceous faults in the basin side, and on the terrace side, the lateral persistence of the reflection reduced but was not affiliated with faults. The horizon stops at the Trøndelag Platform and the Frøya High.

The Top Early Santonian (ES) was correlated with the near top Kvitnos Formation and it is characterized by a low amplitude, discontinuous positive reflection. In the basin side, the fill is relatively chaotic at the northern part of study area. In the southern part, the lateral persistence of the reflection becomes even worse both in the basin side and the terrace side.

The Intra Mid-Campanian (MC) was mapped as the near top Nise Formation in the lithostratigraphy. The reflection quality is similar to the ES which is low amplitude and discontinuous. To the northern part, the reflection is discontinuity in the Rås Basin. It is recorded at 2-2.5 s TWT in the seismic lines.

The Base Cenozoic (BC) was interpreted as the Top Shetland Group which is a relative continuous strong to intermediate positive reflection throughout the study area. It was mapped at 1-3 s TWT from the Halten Terrace to the Rås Basin. In the northern part of the Helland-Hansen Arch, the reflection goes to less than 2 s TWT. Seven wells all penetrated through the Base Cenozoic. At the Helland-Hansen Arch in the Vøring Basin, the Base Cenozoic is weak in reflection.

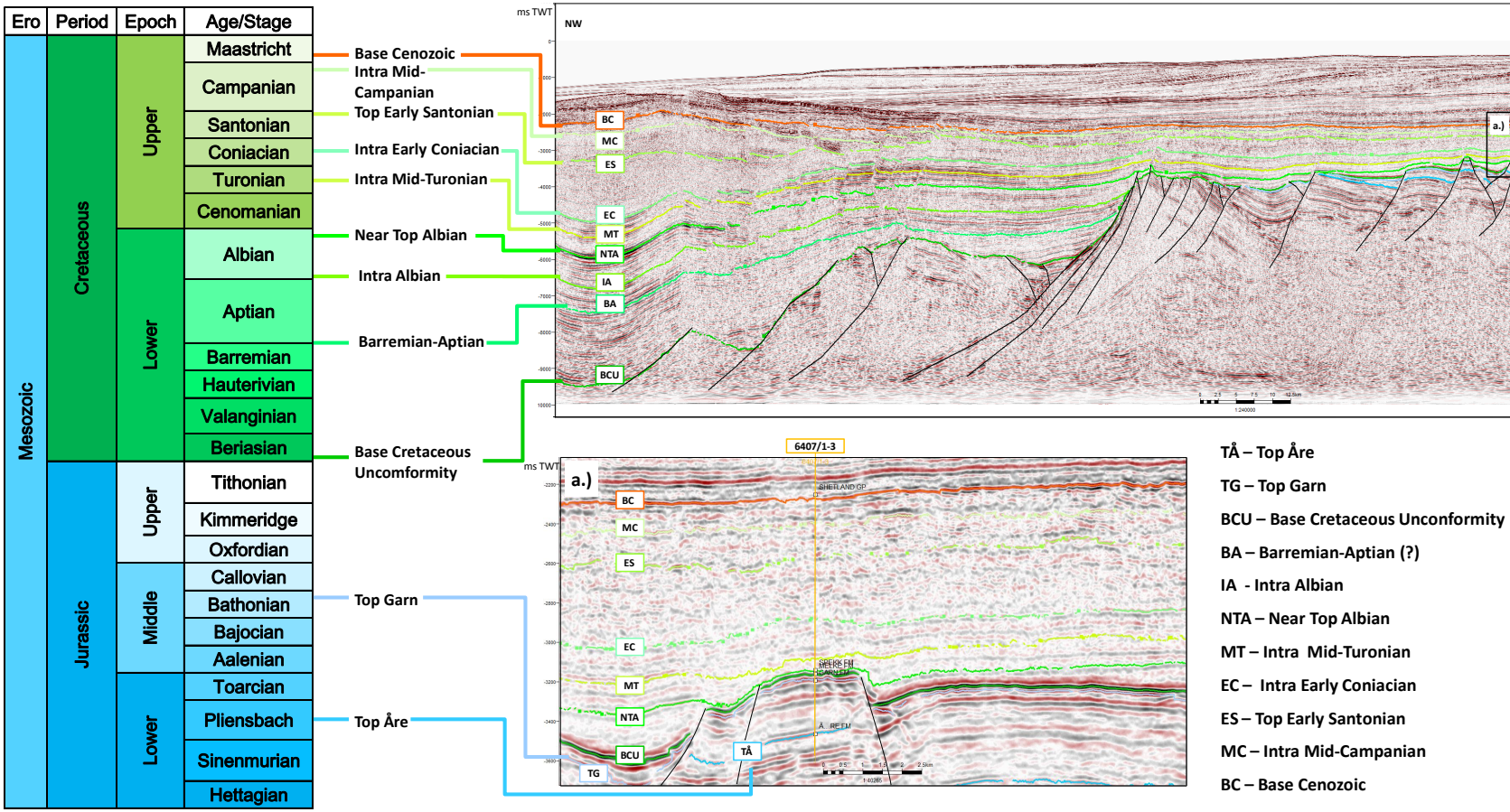

Figure 3.9: Well 6407/1-3 tied with one key profile. Location of well 6407/6-3 can be seen in Figure 3.3. Eleven horizons presented in different colors are tied with the lithostratigraphic column (Figure 3.7). Abbreviations are used for representing different horizons in their corresponding ages/stages.

3.6 BCU Time-structure Map

The Klakk Fault Complex separates the Halten Terrace to the east from the Rås Basin to the west. The fault was generally discussed by Blystad et al. (1995) having N-S strike. In this section, the geometry of the Klakk Fault Complex will be depicted, and the adjacent structural elements of the Klakk Fault Complex will be shown both in the 2D and 3D time-structure maps.

Figure 3.10 demonstrates the time-structure map of the BCU in the 2D window stretches from *c*a. 63°40′N to *c*a. 65°30′N in latitude and from *c*a. 4°40′E to *c*a. 8°10′E in longitude, with an depth-related illustration of the study area. The primary variation of elevation disperses along E-W. In general, the BCU time-structure map shows the topography that high in the east and descends to the west (Figure 3.11).

The shallowest area is found in the far eastern side on the Trøndelag Platform at *c*a. 2 s TWT, and the deepest is located in the deep Rås Basin at west, which reaches the maximum at *c*a. 9 s TWT. From the highest platform area to the second highest area, the Halten Terrace occupied a relative large area and with a slightly dip from *c*a. 3 s TWT at east to *c*a. 4.5 s TWT at west. But along the western margin of the Halten Terrace, elevation time rebounds from *c*a. 4.5 s TWT to *c*a. 3.5 s TWT, especially at the northern part in the orientation of NE-SW. The Klakk Fault Complex divide the study area into two parts, the basin side to the west and the terrace side to the east (Figure 3.11). The sharpest fall takes place along the Klakk Fault Complex, from the Halten Terrace to the sub-terrace, which the elevation time drops to 6-6.5 s TWT. The sub-terraces, from north to south, vary in width. It can be seen simply and directly from the 2D time-structure map of the BCU (Figure 3.10) that three rhomboids are located to the west of the Klakk Fault Complex. The widest rhomboid-shaped sub-terrace is corresponding to the most curvilinear segment of the Klakk Fault Complex at south, the smallest one is in the middle part corresponding to the less curvilinear segment. One phenomenon occurred along the western margin of three rhomboidal sub-terrace, which along the NE-SW orientated margin, similar elevation time rebound also took place. The time elevation rebounded slightly to *c*a. 5 s TWT from 6-6.5 s TWT. The westernmost in the study area comprises the intrabasinal high and ridge (Figure 3.11). Generally, except the two obvious shallower time elevation at the Grip High to the south and the Slettringen Ridge to the north, the basin is deepening towards west until the deepest part in the western side of the Slettringen Ridge. The basin is divided by the two high-elevation ridge and high, forming two sub-basins at the both sides. Between the sub-terrace and the two shallow-time-elevation ridge and high, two roughly NE-SW orientated accommodation zones can be seen clearly at around 7.5 s TWT. The sub-basin at the east of the Slettringen Ridge extends NE-SW to the south, but shift to N-S strike to the north, which shows a similar strike as the Slettringen Ridge from south

to north. Analogously, the sub-basin at the east side of the Grip High displays similar strike as the Grip High, which both of them extend in NE-SW direction.

3.7 Structural Outline of Key Profiles

Based on the strike of the Klakk Fault Complex and its adjoining structures, three segments are divided from south to north and the cross-sectional structural outlines of the segments are illustrated by seven key profiles.

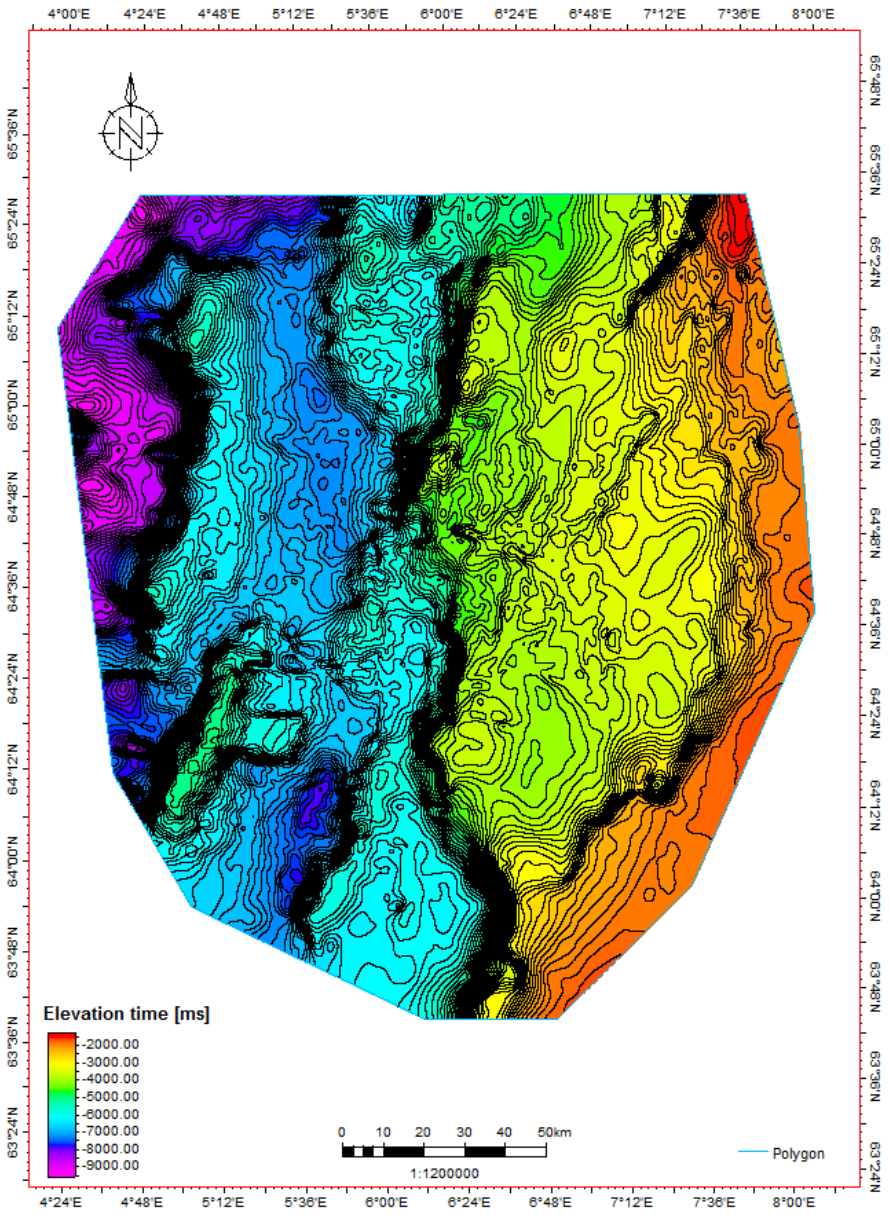

Figure 3.10: 2D time-structure map of the BCU shows the transition from the platform in the east to the deep basin in the west. The Klakk Fault Complex divided the study area into the shallower time elevation terrace and the deeper time elevation basin from east to west. The Klakk Fault Complex orientates in two directions in general: NW-SE and NE-SW.

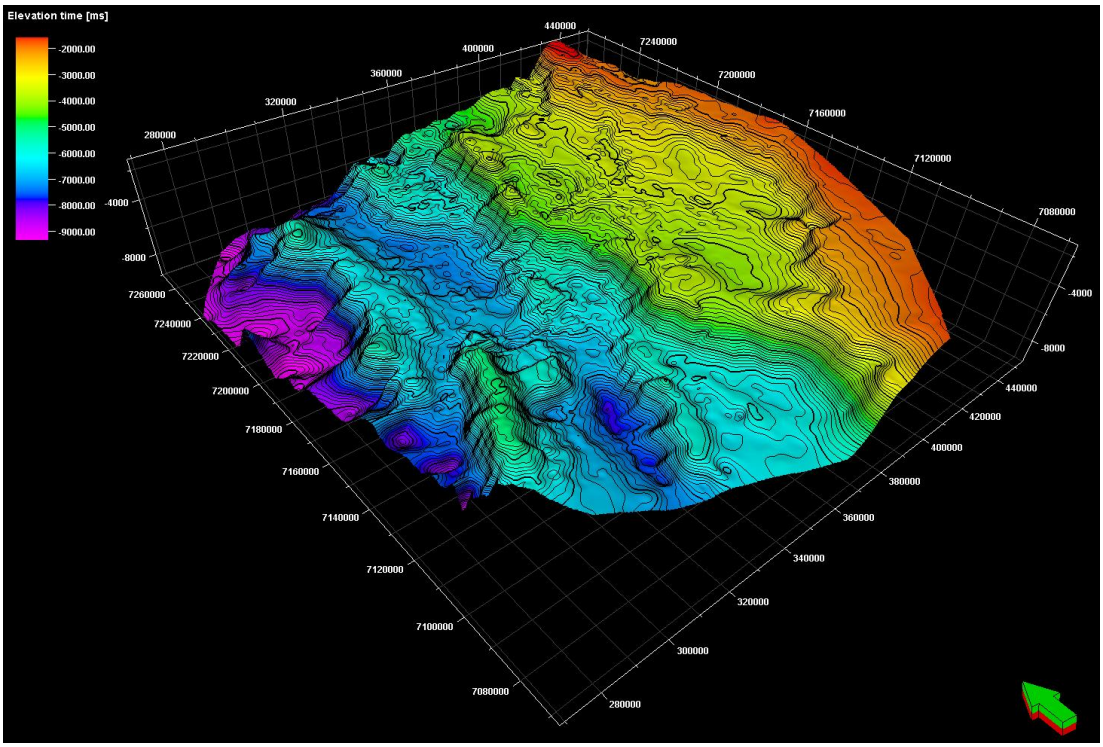

Figure 3.11: 3D time-structure map of the BCU shows a general topography that is high in the east and descends to the west. The whole area appears to a four-step morphology. From highest step to the lowest one are the Trøndelag Platform, Halten Terrace, sub-terrace and the deep Rås Basin. The Klakk Fault Complex divided the study area into two parts, the basin side and the terrace side to the west and east respectively. The Halten Terrace shows a rhomboidal shape and the sub-terrace at the downthrown side of the Klakk Fault Complex display analogous shape as the terrace. To the west the Slettringen Ridge and the Grip High are located in the basin center with a general strike of NE-SW.

The Klakk Fault Complex mainly comprises two strikes: NE-SW and NW-SE, which linked as a continuous N-S fault complex. It terminates at Ytreholmen Fault Zone (*c*a. 65°30′N) to the north and to the south, it extends to the Frøya High (*c*a. 63°5′N) (Blystad et al., 1995). The southern part of the Klakk Fault Complex is not involved in the study. The study mainly focus on the north, from *c*a. 63°40′N in the SE Vøring Basin. Based on the plan view, the fault array of the Klakk Fault Complex is composed of two sets of faults. The predominant displacement took place along the NE-SW orientation. Therefore, the Klakk Fault Complex was divided into three segments (Figure 3.12). Segment I and II constitute two fault strikes, while Segment III only strikes NE-SW. Three segments can be visualized in Figure 3.12 which illustrates Segment I and II as the ideal half-graben geometry in similar polarity. Segment I shows a more curvilinear morphology on map view when compare with Segment II. Furthermore, Segment I extends more in length than Segment II. It also illustrates that Segment I and II are bounded by sub-terraces that displays an obvious rhomboidal geometry.

Each of the segment is represented by two or three seismic profiles (Figure 3.13), and all the profiles are dip lines and oblique lines (Figure 3.4) crossing the Klakk Fault Complex. On account of the ratio between the vertical and horizontal scales in the seismic profile,

real structural outlines are difficult to show in 1:1 cross-section. Therefore, in order to understand the more realistic geometry of the faults on the seismic profiles, one 1:1 cross-section was generated to compare with the 1:5 (vertical scale : horizontal scale). From the Figure 3.14, bordered faults are all portrayed of low angles (< 30°-40°). With depth increasing, however, the two-way-travel time accelerates. The relationship between the real depth and two-way-travel time is not following a linear function but a quadratic formula, or even higher order equation. Therefore, the structural outline in 1:1 cross-section becomes inevitably inaccurate with depth increasing.

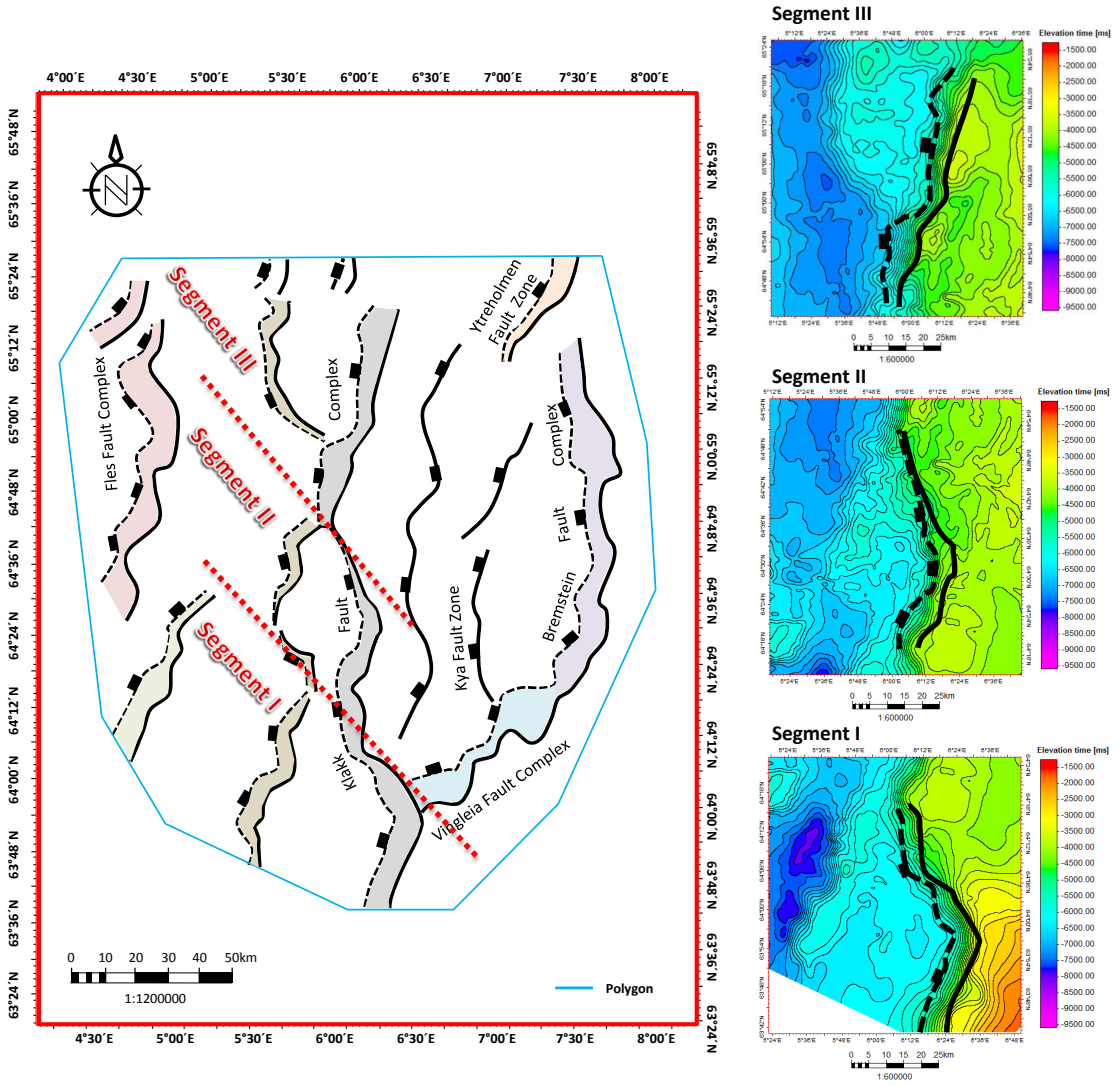

Figure 3.12: Two red dash lines divided the Klakk Fault Complex into three segments. Segment I and II show the ideal half-graben on the plan view, and Segment III strikes NE-SW. Three segments all follow the similar polarity. The fault polygon was drawn based on the time-structure map of the BCU, and other faults in the study area also were drawn by the fault polygons. N-S trending faults on the Halten Terrace were draw based on the fault polygon generated in *Petrel*. Three separated fault segment polygons are exhibited to the right with the time-structure maps underneath.

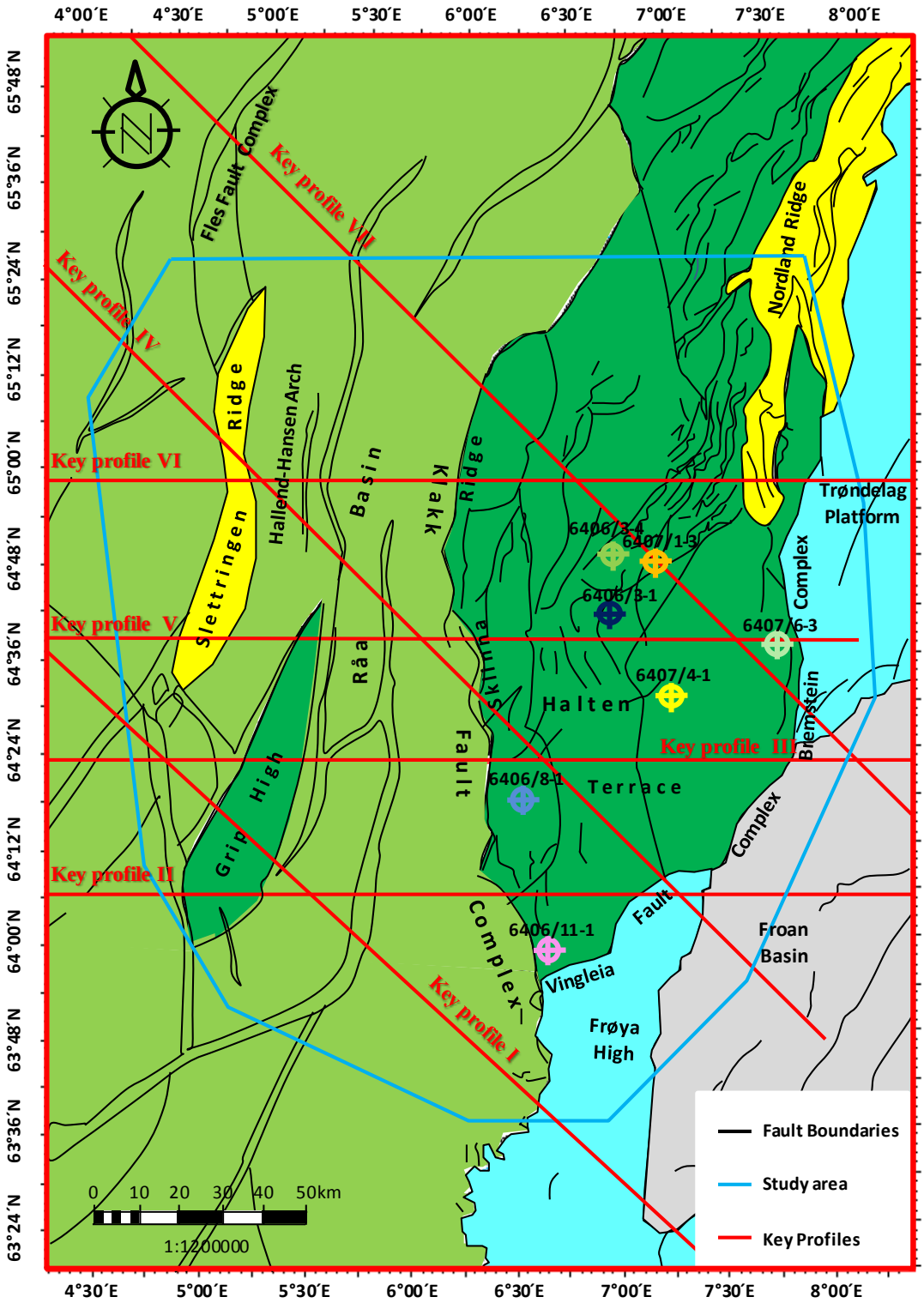

Figure 3.13: Seven key profiles were selected for displaying the cross-sectional morphology of the Klakk Fault Complex in NW-SE and E-W orientations. Key profile V and VII are tied with the exploration wells 6407/6-3 and 6407/1-3 respectively (detail information can be seen in Table 3.1 and Table 3.2). Redrawn from Blystad et al. (1995).

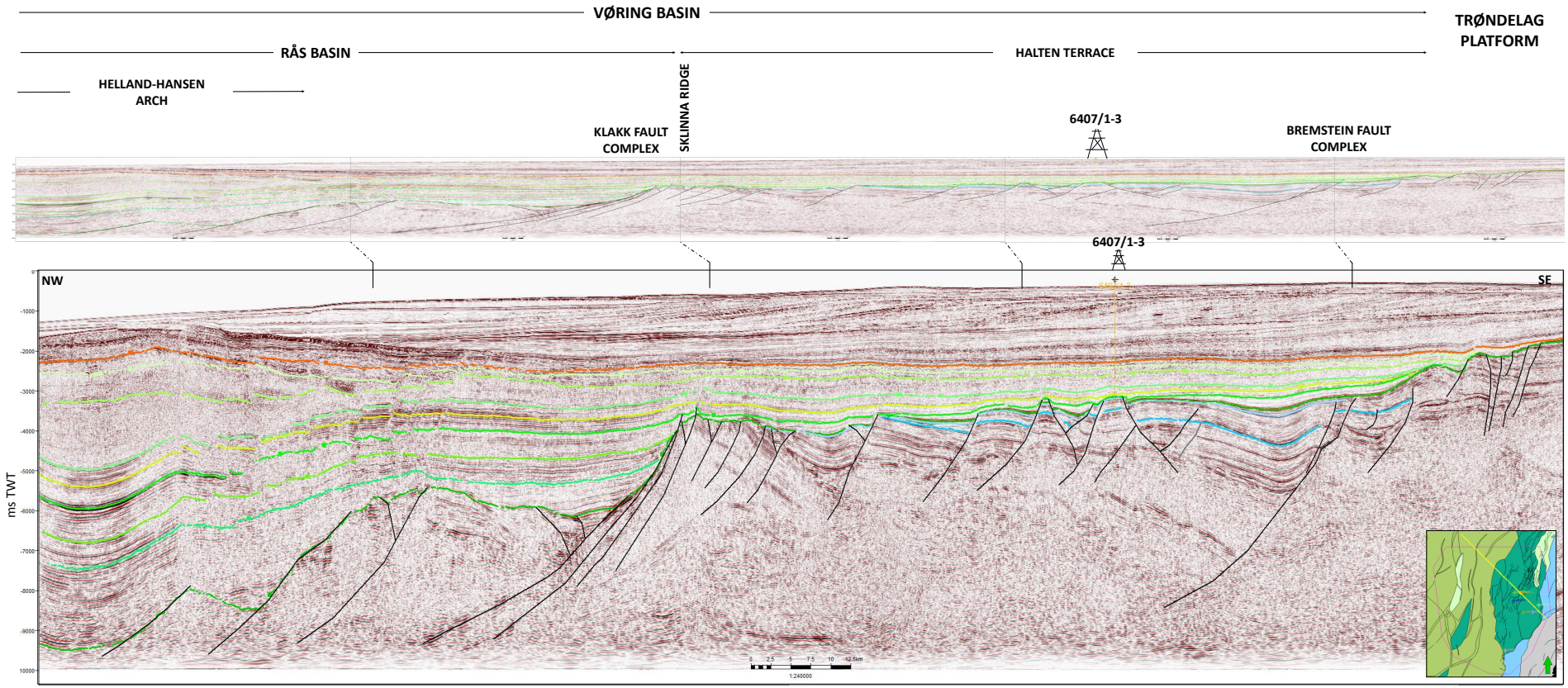

Figure 3.14: The 1:1 and 1:5 (vertical scale : horizontal scale)seismic profiles. The lines in the 1:1 seismic profile (the upper one) are correlated to the lines in the 1:5 seismic profile (the lower one). Structural elements and location of exploration well6407/1-3 are marked on the top. Border faults are visualized as low angle listric faults in this seismic profile.

3.7.1 Segment I

Segment I (Figure 3.12 and Figure 3.15) is located in the southwest Halten Terrace extended to the Frøya High in western-facing polarity. As mentioned in Chapter 3.7, southern part of Segment I will not involved for detail analysis. Cross-sections are demonstrated by Key profiles I and II (Figure 3.15). The NE-SW striking fault segment is represented by Key profile I (Figure 3.16) and NW-SE striking fault segment is represented by Key profile II (Figure 3.17).

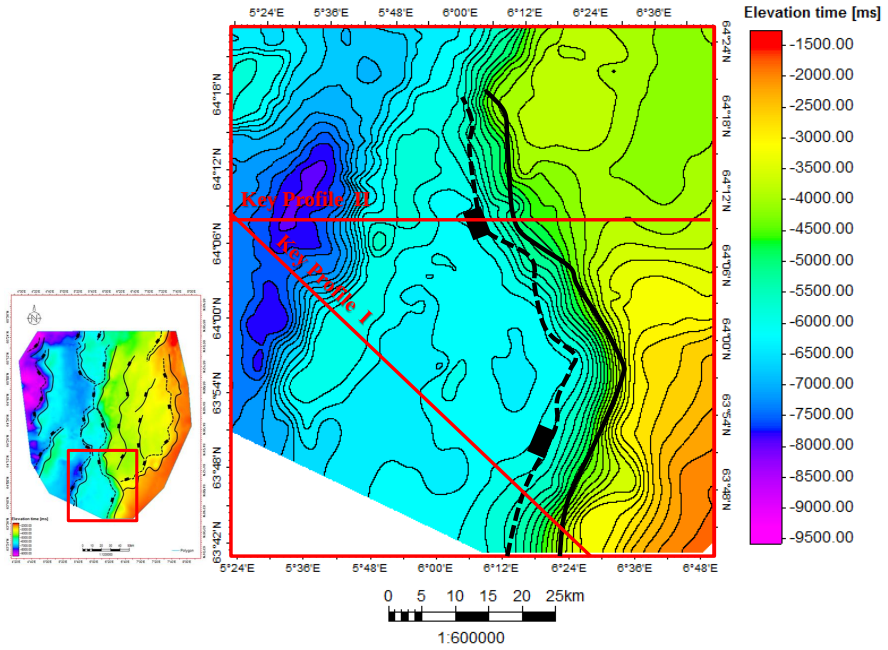

Figure 3.15: Segment I is in the southern part of the Klakk Fault Complex. Fault polygon is based on the time-structure map of BCU. Key Profile I represents the cross-sectional morphology of the NW-SE oriented segment of the Klakk Fault Complex.

Key profile I (Figure 3.16) is the dip line (Figure 3.4) cutting through the Klakk Fault Complex in NE-SW strike, traversing the Frøya High and Rås Basin. The Klakk Fault Complex is dominated by a west-dipping listric fault separating the Frøya High to the east from the Rås Basin to the west. This fault has a relative high angle and a short planar fault locates at east of it. The sub-terrace is constituted by two main tilted huge fault blocks bounding by two listric normal faults. The Grip High which bounded by west-dipping faults at west is suited at west of the sub-terrace. These two shallower structures formed a depocenter in between. The western part of the Grip High is more affected by listric normal faults. The southernmost of the Slettringen Ridge may be at the west of the Grip High, which shows a shallower structure. The western flanks of the normal faults all exhibit an uplift and subjected to the BCU erosion. Some of the fault blocks have a divergent reflections splaying towards the fault planes. The western margin of the sub-terrace were subjected to exposure until the Intra Albian time. The Barremian-Aptian and Intra Albian reflections are slightly tilted towards west and were onlap the fault plane of the Klakk Fault Complex. Sedimentary strata were upwarped on

top of the dip point of the Klakk Fault Complex. In Cretaceous, the sediment successions display relative uniform features, but at the eastern top of the Grip High, the reflections are slightly folded and the onlap displays a rollover geometry. Smaller fold can be seen at the western side of the Grip High. The strongest folded reflections are Barremian-Aptian and the Intra Albian, especially between two tilted fault blocks.

Key profile II (Figure 3.17) illustrates a cross-sectional geometry of Segment I that strikes in NW-SE. The BCU displays a high-amplitude undulation from the Frøya High at east to the Grip High in the Rås Basin at west in the study area. The Klakk Fault Complex is bounding the Halten Terrace at the uplifted western margin. The BCU is displaced slightly by the fault plane, so that, from the Halten Terrace to the Rås Basin, the Klakk Fault Complex has smaller displacement and the dip angle is higher. With the significant fault dip, big uncertainty exists. To the west of the Klakk Fault Complex, a horst structure can be observed with deep erosion on the top. On the graben sides, two depocenters occur. In the deep part of the Rås Basin, the Grip High is bounded by the westward-dipping fault to the west. During the Barremian-Aptian time, the deposition only took place in the west graben of the horst. The Intra Albian horizon is relative flat-lying. The onlaps of the Intra Albian on the Grip High and the Klakk Fault Complex are different from each other. Onlap at the Grip High side is flat towards on the Grip High, while on the Klakk Fault Complex, it shows a normal drag onlap along the fault plane. After the Near Top Albian, sedimentary successions drowned the whole terrace and the basin, and show relative uniform thickness. Horizon Near Top Albian is upwarp at the top of the Klakk Fault Complex. At the terrace area, the deposition in the Cretaceous tilted slightly towards west. After the Intra Mid-Turonian, sediments deposited on the Grip High.

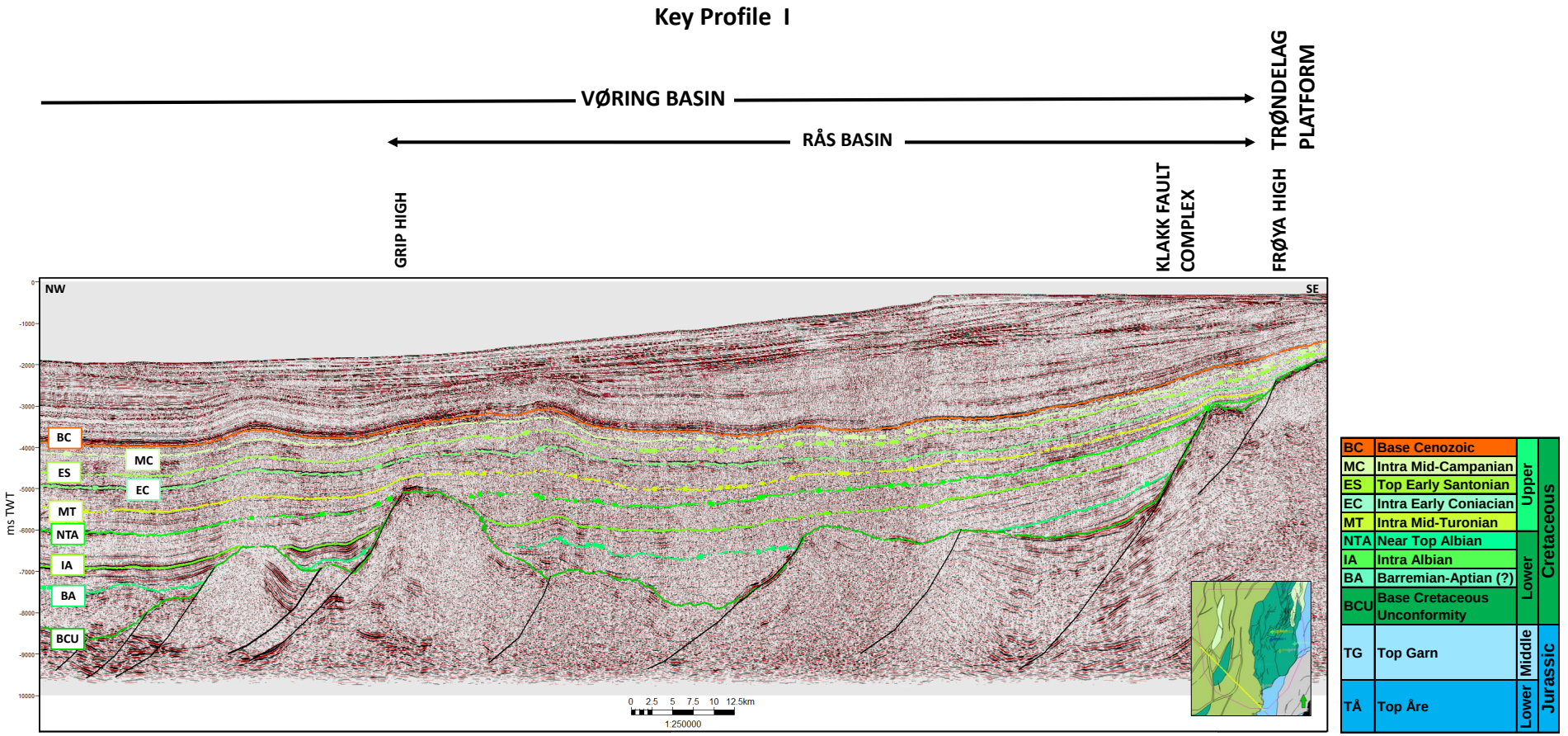

Figure 3.16: Key profile I represents the Segment I with the strike of NE-SW. The structural elements are represented on the top of the seismic line. The yellow line in the map view at the left bottom shows the coverage of the structural elements by Key profile I. The abbreviation of horizons in different ages/stages is shown in the table with corresponding color codes of the interpreted horizons in the seismic profiles.

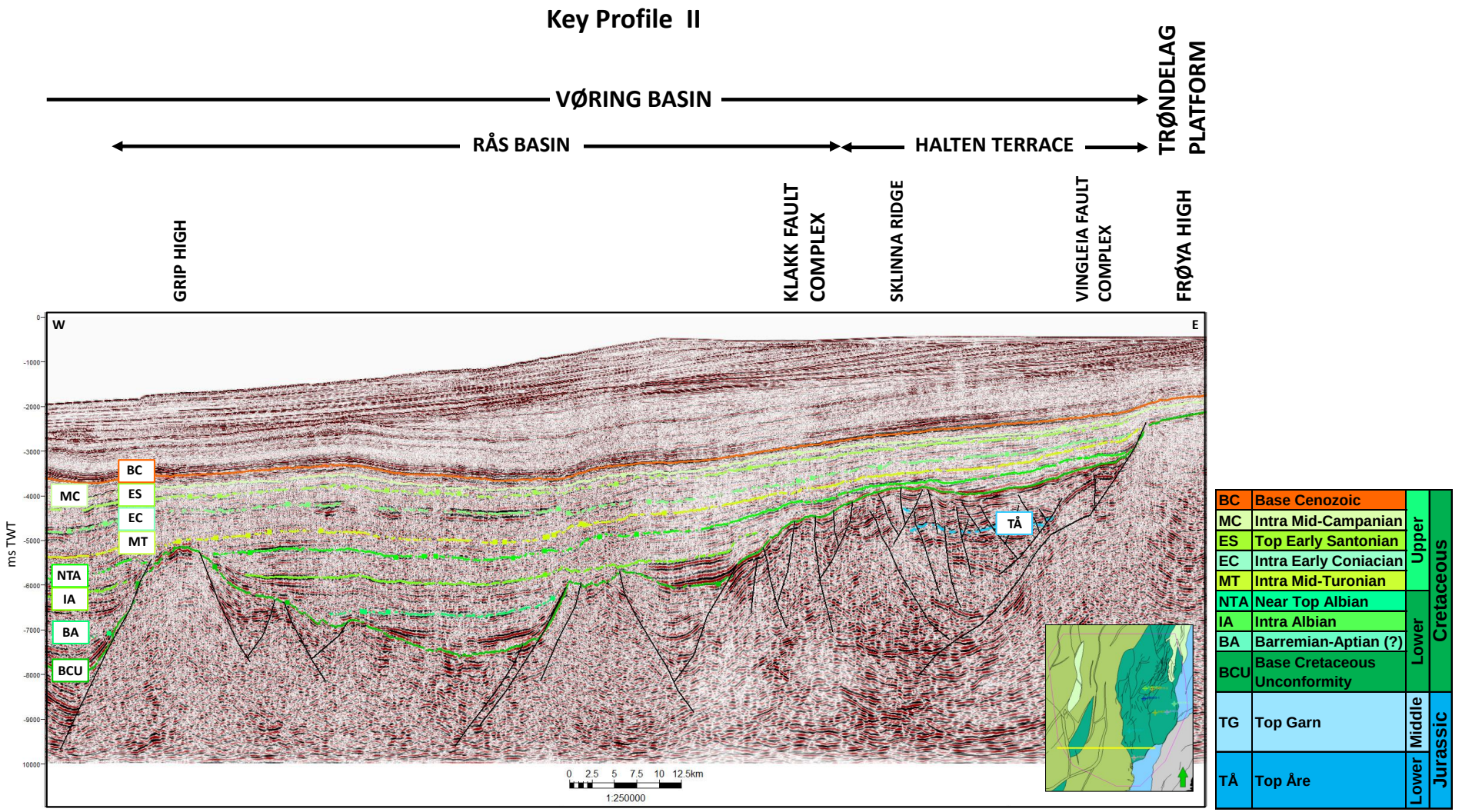

Figure 3.17: Key profile II represents the Segment I with the strike of NW-SE. The structural elements are represented on the top of the seismic line. The yellow line in the map view at the left bottom shows the coverage of the structural elements by Key profile II. The abbreviation of horizons in different ages/stages is shown in the table with corresponding color codes of the interpreted horizons in the seismic profiles.

3.7.2 Segment II

Similar half-graben (Rosendahl et al., 1986) is presented by Segment II, which is portrayed of a predominate arcuate geometry with the western-facing polarity. From the plan view (Figure 3.12), the bisections of Segment II seems mirrored along E-W. Nonetheless, the southern part striking NE-SW shows a low dip listric geometry dipping towards the basin (Figure 3.19), while the northern part of the fault which strikes NW-SE reveals a relative higher dip (Figure 3.20 and Figure 3.21). Figure 3.18 shows that Key profile III (Figure 3.19), Key profile IV (Figure 3.20) and Key profile V (Figure 3.21) represent the cross-sectional morphology of Segment II.

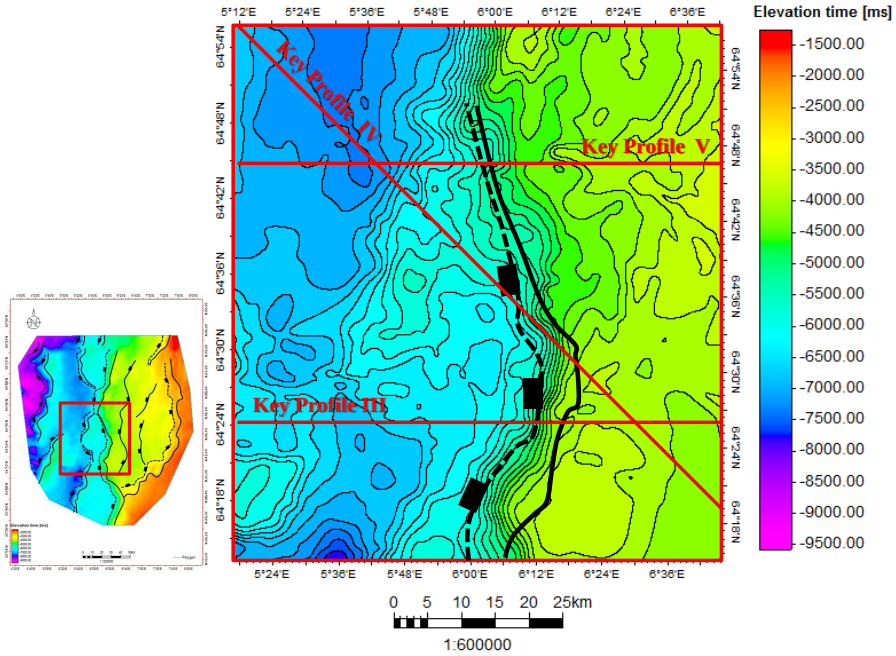

Figure 3.18: Segment II is in the middle part of the Klakk Fault Complex. Fault polygon is based on the time-structure map of BCU. Key profile III represents the cross-sectional morphology of the NE-SW oriented segment of the Klakk Fault Complex, and Key profiles IV and V represent the cross-sectional morphology of the NW-SE oriented segments.

Key profile III (Figure 3.19) illustrates the oblique cross-section (Figure 3.4) of Segment II (Figure 3.13). Due to the difference in strike, profile III has distinct structural pattern from Key profiles IV and V. The profile (Figure 3.19) oriented E-W and demonstrates morphology of the NE-SW striking part of Segment II. From the east to the west, the Klakk Fault Complex separate the Halten Terrace from the Rås Basin, which shows an abruptly transition from the stable terrace to the deep basin. The Klakk Fault Complex is dipping to the basin side with a large displacement. The master fault in the Klakk Fault Complex is a dominated listric normal fault dipping to the basin side, located westernmost among the faults. Faults at the back of the master listric fault are recognized as planar faults with similar dip angles. In the listric normal fault, the change of vertical displacement (throw) is associated with the rotation of the downthrown blocks, and the hade increases with the depth. Footwall uplift took place at the Sklinna

Ridge area, and unconformity exhibited at the top. The BCU primarily displays low-amplitude undulation in Key Profile III. The uplifted Grip High is located at the west of the sub-terrace in the Rås Basin. The faults at the east of the Grip High displays the listric faults with the opposite-dipping antithetic faults. There is no apparent elevation difference separates the Grip High from the sub-terrace in the Rås Basin. Sedimentary successions between Near Top Albian to Top Early Santonian are portrayed of uniform thickness and parallel reflections. On the Halten Terrace. the Lower Cretaceous strata is much thinner than the Upper Cretaceous, while in the basin side, they are generally equivalent in thickness.

The northern part of the Klakk Fault Complex which strikes NW-SE is illustrated by Key Profile IV and V. Key Profile IV (Figure 3.20) shows that, from the terrace to the deep basin, no big displacement caused by the Klakk Fault Complex is evident. The western margin of the Halten Terrace is uplifted. From the Halten Terrace to the Rås Basin, the BCU is flexually transiting. The Klakk Fault Complex is truncated by the BCU on top displaying a flower structure, and tends to join downwards onto a single strand in basement at the west of the Halten Terrac. Due to the poor seismic resolution and the scares of stratigraphic correlation, it does not facilitate mapping the horizons and defining negative or positive structure. The sub-terrace to the western side of the Klakk Fault Complex is bounded by four main listric normal faults dipping NW in a low angle on the western margin. These faults strikes NE-SW which is striking opposite as the NW-SE orientating Klakk Fault Complex (Figure 3.13). The Slettringen Ridge is bounded by three listric normal faults dipping westwards. In the Rås Basin, the Cretaceous sediments were deposited more uniform in thickness in different ages/stages. Horizons younger than Intra Mid-Turonian onlap on the uplifted Sklinna Ridge.

Key Profile V (Figure 3.21) demonstrates similar transition from the terrace side to the basin side. The Klakk Fault Complex bounding the western margin of the Halten Terrace appears as a steeper faults dipping east with the antithetic faults dipping opposite. Due to the poor resolution in the deep part of the seismic lines, the deep extension of the faults remains unclear. A listric normal fault appears at the western side of the Klakk Fault Complex, of which the sub-terrace formed between this fault and the Klakk Fault Complex. Uplift of the western margin of the sub-terrace is exhibited. A depocenter is located between the sub-terrace and the Slettringen Ridge. Several west-dipping, deep-seated listric normal faults in the Rås Basin formed the tilted fault blocks. Large wedge-shaped syn-rift deposits are clear shown in the seismic line. The reflections are divergent towards the fault plane, especially towards the Klakk Fault Complex. Sediments younger than the Near Top Albian are thicker than the older deposition in the Cretaceous in the Rås Basin.

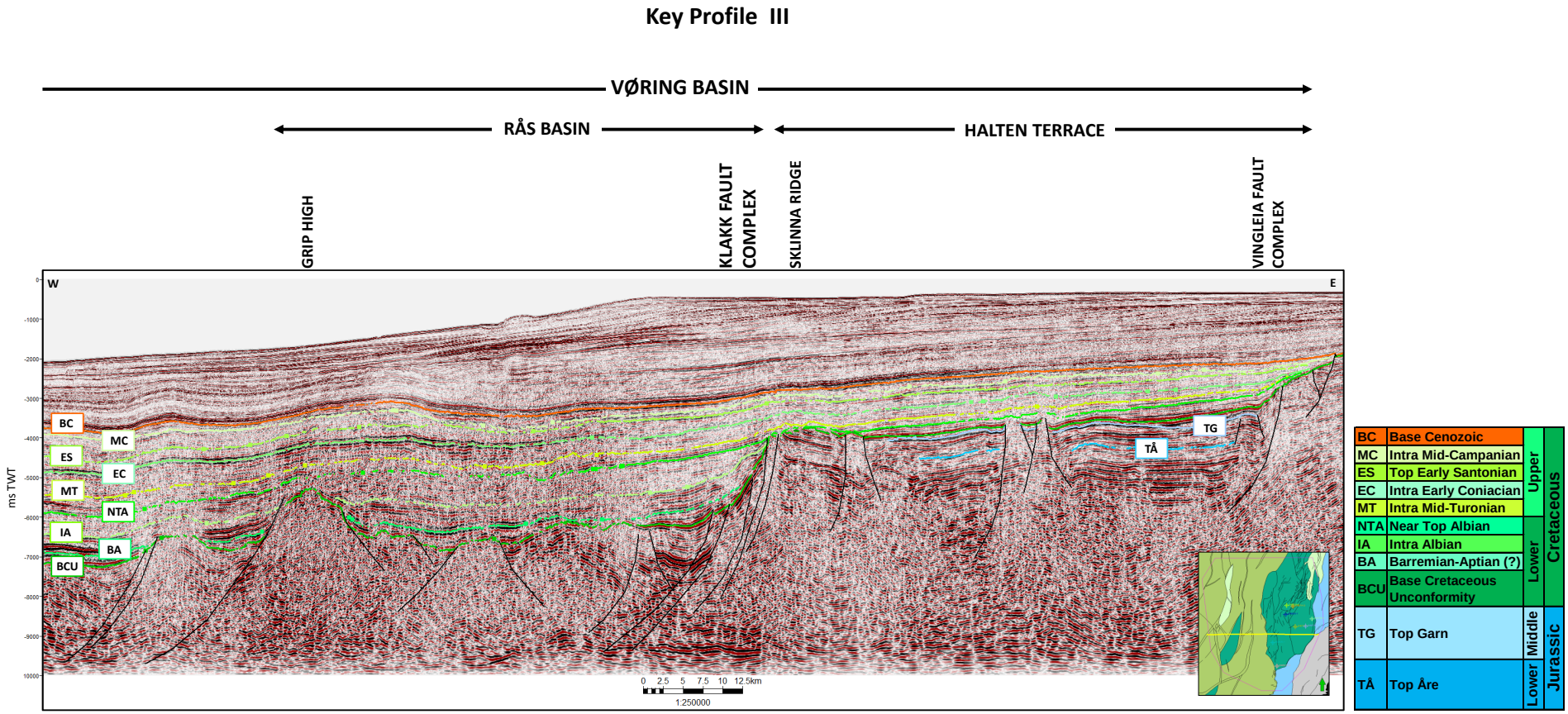

Figure 3.19: Key profile III represents the Segment II with the strike of NE-SW. The structural elements are represented on the top of the seismic line. The yellow line in the map view at the left bottom shows the coverage of the structural elements by Key profile III. The abbreviation of horizons in different ages/stages is shown in the table with corresponding color codes of the interpreted horizons in the seismic profiles.

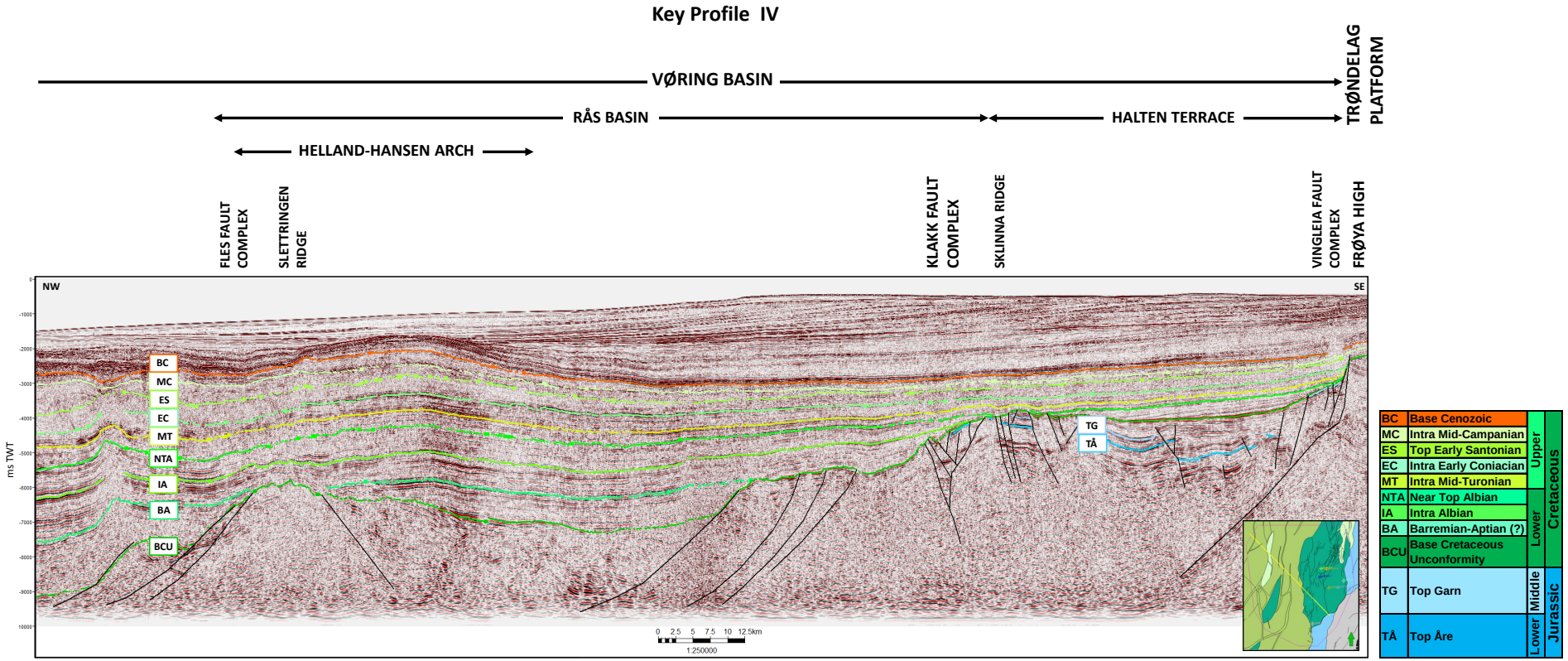

Figure 3.20: Key profile IV represents the Segment II with the strike of NW-SE. The structural elements are represented on the top of the seismic line. The yellow line in the map view at the left bottom shows the coverage of the structural elements by Key profile IV. The abbreviation of horizons in different ages/stages is shown in the table with corresponding color codes of the interpreted horizons in the seismic profiles.

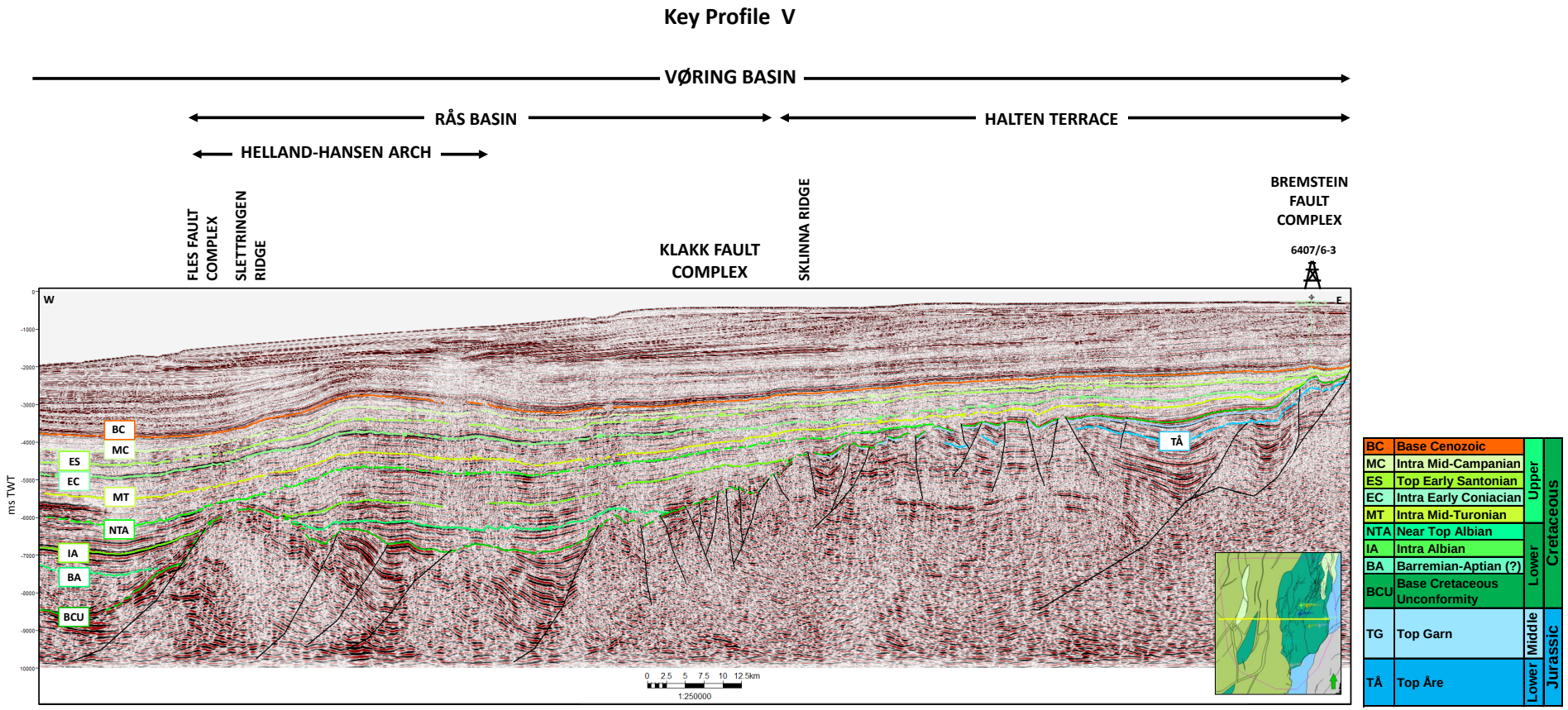

Figure 3.21: Key profile V represents the Segment II with the strike of NW-SE. The structural elements are represented on the top of the seismic line. The yellow line in the map view at the left bottom shows the coverage of the structural elements by Key profile V. The abbreviation of horizons in different ages/stages is shown in the table with corresponding color codes of the interpreted horizons in the seismic profiles.

3.7.3 Segment III

Segment III is striking NE-SW without typical ideal half-graben geometry (Rosendahl et al., 1986) in the map view (Figure 3.12), which is distinct from Segments I and II. The Klakk Fault Complex dips towards NW, bordered along the Sklinna Ridge at west with biggest throw when compare to other faults in the study area. Key Profile VI and VII illustrate the cross-sections of the Segment III (Figure 3.22, Figure 3.24 and Figure 3.25). Two key profiles cross the Klakk Fault Complex and have the intersection on the Halten Terrace.

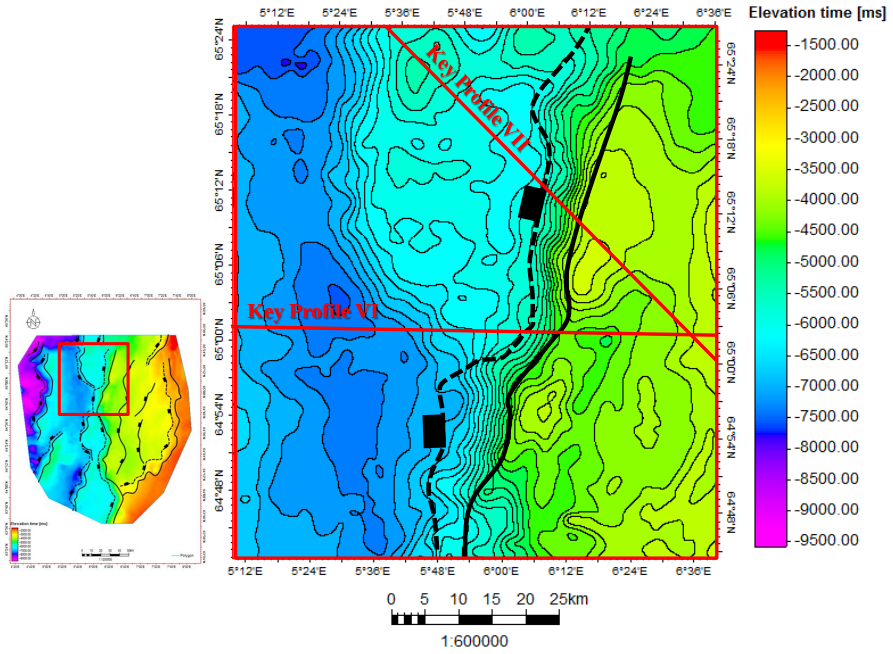

Figure 3.22: Segment III is in the northern part of the Klakk Fault Complex. Fault polygon is based on the time-structure map of BCU. Key Profile VI and VII represent the cross-sectional morphology of the NE-SW oriented segment of the Klakk Fault Complex.

Key profile VI (Figure 3.24) presents Segment III in strike E-W as the oblique line (Figure 3.4). On the Halten Terrace, faults are characterized by listric faults dipping to the west with several antithetic faults in the opposite dip. The Klakk Fault Complex separates the terrace from the basin, which is portrayed by a listric normal fault as the outer master fault. This westernmost NW-dipping listric master fault has a lower dip angle and is deep-seated. Faults at the eastern side of the listric master fault display a relative more planar character. Footwall uplift is evident at the western margin of the Halten Terrace and it is truncated by the BCU. Huge displacement occurred from the terrace to the basin, which the discrepancy of elevation time can reach more than 2 s TWT. On the terrace side, western margin gives apparent horst structure which was experienced erosion of the whole Jurassic sediments. Along the downthrown side of the Klakk Fault Complex, tilted faulted-blocks build a sub-terrace from the Halten Terrace to the Rås Basin. The planar antithetic faults are cut by the outer master fault system. At the downthrown side, tilted fault blocks in the Rås Basin are rotated dramatically

to the center of the Rås Basin. The sub-terrace is bounding by two deep-seated, west-dipping listric faults to the west. The Slettringen Ridge is comprised of the uplifted shoulder of a huge tilted fault block. The syn-rift deposits are identified by clear wedge-shaped seismic reflections. On the terrace area, the BCU is tilted towards west in a range of 2.5-4 s TWT. Cretaceous reflections in the basin area can be found onlaps on both fault scarps and truncation. The Slettringen Ridge was not buried by sediments, at least, in the Barremian-Aptian time. On the Klakk Fault Complex, horizon of the Barremian-Aptian shows an normal drag onlapping the fault zone. Similarly, reflection of Intra Albian also has this appearance.

Key profile VII (Figure 3.25) is a NW-SE orientated seismic line that covers the entire Halten Terrace and extends to the Rås Basin. It crosses Segment III as a dip line (Figure 3.4). Well 6407/1-3 was tied to this profile on the Halten Terrace. The Klakk Fault Complex ranges from *c*a. 4 s to 9.5 s TWT in the cross-section, which shows a low-angle listric master normal fault dipping towards NW at the westernmost side of the Klakk Fault Complex. Eastwards, faults are portrayed of relative more planar character. The footwall of the Klakk Fault Complex, tilted fault blocks are dramatically eroded in upper Jurassic formations. The truncation cut through the whole Jurassic formations at the uplifted shoulder of the footwall severely. The hangingwall fault blocks tilted towards the Klakk Fault Complex in the Rås Basin, and the upper Jurassic deposits display a typical wedge shape, divergent seismic lines.

Faults in the tilted fault blocks at west of the Klakk Fault Complex show a listric geometry, small antithetic faults dipping opposite are existed. Large tilted fault block formed the Rås Basin to the western side of the Klakk Fault Complex as the hangingwall. These tilted fault blocks formed a sub-terrace between the stable Halten Terrace and the basin center. The BCU on the terrace, from SE to NW, shows a gentle dip towards NW, which consequently have a range in TWT from 3 s to 4 s. On the Sklinna Ridge, the fault block displays as a narrow saddle riding on the westernmost margin of the Halten Terrace.

In the basin side, the BCU varies contrarily, which shows a dip towards SE. From the sub-terrace to the deep Rås Basin, a small tilted fault block against the sub-terrace below 8 s TWT with the same dipping of the BCU. Here, the deepest depocenter of the basin generated. The huge thickness of Cretaceous sediments in the basin with a time-thickness more than 7 s TWT. Cretaceous deposited packages thins towards the Klakk Fault Complex. Onlaps were found on the fault scarps both on the terrace and basin sides. Analogically, these onlaps are characterized by normal drag along the Klakk Fault Complex.

In the deepest basin center of the Vøring Basin, the reflections deeper than the horizon Top Early Santonian and shallower than it in the Cretaceous show variations and subsequently affected the configuration of the sedimentary strata in between. From BCU

to Early Coniancian, these six reflections and the infill packages show a resemblance of the configuration of the basin floor. A very thick sedimentary strata exists between the Early Coniancian and Top Early Santonian, and Top Early Santonian is released reflecting basin floor configuration. Reflections and sedimentation pattern shallower than Top Early Santonian tend to be upwarp.

A zoom-in of the Klakk Fault Complex in Key profile VII (Figure 3.23) illustrates that the Klakk Fault Complex extended into the Near Top Albian, the tip points made the horizon upwarped. At the deep part around 6-10 s TWT underneath the Klakk Fault Complex, an middle amplitude reflection is clearly visualized. This reflection is characterized of a NW-dipping low angle undulated band. The Klakk Fault Complex seated on this reflection and merged into this it.

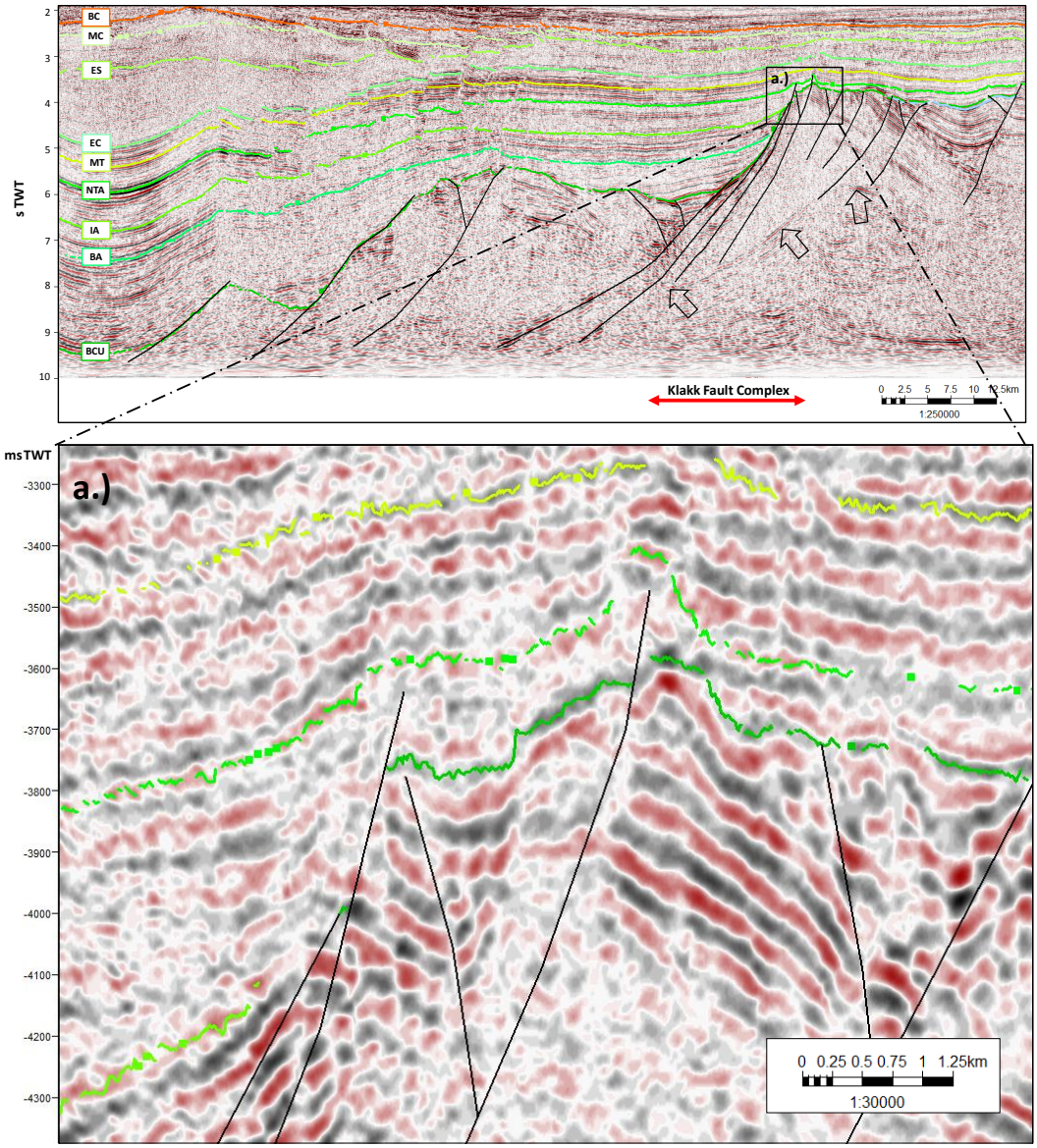

Figure 3.23: Zoom-in of the Klakk Fault Complex in Key profile VII, the red arrow indicates the Klakk Fault Complex area. Arrows show the underlain low angle undulated band. Area a.) is amplified to illustrate the tip points under the Near Top Albian.

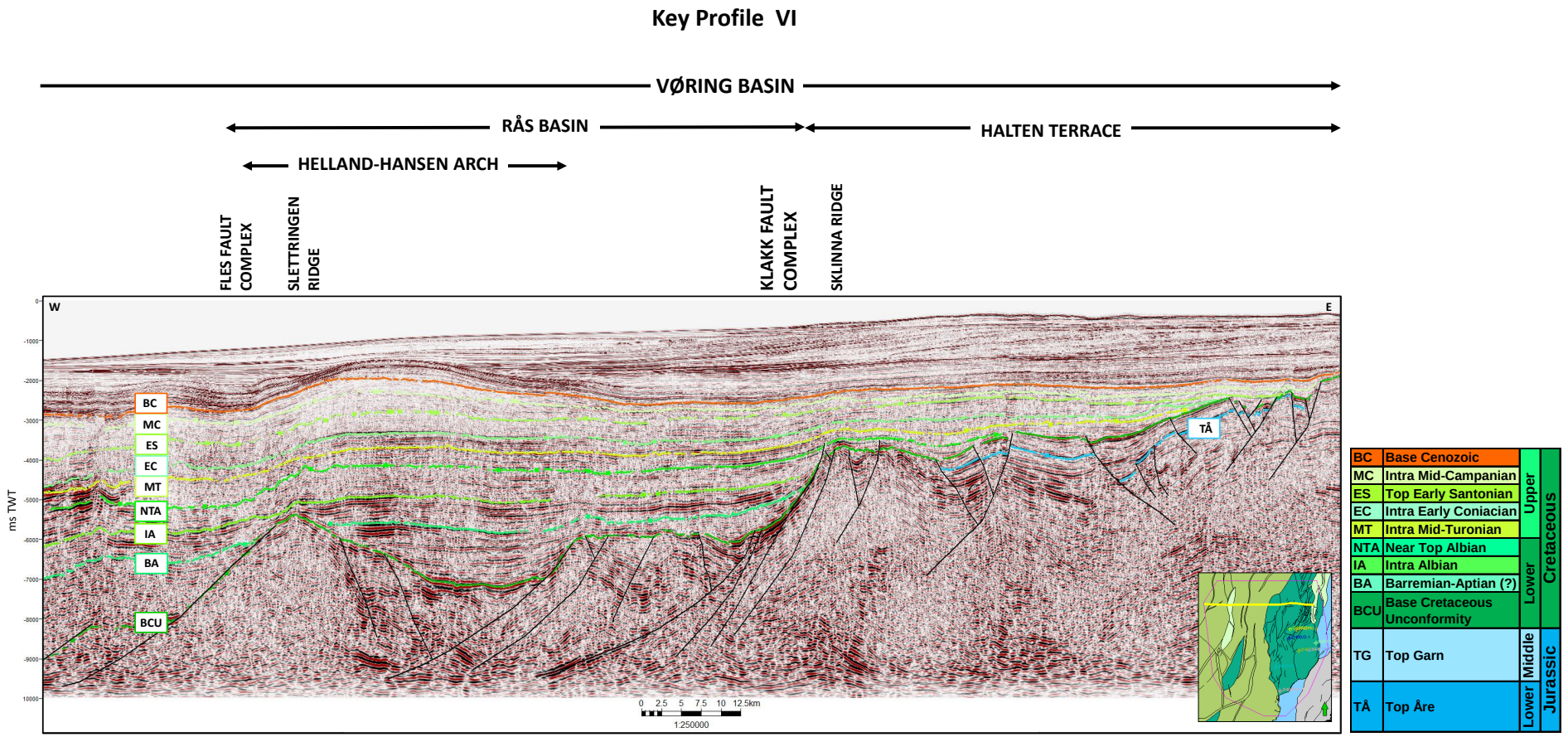

Figure 3.24: Key profile VI represents the Segment III with the strike of NW-SE. The structural elements are represented on the top of the seismic line. The yellow line in the map view at the left bottom shows the coverage of the structural elements by Key profile VI. The abbreviation of horizons in different ages/stages is shown in the table with corresponding color codes of the interpreted horizons in the seismic profiles.

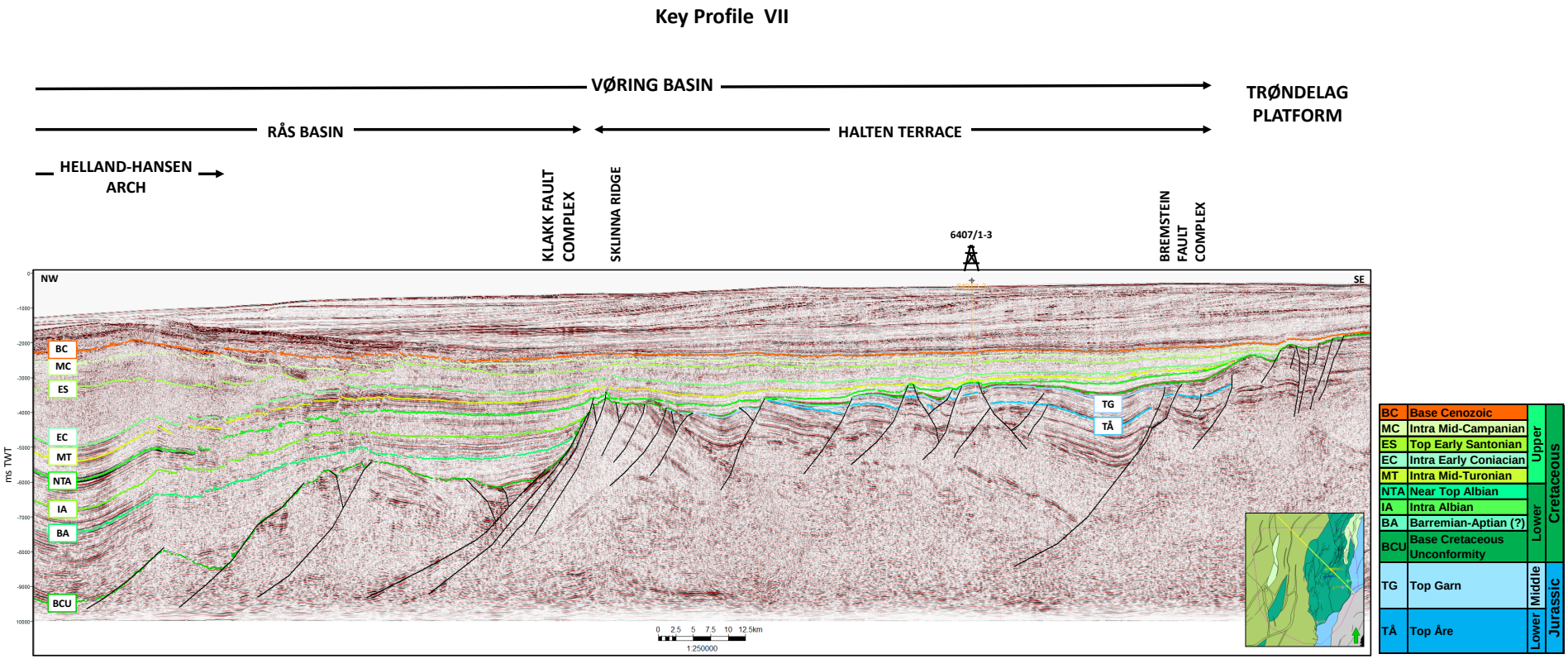

Figure 3.25: Key profile VII represents the Segment III with the strike of NW-SE. The structural elements are represented on the top of the seismic line. The yellow line in the map view at the left bottom shows the coverage of the structural elements by Key profile VII. The abbreviation of horizons in different ages/stages is shown in the table with corresponding color codes of the interpreted horizons in the seismic profiles.

3.7.4 Outline of the Klakk Fault Complex

General description of the key profiles shows that the Klakk Fault Complex not only varies from segment to segment, but also intrinsically differentiates in two strikes in the same segment. Two predominate geometries can be observed in the Klakk Fault Complex. In the NE-SW orientation, a low-angle master listric normal fault exists at the westernmost with several planar faults at the eastern side of it. The master fault is characterized by an uplifted footwall with an eroded top and a wedge-shaped syn-rift sediment package in the hangingwall. Faults all have a western-facing polarity. The Rås Basin is the result of down-to-the-basin faulting along the Klakk Fault Complex in this strike. Cretaceous reflections onlap along the fault plane being portrayed of normal drag. The northernmost part of the Klakk Fault Complex in this strike cut though the lower Albian sedimentary sequence and ceased as the tip points at Near Top Albian.

In the NE-SW strike, the Klakk Fault Complex displays as several high dip-angle faults with the antithetic faults. The faults displaced slightly and the major faults have an eastern-facing polarity. One flower structure is exhibited along the transition belt from the stable terrace to the deep basin. All faults are cut by the BCU on top. From the Halten Terrace to the Rås Basin, therefore, the BCU flexual morphology dominates this transition instead of the huge displaced fault plane. Along the NW-SE strike, poor resolution of the seismic lines leads to uncertainties of the fault interpretation.

3.8 Time-thickness Maps

Time-structure map of the BCU was already introduced in Chapter 3.6, so in this section, eight time-thickness maps were generated to show the post-rift depositional geometry and for purpose of finding evidence of fault reactivation during the Cretaceous time. Time-thickness maps with the overall description will be performed with the fault polygon based on the BCU time-structure map. As mentioned in Chapter 3.4 that BCU to Barremian-Aptian time-thickness map and Barremian-Aptian to Intra Albian time-thickness map on the Halten Terrace have no reference value. Therefore, the main description will focus on the basin side. The structural elements can be found in Figure 3.13.

3.8.1 BCU to Barremian-Aptian

The thickness between BCU to Barremian-Aptian in Figure 3.26 represents the depositions situation at the beginning of the early Cretaceous. The study area was divided by the Klakk Fault Complex into two parts which are the Rås Basin and the Halten Terrace

with the surrounding Trøndelag Platform and the Frøya High. Thickest deposition took place at northwest of the Slettringen Ridge which reaches a time thickness of 2.7 s TWT. Key profile IV Figure 3.20 and VI (Figure 3.24) also show similar large time thickness on the western side of the Fles Fault Complex. No deposition took place at the eastern part where the Halten Terrace, Trøndelag Platform and the Frøya High occupied. It can be observed that along the fault escarpment of the Klakk Fault Complex, the first deposition occurred in the Cretaceous time onlaps there. The three sub-terrace were not all buried at this time, only the northernmost one (Key profile VI in Figure 3.24 and VII in Figure 3.25) fully covered by the Barremian-Aptian sediments. The two southern sub-terrace show a similar deposition situation which no deposition took place along the NE-SW striking western margin during this time. Same result is illustrated in the Key profile I (Figure 3.16) and IV (Figure 3.20). In contrast, thicker sedimentary strata with time-thickness of *c*a. 0.9 s TWT accompanied with the NE-SW striking escarpment of the Klakk Fault Complex to the east, especially can be seen clearly in Key profile I (Figure 3.16). Meanwhile, the thickness of the whole sedimentary strata on the sub-terraces increases northwards.

Considerable deposition took place between the sub-terrace and the Grip High and the Slettringen Ridge. Depocenters existed along the fault escarpments of the faults bounding the sub-terraces on the west. Time-thickness reaches 1.2-1.5 s TWT at the hangingwall side, this also shows in Key profiles I (Figure 3.16), II (Figure 3.17), VI (Figure 3.24) and VII (Figure 3.25). Thickness has a gradual decline until reaching 0 s TWT at the Grip High and the Slettringen Ridge to the west. The northern part of the depocenter also shows a gradient changing on thickness from south to north. The southern part (north of the Grip High) only has less than 0.3 s TWT, while the northern part has sedimentary strata of 1.5 s TWT time-thickness. Therefore, a clear depositional trend is following the orientation of NW-SE.

The Grip High and primarily southern part of the Slettringen Ridge were not buried during this time. This shows the same result as all key profiles covered the Slettringen Ridge (Figure 3.16, Figure 3.17, Figure 3.19, Figure 3.20, Figure 3.21 and Figure 3.24). The inflection points of the faults bounding to the west of the Slettringen Ridge were still exposed at this time. Northwest of the Slettringen Ridge, more than 1.8 s TWT time-thickness sediments filled this area.

Generally, the whole area was more buried in the north than in the south. The NE-SW oriented segments in the Klakk Fault Complex accumulated more sediments. The same orientation, the west margin of the sub-terrace exposed in the southern part and less sediments deposited in the northern part. The Grip High was exposed during Barremian-Aptian time.

3.8.2 Barremian-Aptian to Intra Albian

Time-thickness of Barremian-Aptian to Intra Albian in Figure 3.26, in general, is thinner than in BCU to Barremian-Aptian. Same observation are found in key profiles (Figure 3.16, Figure 3.20, Figure 3.21, Figure 3.24 and Figure 3.25).

The largest depocenter during the Albian time occurred on the sub-terrace instead of the western side of the sub-terrace in Barremian-Aptian. More than 0.9 s TWT time-thick sediments accumulated on the southernmost sub-terrace at the scarp of the Klakk Fault Complex in orientation of NE-SW. Correspondingly, northwest margin deposited not more than 0.15 s TWT time-thick sediments. This is found also in Key profile I (Figure 3.16). Same situation can be observed in the middle sub-terrace. The northernmost sub-terrace was laterally buried by sediments in a relative uniform thickness with around 0.5-0.6 s TWT. Overall, the thickness of the whole sedimentary strata on sub-terrace is descendant northwards.

Most part of the Slettringen Ridge was buried during this time (Figure 3.20), except the southern ridge (Figure 3.24). The Grip High was still exposed during this time, which can be found in the key profiles (Figure 3.16, Figure 3.17 and Figure 3.19). Sedimentary strata with a time-thickness of 0.75-0.9 s TWT accumulated in the area between the sub-terrace and the Grip High, the Slettringen Ridge.

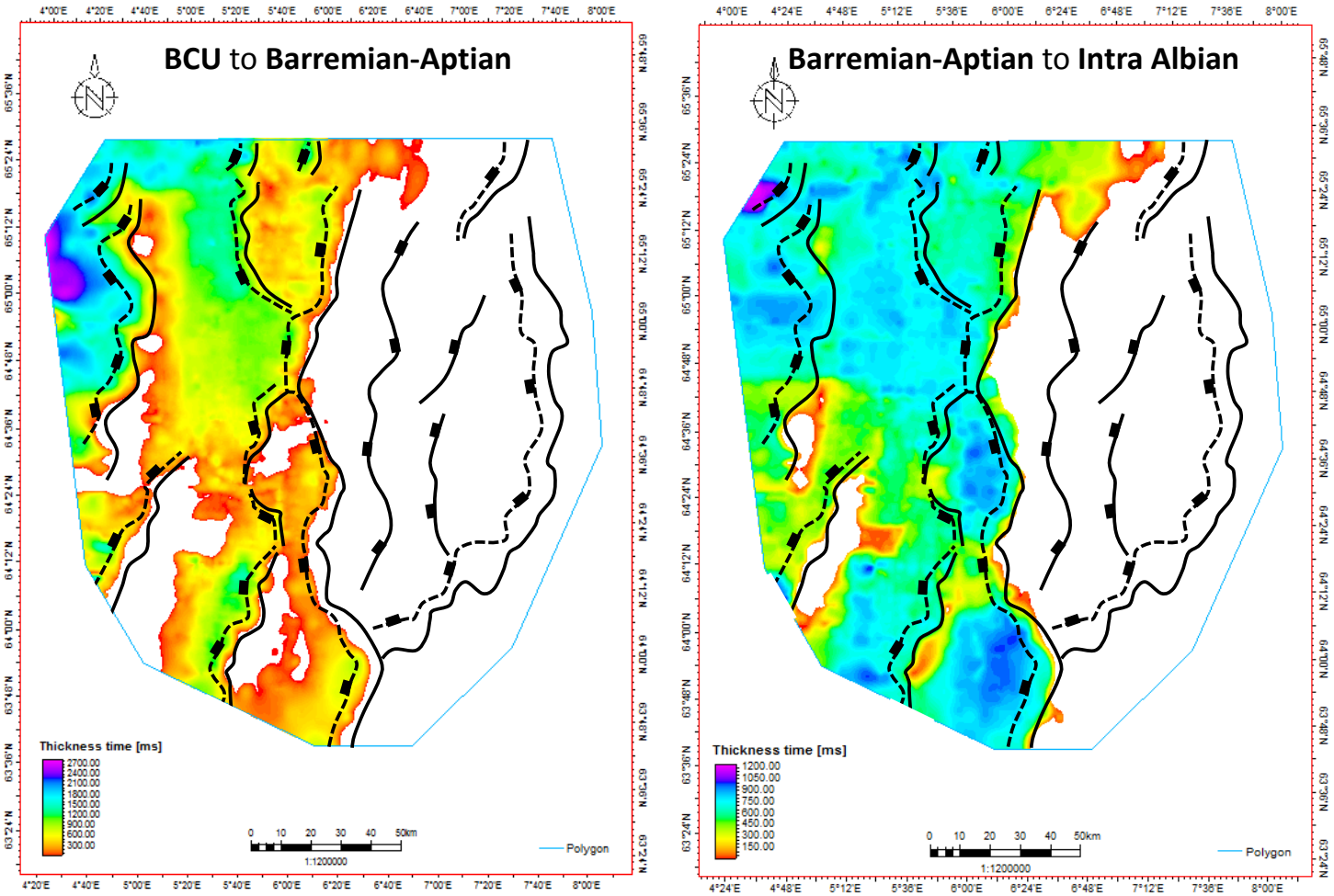

Figure 3.26: Time-thickness maps of BCU to Barremian-Aptian to the left, which shows that no deposition took place at the eastern part of the study area. Thickness map of Barremian-Aptian to Intra Albian to the right shows that the main depocenter occurred along the NE-SW orientated escarpment of the Klakk Fault Complex. Detail description can be seen in the text.

3.8.3 Intra Albian to Near Top Albian

Thickness map of Intra Albian to Near Top Albian reveals the deposition situation at the late Early Cretaceous time (Figure 3.27, left). Whole sedimentary strata is even thinner than Barremian-Aptian to Intra Albian (Figure 3.26, right). The Halten Terrace was subjected to subsidence, which the whole area was almost buried with exceptional area in the southwest and northeast. The Sklinna Ridge at the western margin of the Halten Terrace experienced exposure on some area at north and south. The average time-thickness is approximate 0.3 s TWT on the Halten Terrace. Due to the influence of the NE-SW oriented faults, the thickness can reach 0.45 s TWT at the scarps of these faults.

The three sub-terrace were all covered by the sediments, and nonuniform succession from south to north can be observed on the time-thickness map. In the south, time-thickness ranges from 0.3 s TWT to 0.45 s TWT, while in the north, more than 0.6 s TWT time-thickness strata accumulated locally. Shift of the depocenter happened during this time. Thickest deposition took place between the middle sub-terrace and the south Slettringen Ridge, in an orientation of NW-SE. Here, the time-thickness reaches more than 0.9 s TWT. In key profiles (Figure 3.16, Figure 3.20, Figure 3.21, Figure 3.24 and Figure 3.25) sedimentary strata between Intra Albian and Near Top Albian varies laterally in thickness, it appears that more subsidence took place far away in the west of the sub-terrace. During this time, the Slettringen Ridge was totally covered by sediments, but the Grip High remained exposed.

3.8.4 Near Top Albian to Intra Mid-Turonian

The right figure in Figure 3.27 displays the subsidence from Near Top Albian to Intra Mid-Turonian. The transition from the Lower Cretaceous and Upper Cretaceous occurred in this succession. As seen from the thickness map, the whole area was buried except the east bounding platform and high. Time-thickness of sediments on the Halten Terrace is descendant eastwards, but the average can reach 0.2 s TWT. The northwest margin deposited thicker which is *c*a. 0.3 s TWT in time-thickness.

During this time, no obvious gradient change of the strata thickness can be seen on the sub-terrace. The southernmost one has a time-thickness of 0.4 s TWT, and the northernmost one is 0.36 s TWT in time-thickness. The middle sub-terrace shows a relative weaker subsidence with a time-thickness of 0.24 s TWT. Nevertheless, no big discrepancy of subsidence on the sub-terrace existed. Until the Turonian time, the Grip High was totally buried by the sediments. Relatively, sedimentary strata deposited in a relative uniform thickness in the Rås Basin during this time.

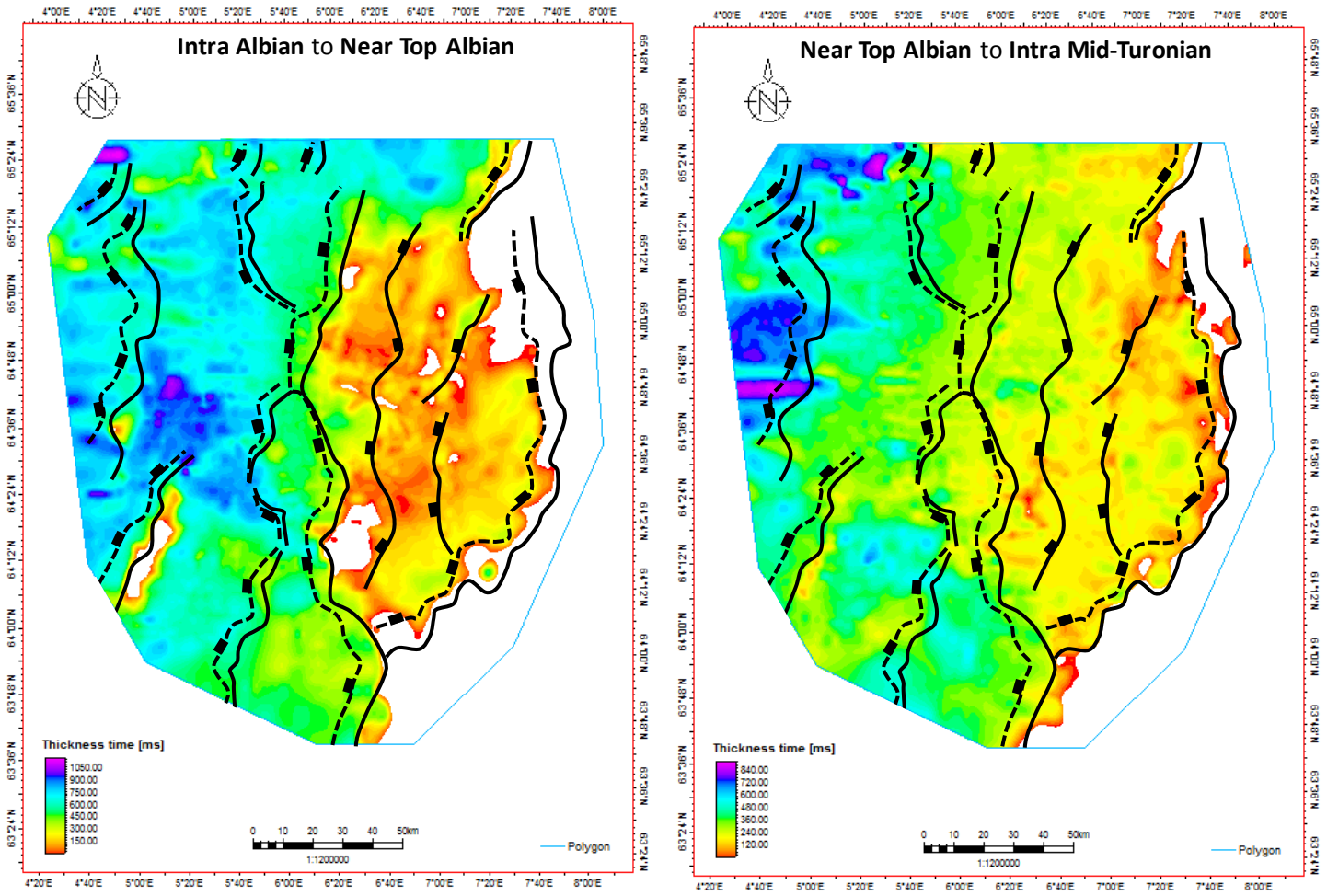

Figure 3.27: Time-thickness maps of Intra Albian to Near Top Albian to the left, which shows that the average time-thickness is approximate 0.3 s TWT on the Halten Terrace and sub-terraces were all covered by the sediments with a gradient changing on thickness from south to north. Thickness map of Near Top Albian to Intra Mid-Turonian to the right shows that the thickness of sediments on the Halten Terrace is descendant eastwards, but the average can reach 0.2 s TWT. Detail description can be seen in the text.

3.8.5 Intra Mid-Turonian to Intra Early Coniacian

Thickness map of Intra Mid-Turonian to Intra Early Conianian in Figure 3.28 has a similar coverage of the study area as it in Near Top Albian to Intra Mid-Turonian. However, thickness variation changes. On the Halten Terrace, similar gradient change on thickness took place, but on the sub-terrace, sedimentary strata is thicker (*c*a. 0.36 s TWT) on the north and thinner (*c*a. 0.2 s TWT) on the south. Similarly, on the western side of the sub-terrace, more than 0.72 s TWT time-thick sediments accumulated at the east of the Grip High, while only 0.3 s TWT time-thick sediments deposited to the north.

3.8.6 Intra Early Coniacian to Top Early Santonian

From Intra Early Conianian to Top Early Santonian (Figure 3.28, right) the Frøya High was berried by sediment, left Trøndelag Platform exposed to the east of study area. Relative thicker sedimentary strata laterally deposited uniform on the Halten Terrace and the Rås Basin. The whole sedimentary strata reaches an average time-thickness in 0.4 s TWT (range from 0.35 s TWT to 0.45 s TWT).

3.8.7 Top Early Santonian to Intra Mid-Campanian

Thickness map of Top Early Santonian to Intra Mid-Campanian (Figure 3.29, left) shows that the predominant deposition is still at the northwest. Sedimentary strata becomes much thinner (not more than 0.15 s TWT) on the Halten Terrace, and even thinner at the southeast part. The Trøndelag Platform was still unburied. On the sub-terrace, time-thickness is descendant southwards, so is the distribution of sediments in the deep basin.

3.8.8 Intra Mid-Campanian to Base Cenozoic

The study area was buried after Intra Mid-Companian (Figure 3.29, right). Time-thickness is relative equivalent to Top Early Santonian to Intra Mid-Campanian, which is about 0.15 s TWT. Except the northwest part (around the Slettringen Ridge), the rest of the study area was deposited by relative uniform sedimentary strata. No obvious gradient change in strata thickness can be observed during this time.

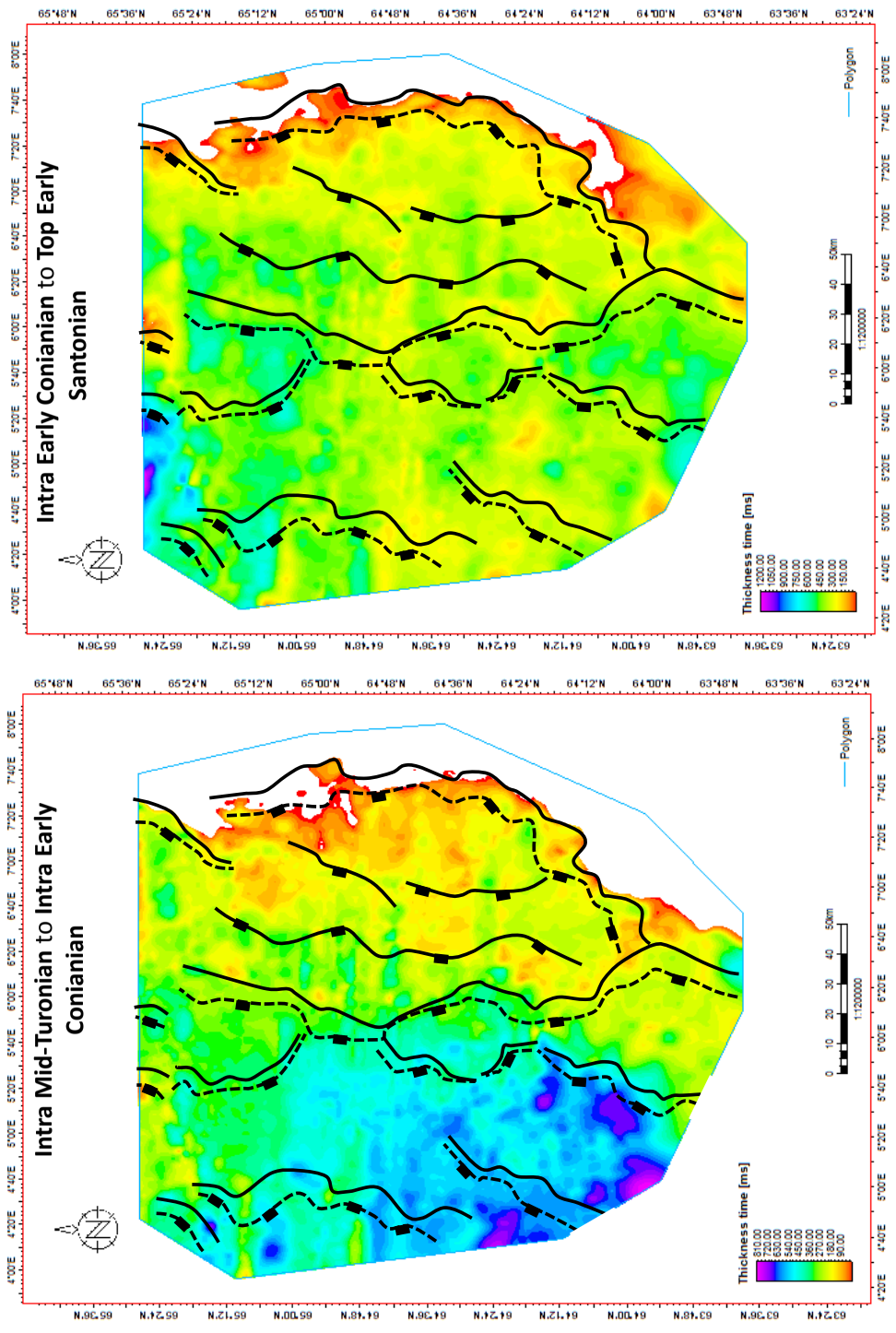

Figure 3.28: Time-thickness maps of Intra Mid-Turonian to Intra Early Coniacian to the left, which shows gradient changes in thickness on the Halten Terrace and the west-bounding sub-terrace. Thickness map of Intra Early Coniacian to Top Early Santonian to the right shows relative thicker sedimentary strata laterally deposited uniform on the Halten Terrace and the Rås Basin, which the sedimentary strata reaches an average time-thickness in 0.4 s TWT. Detail description can be seen in the text.

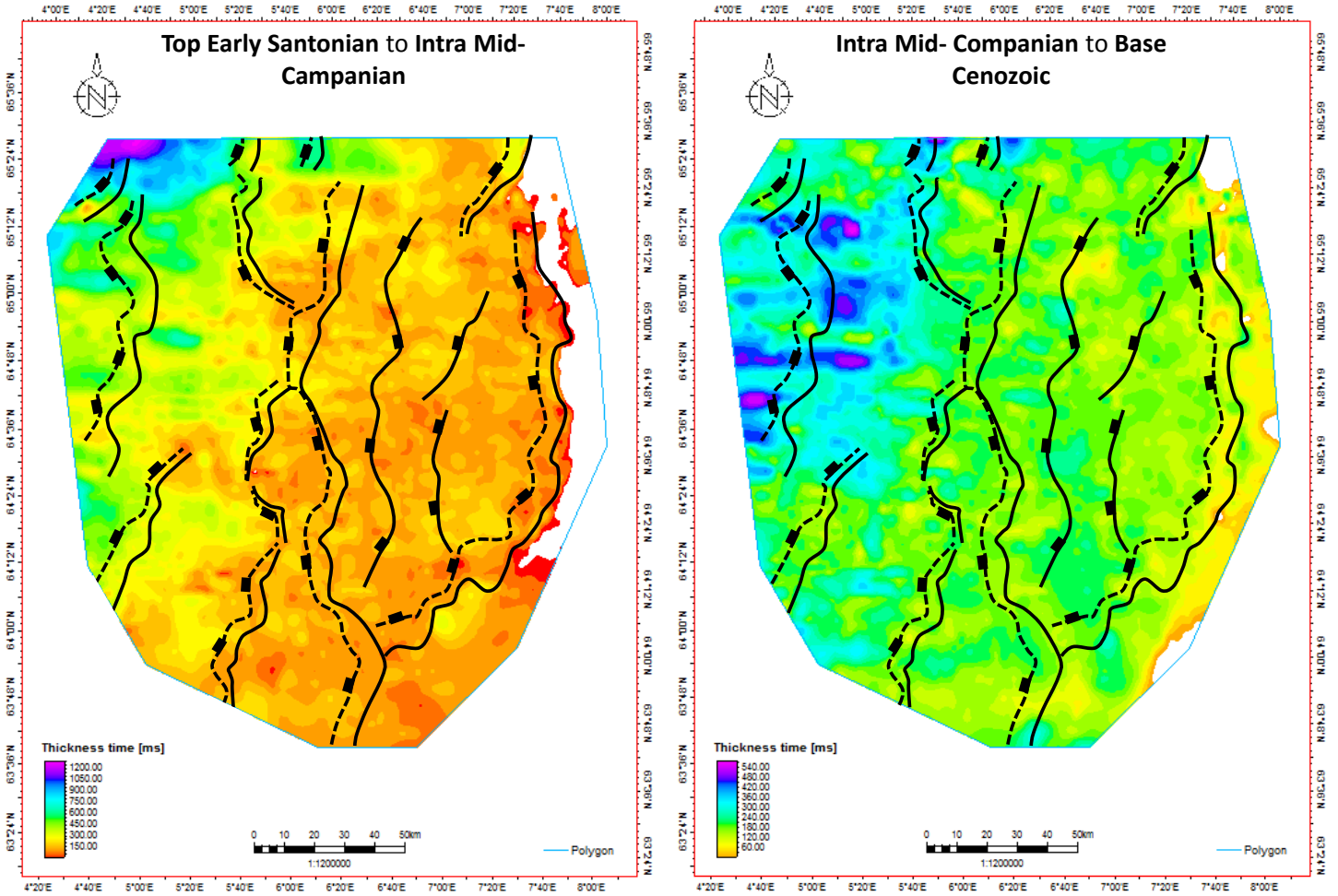

Figure 3.29: Time-thicknees map of Top Early Santonian to Intra Mid-Campanian to the left demonstrates that the predominant deposition is still at the northwest. Sedimentary strata becomes much thinner on the Halten Terrace, and even thinner at the southeast part. Thickness map of Intra Mid-Campanian to Base Cenozoic to the right demonstrates that the time-thickness is about 0.15 s TWT in relative uniform thickness. Detail description can be seen in the text.

Chapter 4

Discussion

The purpose of this study, as introduced in Chapter 1, is to understand the mechanisms responsible for the structural geometry observed on the mid-Norwegian continental margin, particularly the Klakk Fault Complex and its immediate vicinity. In this section, the results and observations from the seismic interpretation and time-thickness maps in Chapter 3 will be discussed, emphasizing on (1) structural architecture of extensional basins; (2) structural inheritance – the role of pre-existing zones of weakness; (3) strike-slip components; and (4) tectonic evolution – regional implications. Many published accounts have been done on the structural geometry of the mid-Norwegian continental shelf, e.g., Bukovics et al. (1984); Gabrielsen (1986); Caselli (1987); Brekke and Riis (1987); Schmidt (1992a); Knott (1993); Blystad et al. (1995); Lundin and Doré (1997); Swiecicki et al. (1998); Brekke (2000); Færseth and Lien (2002); Faleide et al. (2008); Gabrielsen (2010); Faleide et al. (2010); Bell et al. (2014), but the detailed knowledge about the Klakk Fault Complex and its immediate vicinity is still scarce. These previous works will be consulted in the discussion to help focusing on the Klakk Fault Complex analysis, in regards to augmentation and results.

4.1 Extensional Basins

According to many previous works, including Gabrielsen and Doré (1995) and Blystad et al. (1995), the structural style of the late Middle Jurassic-Early Cretaceous rifting episode on the continental margin indicates extension and crustal stretching/thinning as mid-Norwegian driving mechanism. The detail interpretation of the kinematics and dynamic development, however, is in different patterns. This section provides a brief overview of the perspectives of the extensional basins, which includes the architecture of extensional basins (Gabrielsen, 1986, 2010) and the associated transfer/accommodation

zones.

Structural Architectures of Extensional Basins

Many previous works (Bukovics et al., 1984; Gabrielsen, 1986; Brekke and Riis, 1987; Schmidt, 1992a; Knott, 1993; Blystad et al., 1995; Lundin and Doré, 1997; Swiecicki et al., 1998; Brekke, 2000; Færseth and Lien, 2002; Faleide et al., 2008; Gabrielsen, 2010; Faleide et al., 2010; Bell et al., 2014) delineated and suggested that the mid-Norwegian continental margin experienced a long history of rifting and correspondingly formed a series of basins with extensional structures during Jurassic to Early Cretaceous time. The architecture of these rift basins and the basin fill are strongly affected by the displacement geometry on the bounding normal fault systems (Gibson et al., 1989). The structural architecture of the rift basin should be examined firstly. In our case, the Vøring Basin which constitutes the Bremstein and Vingleia Fault Complexes, Halten Terrace, Sklinna Ridge, Klakk Fault Complex, the sub-terraces and Rås Basin are supposed to be found and related to the structural elements in extensional basins.

Gabrielsen (1986) did comparisons of many extensional basins and proposed that these extensional basins have many architectural elements in common. The principal sketch (Figure 4.1) of the extensional regime elaborates the development of the structural elements in rift basin. The *platform* is characterized by a relative flat tectonic unit which comprises a few broad, and only slightly tilted structural traps (Gabrielsen, 2010). The fault system here is active during the early time of the basin development, while when subsidence accelerated in the inner part of the graben system, it slowed down or became arrested. The *marginal platform high* usually exists on the basinward side. On the distal side of the marginal platform high, the *sub-platform* is delineated as heavily faulted fault blocks. The *outer master fault system* separates the platform from the sub-platform which is delineated by the marginal platform high on its distal side and the interior graben on the other. It is bounded by the *inner marginal fault system* to the graben side. The most profound zones in the rift basin is the inner marginal fault system together with the extra-marginal fault complex, and the two are likely to be linked along principal detachment found within the lower crust.

In the study area, similarly, the Halten Terrace shows a relative stable and flat tectonic unit (Chapter 2.3.2) where the faults were active during the late Middle Jurassic to Early Cretaceous. According to Brekke (2000), the Halten Terrace as an individual element was initiated by faulting in the Late Jurassic time and its main subsidence did not take place until later in Cretaceous time. Thus the Halten Terrace is a relative stable element which was subjected to tectonic activity in a short period and then experienced a relative long quiescence time. By comparing the fault system on the Halten Terrace with the perspective of Gabrielsen (1986), it follows analogously that the faults were

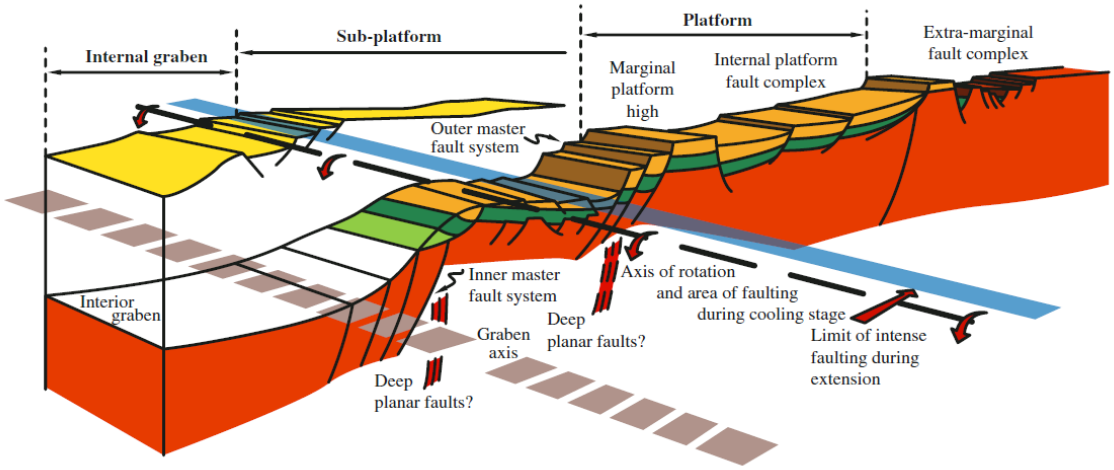

Figure 4.1: Principal sketch of major structural elements in graben system displays similar architectural elements in the study area (Gabrielsen, 2010).

active in the Late Jurassic time and arrested by the subsidence later in Cretaceous. Moreover, the delineated marginal high on the basinward side can be also found on the Halten Terrace, which is named Sklinna Ridge by Blystad et al. (1995). Therefore, we defined the Halten Terrace as the platform and the Sklinna Ridge as the marginal platform high. Instead of using the term sub-platform of Gabrielsen (1986) we prefer to use sub-terrace for the down-faulted area between the Halten Terrace and the Rås Basin. The Klakk Fault Complex and the faults bounding the sub-terrace to the west are the outer master fault system and inner marginal fault system respectively. Similar structural elements in the study area can be visualized in the 3D sketch graben margin with main structural elements (Figure 4.2) proposed by Gabrielsen (2010). As mentioned in Chapter 3.6 that the Klakk Fault Complex has the biggest displacement in NE-SW strike. Correspondingly, the Halten Terrace and its west-bounding rotated fault blocks all experienced footwall uplift following the same NE-SW orientation. Along NW-SE strike, the Klakk Fault Complex exhibits obvious different pattern from the northwest-dipping listric and planar faults in the NE-SW strike. Thus, in NW-SE orientation the Klakk Fault Complex, at least, was subjected to a different deformation mechanism that generated the small displacement and steeper faults. The extensional trend, therefore, follows NW-SE orientation, which is in accordance with Graue (1992); Grunnaleite and Gabrielsen (1995) and Reemst and Cloetingh (2000) that the main direction of extension during the Middle Jurassic-Early Cretaceous was NW-SE in the northeastern part of the Møre Basin. Gabrielsen et al. (1999) demonstrated more specific that the Møre Basin and Vøring Bsin were estimated to experience the NW-SE orientation extension from the late Permian-Triassic to Jurassic-early Cretaceous, until inversion took place in the Tertiary.

Figure 4.2: Graben margin with its main structural elements in 3D is visualized in the lower figure proposed by Gabrielsen (2010). Red dash-lined realm (a.)) was found as a high similarity to the structural elements in the study area (BCU time-structure map to the right). Hypothetical structural elements were marked in left upper figure a.). Modified after Gabrielsen (2010).

According to Gabrielsen (2010), the second-order faults flatten along detachment at shallower levels than both the primary master faults of the marginal fault complex and the inner and outer marginal fault system. This is also compatible with Osmundsen et al. (2002) and Gómez et al. (2004) in the deep structure of the rift margin. As mentioned in Chapter 3.4, the seismic lines have limited record length so that this detachment does not appear deeper than 10 s TWT. Comparison between the Osmundsen et al. (2002) and Key profile VII (Figure 3.25) is visualized in Figure 4.4. Geoseismic cross-section traversing the study area from Osmundsen et al. (2002) demonstrates a basinward-dipping detachment under the Trøndelag Platform; a deep, antiformal culmination with crest located at *ca.* 4.5 s TWT in the vicinity of well 6407/7-1; and the ramp-flat geometry of the Bremstein-Vingleia Fault Complex (Figure 4.4, lower). In vicinity of the Klakk Fault Complex, this detachment is defined as a deep-seated reflection band at *ca.* 10 s TWT (Figure 4.3 and Figure 4.4, upper). To the deep Rås Basin, it can not be mapped in Key Profile VII.

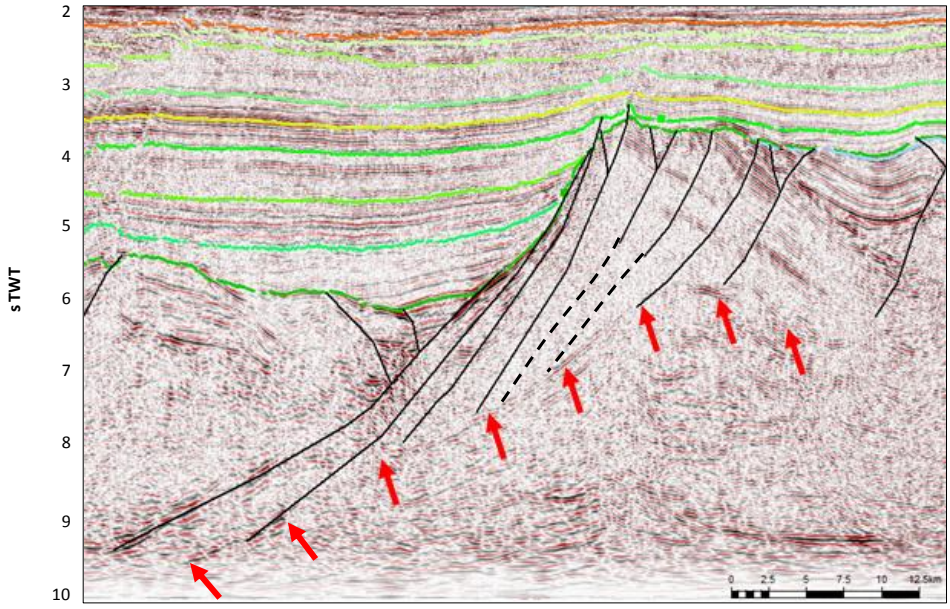

Figure 4.3: Deep-seated detachment in vicinity of the Klakk Fault Complex. The reflection of the detachment is recognized by intermediate amplitude marked with red arrows. The second order faults are flatten along this detachment at shallower levels than the master fault to the basin side. Triangular rider blocks associated with the Klakk Fault Complex can be observed. A larger view of the geoseimic profile compared with Osmundsen et al. (2002) can be seen in Figure 4.4.

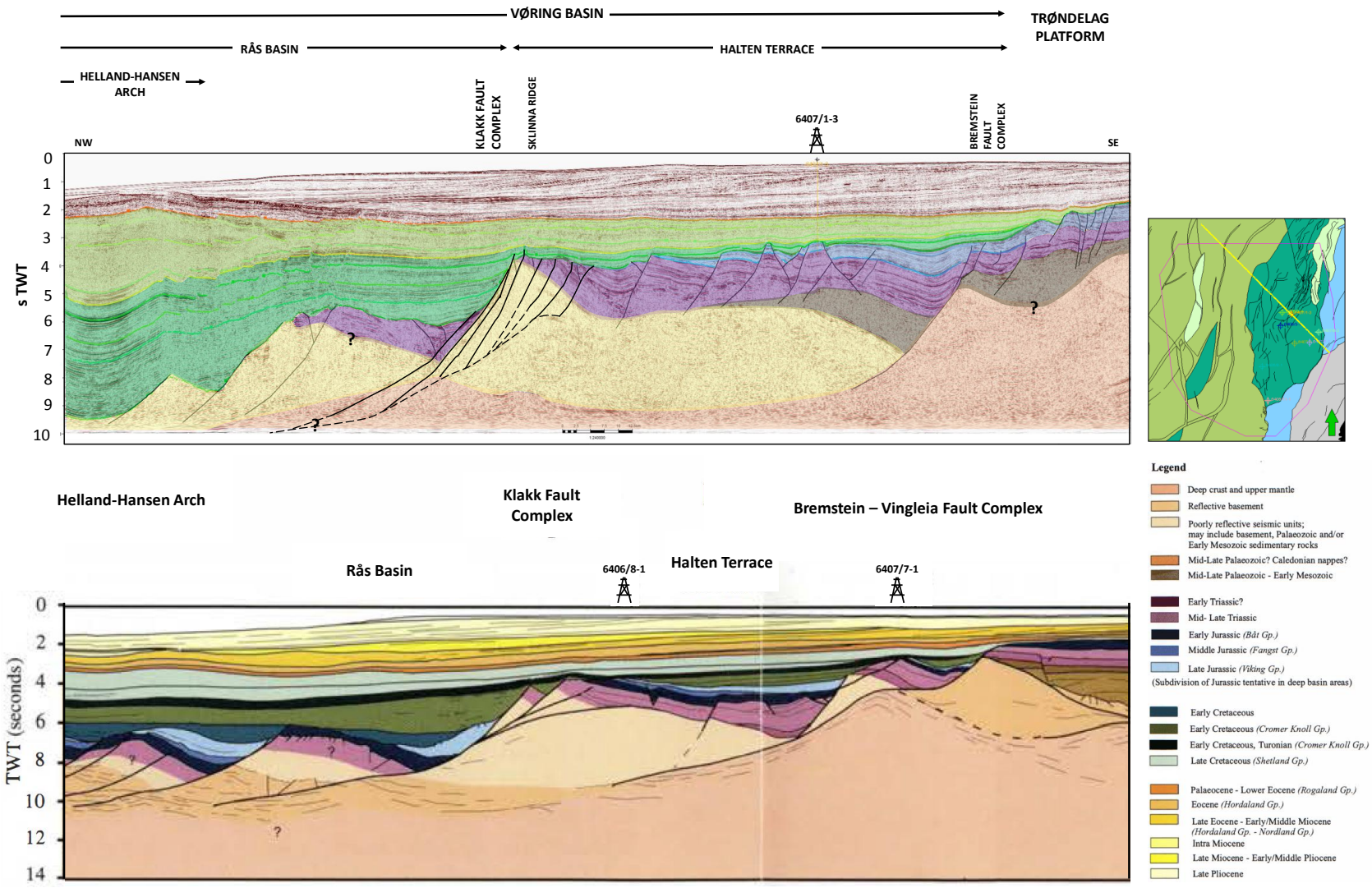

Figure 4.4: Comparison between Key profile VII and the geoseicmic section in Osmundsen et al. (2002) which transverses the Trøndelag Platform, Halten Terrace and the southern Vøring Basin. Very similar deep detachment can be found in Key profile VII by a deep-seated reflector band. The olive-green marks the probable Permian-Triassic terrain dipping southeast. While uncertainties exist beneath the Trøndelag Platform. Modified after Osmundsen et al. (2002).

Furthermore, Gabrielsen (2010) noted that the overall transgression and onlap of the crestal areas may be expected towards the end of the active stretching stage due to the overall subsidence of the rifted area. Usually, sediment starvation happens when subsidence outpaces sediment supply. On a regional scale, the relief may be enhanced by upheaval of graben shoulders due to isostasy and elastic response to faulting. This can be seen in our case (Figure 3.25) that the the fault blocks in immediate vicinity of the deepest depocenter usually are more severe rotated and more significant eroded on the shoulder of the footwall blocks. The erosion polygon of the intrabasin synthetic fault blocks in the whole study area is not possible to draw which was mentioned in Chapter 3.4.

Transfer/accommodation zones

The PROBE (Proto-Rifts and Ocean Basin Evolution) model proposed by Rosendahl et al. (1986) of the ideal half-graben was first referred to the structural expressions of rifting in Lake Tanganyika, Africa. Subsequently, it was applied to North Viking Graben by Scott and Rosendahl (1989). The linking modes are divided into three families (Figure 4.5). Based on the plane view of these modes, we infer the family 3 as the Klakk Fault Complex, especially, the case 7 and 8 can be clearly observed in the study area (Figure 3.10 and Figure 3.12). This also coincides with the segment division in Chapter 3.7 (Figure 3.12) that each of the segment follows the similar polarity half-graben geometry (family 3 in Figure 4.5). A simple fundamental unit of an ideal half-graben is presented by Segment I (Figure 3.15) and II (Figure 3.18), which shows an intrinsic geometry of a predominate arcuate bounding fault in map view (Rosendahl et al., 1986). In this model, the main characteristics of the fundamental unit is the

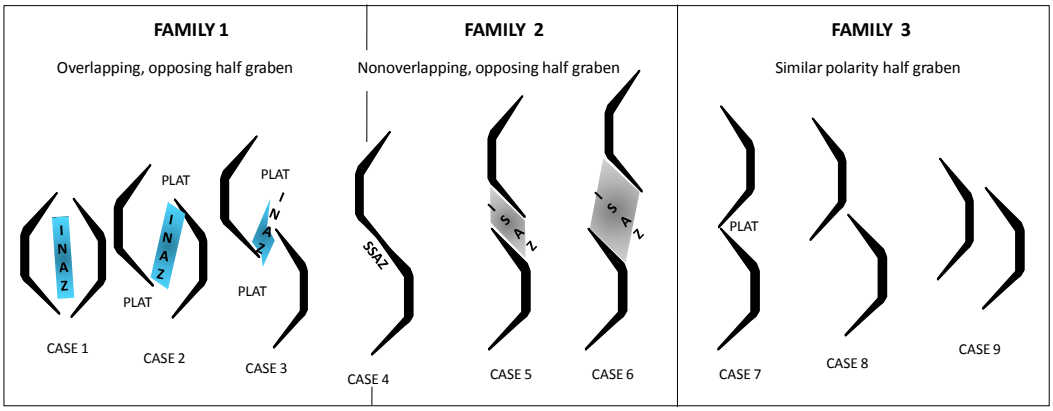

Figure 4.5: Possible half-graben linking modes. The mechanical consequence of these geometries are marked in the shade area and abbreviations. INAZ-interference accommodation zones (marked in blue); ISAZ-isolation accommodation zones (marked in grey); SSAZ-strike-slip accommodation zones; PLAT-platforms. Redrawn from Rosendahl et al. (1986), Rosendahl (1987) and Scott and Rosendahl (1989).

arcuate geometry in the view, and it requires listric border fault geometries in cross-section. Along the ends of the fundamental unit, shear and rotation mandate in turn. In the Klakk Fault Complex, along the NE-SW strike, the listric border master fault is present and can be observed in the seismic sections (Chapter 3.7: Figure 3.16, Figure 3.19, Figure 3.24 and Figure 3.25); along the NW-SE strike, faults become steeper and have the feature of shearing and may have horizontal displacement to some degree. Two fundamental units linked as the family 3 mode shown in Figure 4.5.

The linkage between two fundamental units was proposed in more detail by Morley (1988) and later was improved by Morley et al. (1990) applied to the east African rift system. These concepts can be utilized in the Klakk Fault Complex and to well explain the transfer zones. Figure 4.6 illustrates the transfer zone classification, the Klakk Fault

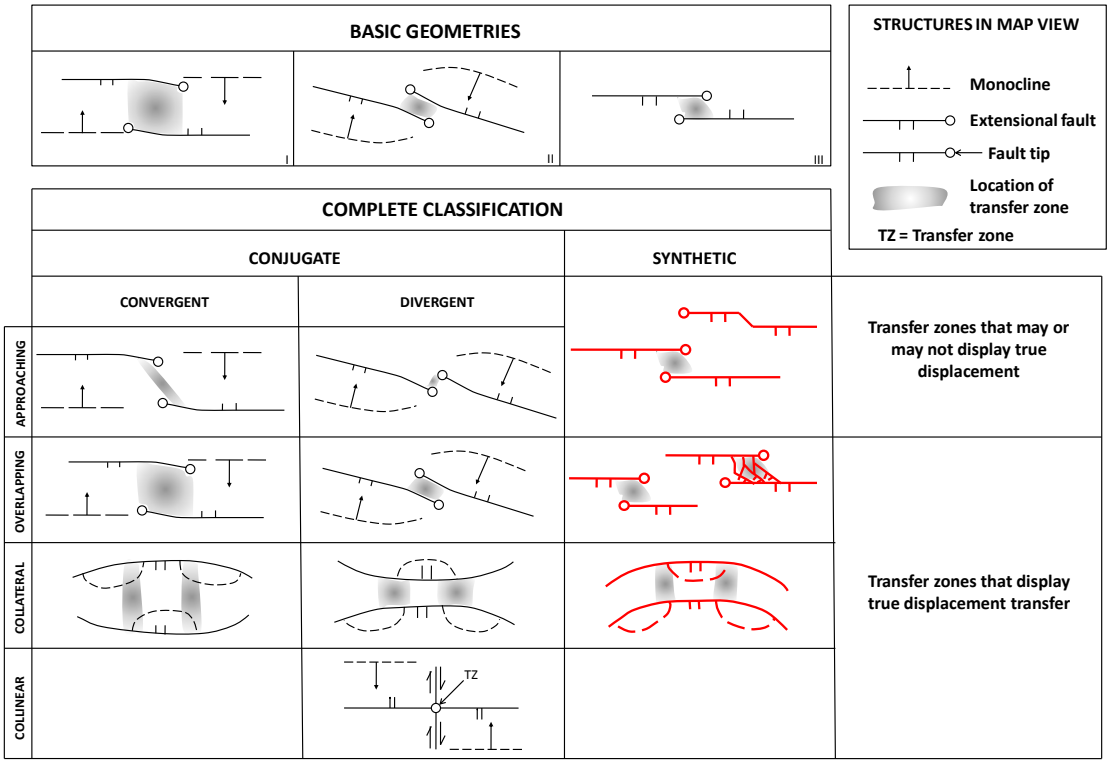

Figure 4.6: Transfer zone classification scheme modified after Morley et al. (1990). Transfer zones are mainly classified into three basic types by Morley (1988). Transfer zones can occur between faults that dip in opposite directions (conjugate, I and II) and in the same direction (synthetic, III). The complete classification divides these three basic type into four subdivisions: approaching, overlapping, collateral and collinear. In the study area, three subdivisions of the synthetic fault segment (highlighted in red color) can be observed along the Klakk Fault Complex and the west-bounding faults of the sub-terraces.

Complex coincides with the classification of synthetic class that is highlighted in red color. The Klakk Fault Complex dips NW in the major faults in all three segments (Chapter 3.7: Figure 3.16, Figure 3.19, Figure 3.24 and Figure 3.25). Transfer zones between the master listric faults in the Klakk Fault Complex occur where these two tips

of the master faults have failed to propagate past each other. From the time-structure map of the BCU (Figure 4.7), the transfer zones exist in NW-SE strike in the Klakk Fault Complex and no overlapping can be found between two master faults. Faults evolve from isolated faults to the interacting faults through the linkage. According to the fault segmentation and linkage mode in Kim and Sanderson (2005), the linkage relationship in the Klakk Fault Complex is supposed to belong to the hard-linked segment faults. This was also demonstrated by Gómez et al. (2004) that the Klakk Fault Complex appears to be linked on the scale of the map as hard-linked faults. However, when the west-bounding faults of the sub-terraces are taken into account, overlapping and collateral relationships are identified integrating with the Klakk Fault Complex.

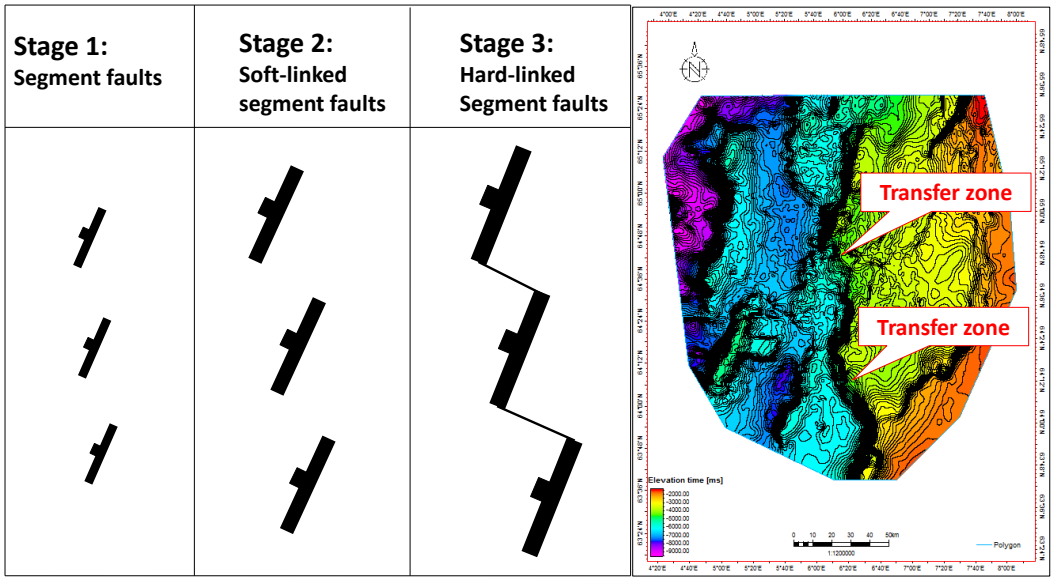

Figure 4.7: A simplified sketch of the faults propagation and linkage between each other. Three master faults are dipping in the same direction which is belong to the synthetic classification. The linkage between the master faults occurs where the tips of two faults failed to overlap each other.

4.2 Structural Inheritance – the Role of Pre-existing Zones of Weakness

The lineament pattern in the NE Atlantic margin is dominated by three major sets (Figure 4.8) which are characterized by a dominant NE-SW lineament, a subordinate but distinct N-S grain and a more diffuse cross-cutting NW-SE set observed through lineament terminations and offsets (Doré et al., 1997b). Similar fracture patterns on-shore Norway also be strongly repeated and observed in landsat lineament mapping (Gabrielsen and Ramberg, 1979).

The NE-SW trend in the study area is highly repeated in the Klakk Fault Complex and

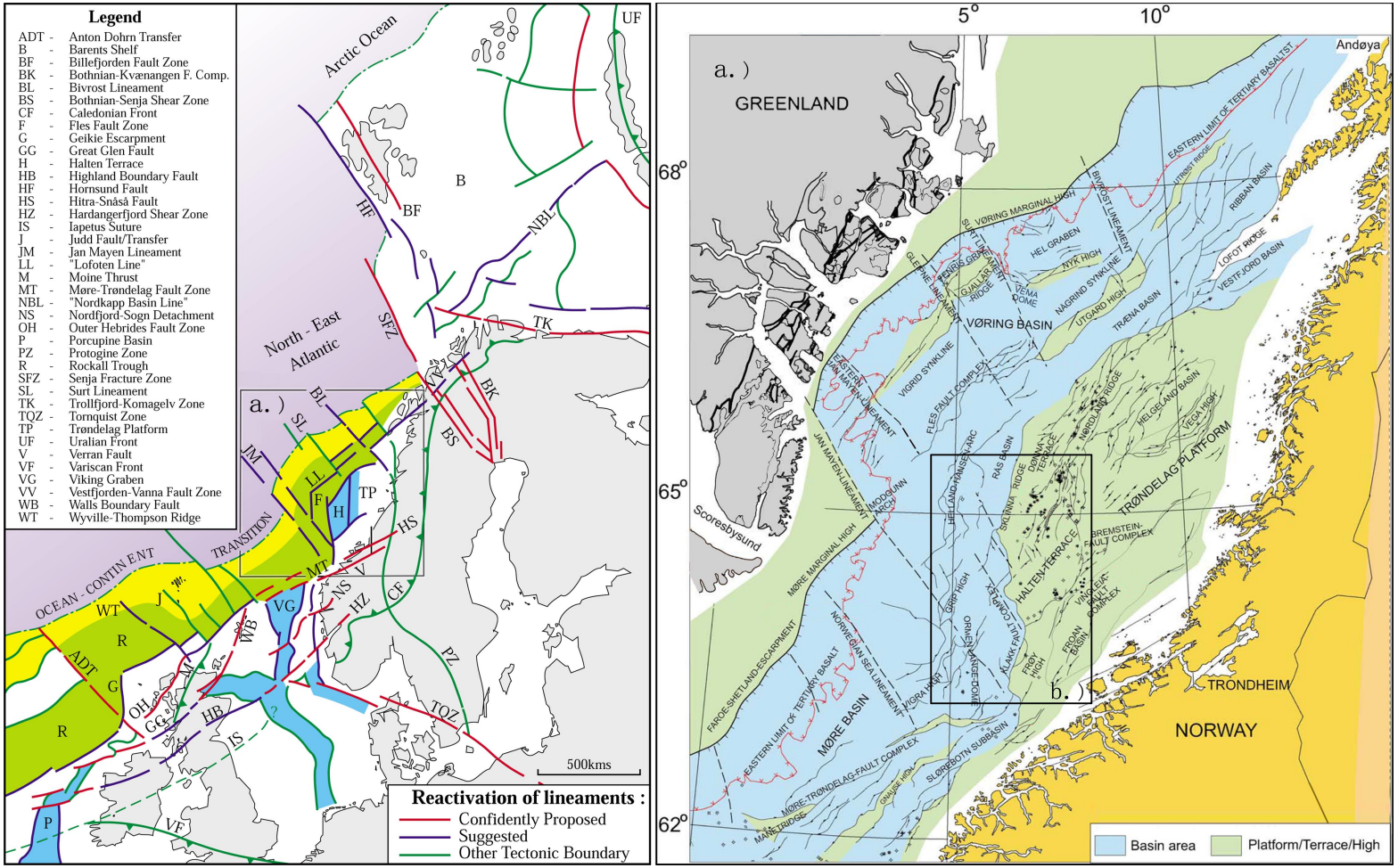

Figure 4.8: The Klakk Fault Complex is situated east of the Jan Mayen Fracture Zone and northeast of the Møre-Trøndelag Fault Complex. The reactivation of lineaments are presented in the left figure, area a.) is amplified to the right. Figure a.) to the right illustrates the detail of the study area. The dash lines represented the probable transfer zones which interposed by NE-SW striking faults, creating an overall rhomboidal geometry. Area b.) is amplified in Figure 4.9, left. After Doré et al. (1997b) and Færseth and Lien (2002).

the faults on the terrace and sub-terrace. Especially along the Klakk Fault Complex, the weakness zones in this orientation are the prototypical representation where the Klakk Fault Complex generated the maximum displacements and formed the huge northwesterly dipping fault blocks. The southeastern-bounding Vingleia Fault Complex and numerous small-scale faults on the Halten Terrace are also expressed in NE-SW trends. According to Doré et al. (1997b), rifting was refocused on the NE Atlantic margin (Rattey and Hayward, 1993; Earle et al., 1989), initiating the chain of broad NE-SW Cretaceous-Cenozoic basins, i.e., Vøring Basin, Møre Basin, Faeroe-Shetland Basin and Rockall Trough, and overprinting the Jurassic (and earlier) rift network. The NE-SW grain was emphasized later by the extensional episodes of mid-Cretaceous (probably Cenomanian) and latest Cretaceous to Palaeocene age. According to Færseth and Lien (2002), these major NE-SW normal faults are not merely as a result of proximity to the Atlantic margin, but also to reflect the influence of the prominent NE-SW basement grain represented by the long-lived Møre-Trøndelag Fault Complex (Figure 4.8, right). According to Skilbrei and Olesen (2005), in the Trøndelag Platform area, there are a series of pre-Cretaceous structural highs and lows with a NE-SW grain separated by N-S structures, which make up eye-with-eye patterns within the Trøndelag Platform and one major rhomboid feature from the Møre-Trøndelag Fault Complex in the south to the Vestfjorden Basin in the north (the Trøndelag Platform). Skilbrei and Olesen (2005) also stated that the principal trend is NE-SW in the Møre and Vøring Basins, except for the area dominated by N-S grain between 64°N and 65°30′N (the area is dominated by the Halten Terrace). Although the Halten Terrace is trending N-S, the internal grain of the terrace is still dominated by NE-SW. He postulated that these might be the result of major faults being superimposed on Devonian extensional collapse structure. While from the BCU time-structure map (Figure 3.10 and Figure 3.11) in the study area, the dominated grains are more likely to be NE-SW and NW-SE. The eye-with-eye-patterned sub-terraces to the west of the Halten Terrace are also constrained by NE-SW and NW-SE grains.

The N-S trend is suggested widely by the previous work (Blystad et al., 1995; Doré et al., 1997b, 1999; Pascal and Gabrielsen, 2001; Skilbrei et al., 2002; Osmundsen et al., 2002; Færseth and Lien, 2002; Skilbrei and Olesen, 2005; Osmundsen and Ebbing, 2008) on the eastern and western bounding faults of the Halten Terrace. This trend at least can be dated back to Permian, although it is a regional expression of the Jurassic rifting. Doré et al. (1997b) regarded that the N-S trending appears to interpose between the dominant NE-SW lineaments, creating an overall rhomboidal geometry evident and this suggests that the two fault sets may have a common origin. However, in our study area, the detailed fault interpretation in the seismic sections transversing the Klakk Fault Complex and the refined interpretation of the BCU reveal that the western bounding faults of the Halten Terrace actually varies in segments, mainly following the NE-SW and NW-SE trends (Chapter 3.7.4). The rhomboidal geometry, therefore, is constrained

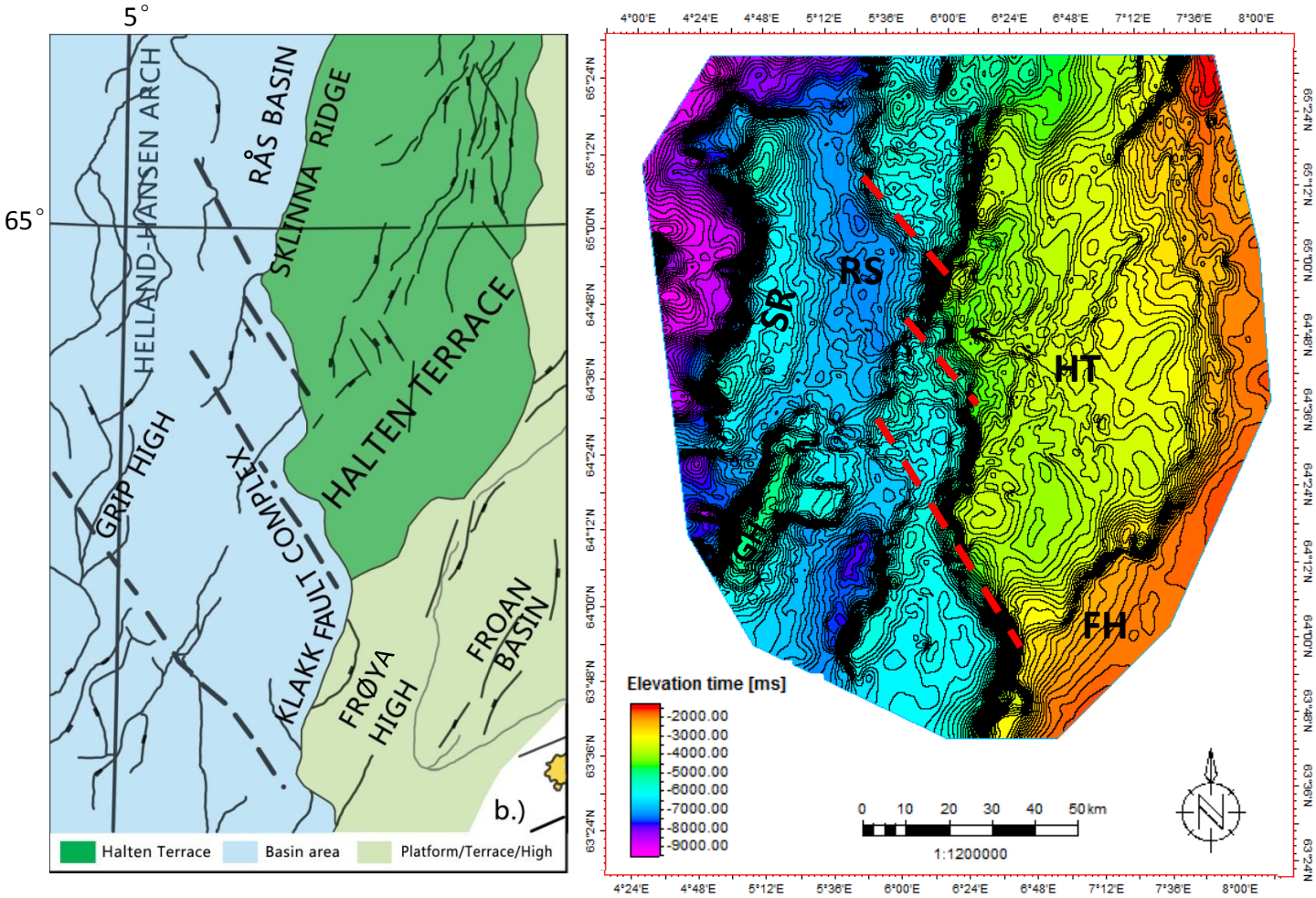

Figure 4.9: The left figure demonstrates the two main lineaments, modified after Færseth and Lien (2002). It represents the area b.) in Figure 4.8, a.). Black dash lines are the suggested NW-SE transfer zones by Færseth and Lien (2002). The right one is the BCU time-structure map of the study area, red dash lines are the transfer zones interpreted in this thesis. Comparison of the BCU time-structural map of the study area with the NW-SE trending structural inheritance suggested by Færseth and Lien (2002), a high similarity appears that the sub-terraces bounding by two fault sets which are NW-SE and NE-SW creating the overall rhomboidal geometry. HT=Halten Terrace, RS=Råss Basin, FH=Frøya High, GH=Grip High, SR=Slettringen Ridge.

by NE-SW and NW-SE lineaments (Figure 4.8 and Figure 4.9) instead of N-S and NW-SE lineaments. N-S does not appear to be an important trend in the Klakk Fault Complex.

The NW-SE "transfer" trend segmented the Mesozoic-Cenozoic basin system (Doré et al., 1997b), e.g., Jan Mayen Lineament, which is coincident with a main southeastwards offset of the basin chain, displaces the ocean-continent boundary and extends into one of the most significant transforms in the North Atlantic (Blystad et al., 1995). The transfer zone is very difficult to assign a basement origin (Doré et al., 1997b). Nevertheless, it is established in Romer and Bax (1992) that NW-SE feature systems are prominent in the Precambrian basement as striking faults zone on both sides (south and north) of the Caledonian orogen. Strömberg (1978); Henkel and Eriksson (1987) noted that the NW-SE trend in the mid-Norwegian continental shelf has been previously attributed to Proterozoic shear zone, which coincides with Romer and Bax (1992) that Proterozoic faults defined basement rocks. While Skilbrei and Olesen (2005) interpreted this trend as the Devonian detachment or shear zones that can be approximately followed to the central part of shelf. This detachment zones are connected to detachments in East Greenland by Olesen et al. (2004). In our study area, the NW-SE striking Klakk Fault Complex segments are also considered as the transfer zones. The mechanism of these transfer zones are poorly understood, but referring to the previous published accounts (Blystad et al., 1995; Doré and Lundin, 1996; Doré et al., 1999; Gabrielsen et al., 1999), it may be caused by the basement inhomogeneities. As stated by Færseth and Lien (2002), these NW-SE transfer zones may play an important role since they result in a well-defined along-strike margin segmentation (Figure 4.8, right and Figure 4.9) and some of them appear to have had a prolong history of activity and correlate with major basement inhomogeneities (Blystad et al., 1995; Doré and Lundin, 1996; Doré et al., 1999; Gabrielsen et al., 1999). Moreover, NW-SE transfer zones are observed as termination and offset of structural features, changes in fault patterns, and they may have acted as persistent barrier to rift propagation (Tsikalas et al., 2001).

From the above, the Klakk Fault Complex with predominate NE-SW and NW-SE trends combined with the west bounding rhomboidal-shaped sub-terraces are most likely to be the structural inheritance of the basement lineament. It may be the combined effect of Proterozoic shear zone in the basement and the NW-SE Devonian shear zones, as well as the NE-SW orientation related to Devonian extensional collapse structure and the post-Devonian fault activities.

Lineaments do not only exist offshore, similar lineaments were also found onshore Norway (Gabrielsen and Ramberg, 1979; Gabrielsen et al., 1999; Braathen et al., 2000, 2002; Osmundsen et al., 2003; Skilbrei and Olesen, 2005). The most conspicuous should be the Møre-Trøndelag Fault Complex onshore and offshore with the predominate ENE-WSW structural grain. The Møre-Trøndelag Fault Complex (Figure 4.8 and Figure 4.10) acted

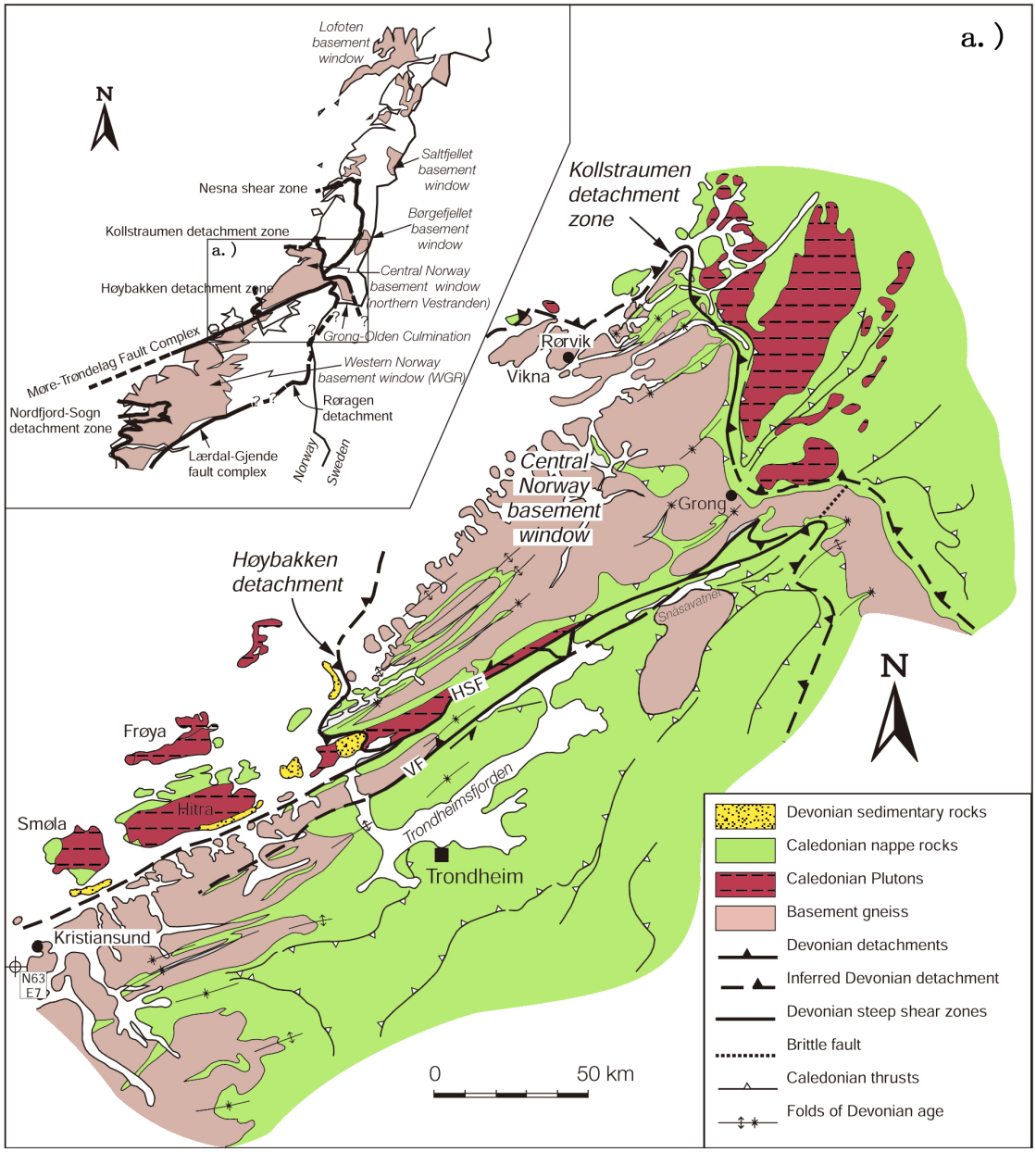

Figure 4.10: Sketch map of central Scandinavian Caledonides and figure a.), simplified tectonic map of Tronheimfjord region where Møre-Trøndelag Fault Complex and Høybakken and Kollatraumen detachment zones located. HSF=Hitra-Snåsa Fault, VF=Verran fault. Modified after Braathen et al. (2000) and Skilbrei and Olesen (2005).

as an crucial role in the Devonian scenario, playing a ductile sinistral shear zone in a developing transtensional and/or transpressional strain regime in the surrounding regions (Roberts, 1983; Krabbendam and Dewey, 1998; Osmundsen et al., 1998; Braathen, 1999; Braathen et al., 2000). In central Norway, a bidirectional, opposed extensional model is stated by Braathen et al. (2000), which is northeast-southwest stretching axis parallel or sub-parallel to the Scandian orogen. According to Braathen et al. (2000), this bidirectional and opposed orogen-parallel transport was net effected by the uplift of high-grade central Norway basement window by tectonic denudation. This NE-SW orientation on land can be also observed offshore. In offshore areas from the central-east Møre Basin

to within Central Norway onshore, there is parallelism between the old basement grain (probably Devonian) and the rift basins (e.g., Rås Basin) and their associated faults (e.g., Klakk Fault Complex, Vingleia Fault Complex) (Skilbrei and Olesen, 2005).

4.3 Strike-slip Movement

One interesting observation from the time-structure map of the BCU (Figure 3.10 and Figure 4.9) in the study area is that the rhomboidal shape is highly repeated in the terrace and sub-terraces. These rhombohedral depressions associated with the Halten Terrace and the west-bounding sub-terraces are very similar in geometry to pull-apart basins described by Crowell (1974). The first theory about pull-apart basins in dextral/sinistral settings were suggested by Caselli (1987) and Brekke and Riis (1987). Before Caselli (1987), the right-lateral shear system was suggested by Gabrielsen and Robinson (1984) by correlating the fault trends of the Kristiansund-Bodø Fault Complex (64°N - 67°N, 6°E - 12°E, the nomenclature of this fault redefined by Blystad et al. (1995) as the Klakk Fault Complex (63°5′N - 65°30′N, 6°E - 6°15′E) and Revfallet Fault Complex (65°15′N - 66°50′N, 7°E - 12°E). with deformation strain ellipsoid for dextral shear system. Caselli (1987) postulated that the pull-apart basin associated with the Halten Terrace is the result of dextral slip movements. In the same year, Brekke and Riis (1987) noted that the rhomboidal shape of the Halten Terrace probably formed as a pull-apart basin in a sinistral fault system during late Kimmerian deformation. Later, this theory was supported by Schmidt (1992b) by doing the structural analysis of the Heidrun Field.

However, strike-slip faults are very difficult to detect in seismic sections. In our case, along the Klakk Fault Complex, the most likely compatible structure we detected is one interpreted flower structure in Key profile IV, and probably the high-angle faults with NW-SE strike. But comparing with the larger-scale Kristiansund-Bodø Fault Complex, including the northern Nordland Ridge postulated by Gabrielsen and Robinson (1984), the Klakk Fault Complex and the shape of Halten Terrace are not compelling to prove the horizontal displacement.

4.4 Tectonic Evolution – Regional Implications

The intermittent extension on the mid-Norwegian margin is well documented from post-Caledonian orogenic collapse in Devonian to post-early Eocene passive margin development (Doré et al., 1999; Roberts et al., 1999; Eldholm et al., 2002; Hooper and Walker, 2003; Tsikalas et al., 2012). Discrete rift events during this period have been defined in Permian-Triassic, Middle-Late Jurassic, earliest Cretaceous, mid-Cretaceous, and Late Cretaceous-Paleocene times (Figure 2.2) (Blystad et al., 1995; Roberts et al., 1999; Doré

et al., 1999; Brekke, 2000; Faleide et al., 2008; Gabrielsen, 2010; Faleide et al., 2010; Tsikalas et al., 2012; Bell et al., 2014). Evidence of these extensional events, in addition to the Cenozoic compressional events, can be visualized on the seismic profiles and time-structure maps from the Halten Terrace and the Rås Basin.

The Permian-Triassic rift event on the mid-Norwegian continental margin is proposed by previous work (Ziegler, 1988b; Tsikalas et al., 2012), but it is not easy to resolve on the eastern part of the Halten Terrace and in the Rås Basin due to the poor seismic resolution at depth and lack of well penetration. Nevertheless, in key profile VII (Figure 3.25, Figure 4.4) it is evident on the Trøndelag Platform area and western part of the Halten Terrace that at around 5 s TWT, W/NW-dipping faults terminates at the Permian reflection. According to Blystad et al. (1995); Pascoe et al. (1999); Withjack and Callaway (2000); Osmundsen et al. (2002) and Osmundsen and Ebbing (2008), this Permian-Triassic extensional event can be found in the form of a block-faulted terrain beneath the Halten Terrace and Froan Basin/Trøndelag Platform as easterly-tilted half-graben. This terrain is only visible in Key profile VII when comparing with Osmundsen et al. (2002) (Figure 4.4). It is characterized by Permian deposits with southeast facing half-graben geometry.

The earliest extensional event confirmed in the Halten Terrace and the Rås Basin is the late Middle Jurassic-Early Cretaceous rifting, which initiated the Klakk Fault Complex and relative small-scale faults on the Halten Terrace and in the Rås Basin. The most significant displacement took place along the western margin of the Halten Terrace, which initiated the Halten Terrace as an individual element in the Vøring Basin independently from the Trøndelag Platform. The typical morphological expression of this extensional event is the huge tilted fault blocks (Chapter 3.7: Figure 3.16, Figure 3.19, Figure 3.24, Figure 3.25). Wedge-shaped syn-rift successions reflect the timing of the event due to the restriction of the Lower Cretaceous succession (Chapter 3.7: Figure 3.16, Figure 3.19, Figure 3.21, Figure 3.24, Figure 3.25), even in the Rås Basin where the seismic quality degrades with depth. The definition of the Base Cretaceous Unconformity plays a decisive role that can tell discrepancies of the fault timing. Skogseid et al. (2000) postulated that the Base Cretaceous Unconformity does not mark the transition from the syn-rift to post-rift sediments in the Late Jurassic-Early Cretaceous rift event. However, alternatives of the definition of the Base Cretaceous Unconformity is still under debate. Nøttvedt et al. (1995) suggested the syn- to post-rift transition to be defined as the point in time when net heat out of the system is greater than net heat into the system. They argued that the transition coincides with a regional shift in tilt from fault block rotation away from the graben axis during the syn-rift stage to tilting directed towards the basin axis during the post-rift stage (Gabrielsen et al., 2001) (Figure 4.11). This can be illustrated in the seismic sections in our study area that the syn-rift and the post-rift sequences have opposite rotations (Chapter 3.7: Figure 3.16, Figure 3.19, Figure 3.24, Figure 3.25). Therefore, our interpretation on the downthrown side of the Klakk Fault

Complex can not see the rifting continuation evidently above the Base Cretaceous Unconformity. The lack of well penetration in the Rås Basin leads to the uncertainty of the activity duration of Klakk Fault Complex. The conceptual sections of the syn-rift succession and post-rift succession, nonetheless, can be well separated by the Base Cretaceous Unconformity in our interpretation.

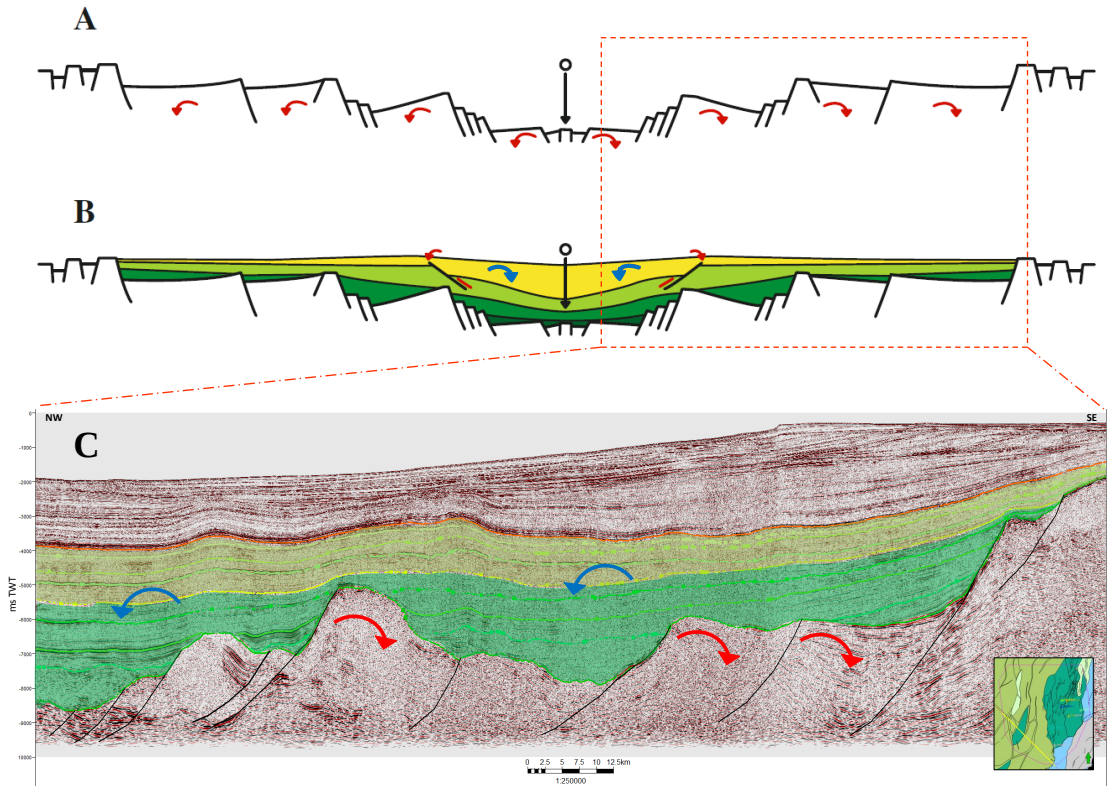

Figure 4.11: Pattern of rotation of sedimentary unites in syn-rift (A) and post-rift (B), Gabrielsen (2010). Key profile I (C) shows the opposite rotations in syn-rift (red arrows) and post-rift (blue arrows). Lower Cretaceous strata and Upper Cretaceous strata are marked with the color codes in Figure 3.7. Seismic section only represent the half of extensional basin (red dash-lined area).

The Jurassic syn-rift sequence, however, represents only a minor constituent of the half-graben fill in the study area. The major part of the sediments, which constitutes the half-graben fill, represents the post-rift stage of basin evolution (Færseth and Lien, 2002). This huge post-rift sedimentary sequence may reveal a period characterized by tectonic quiescence according to Færseth and Lien (2002). On the other hand, an Early Cretaceous rift event on the NE Atlantic margins is postulated by many previous works (Lundin and Doré, 1997; Doré et al., 1999; Tsikalas et al., 2001; Ren et al., 2003) after it was first constrained onshore East Greenland (Surlyk et al., 1981; Surlyk, 1990; Whitham et al., 1999). The biostratigraphical data from the Vøring margin indicate a change from neritic to bathyal conditions and increase in sediment accommodation space in the Aptian–Albian, attributed to eustatic sea-level rise and regional tectonism (Gabrielsen et al., 1999; Tsikalas et al., 2005, 2012). Blystad et al. (1995) have stated that the Klakk Fault Complex was probably reactivated in extensional faulting in the Aptian/Albian. We

mapped three horizons during this time interval: Barremian-Aptian(?), Intra Albian and Near Top Albian. From the first six seismic sections (Chapter 3.7: Figure 3.16, Figure 3.17, Figure 3.19, Figure 3.20, Figure 3.21, Figure 3.24), no reflection evidence shows reactivation of the Klakk Fault Complex during this time. Reflections in this time interval are portrayed of passive infilling feature. At the southern part of the Klakk Fault Complex, reflections show compressional features (Figure 3.16, Figure 3.19) during this time, which may indicate the later inversion associated with intra-plate shortening that took place in the southeastern Vøring Basin and northeastern Møre Basin. From time-thickness maps, the thickness variation along the Klakk Fault Complex can only be observed in the BCU to Barremian-Aptian time-thickness map and Barremian-Aptian to Intra Albian time-thickness map (Chapter 3.8: Figure 3.26), in which deposition is more significant in immediate vicinity of the escarpment of the Klakk Fault Complex along the NE-SW orientation. However, the seismic sections (Figure 3.16, Figure 3.24) illustrated that this is predominantly caused by the hangingwall tilting, which fault scarp has relative more accommodation. There is no reverse drag onlap and wedge-shaped package which can indicate the fault growing in the late Early Cretaceous. Nonetheless, limitation of data set is one restricted condition to date the fault activity associated with this important tectonic phase during Aptian-Albian.

However, a conspicuous difference is visualized in Figure 3.25, which also was mentioned in Chapter 3.7.3 (Figure 3.23) that the Klakk Fault Complex extended into the sedimentary sequence above the Base Cretaceous Unconformity, and the reflection of Near Top Albian was upwarp above the tip points of the Klakk Fault Complex (Figure 4.12). This may reveal that the Klakk Fault Complex was reactivated at the end of Albian time, but this activity did not happen fiercely nor last long. It has been suggested by Brekke (2000); Olesen et al. (2002) and Skilbrei and Olesen (2005) that in the Vøring Basin and perhaps in the Vestfjorden and Ribban basinal area (at north of the Trøndelag Platform), it is likely that a Cretaceous rifting event existed. In addition, referring to the North Atlantic Rift System which experienced an important tectonic phase in Aptian–Albian time related to crustal break-up and sea floor spreading further south in the Atlantic (Ziegler, 1988a, 1992). It is most likely that this activity affected the northernmost part of the study area. The Klakk Fault Complex only activated during the end of Albian at the northernmost, but the rest of the study area remained in tectonic quiescence.

After Albian time, the time-thickness maps (Figure 3.26, Figure 3.27, Figure 3.28) show more relative uniform deposition on thickness along the Klakk Fault Complex. Cretaceous successions show intervals with uniform thickness as well as intervals that are wedge-shaped on the Halten Terrace. Figure 3.19 and Figure 3.20 also illustrate that, at the base or within lower Cretaceous wedge-shaped bodies, the Cretaceous reflections show onlap towards fault block crests as well as fault scarps of the Klakk Fault Complex. Time-thickness maps from Intra Early Conianian to Base Cenozoic (Figure 3.28, left; Figure 3.29) demonstrate a succession with uniform thickness from post-rift time

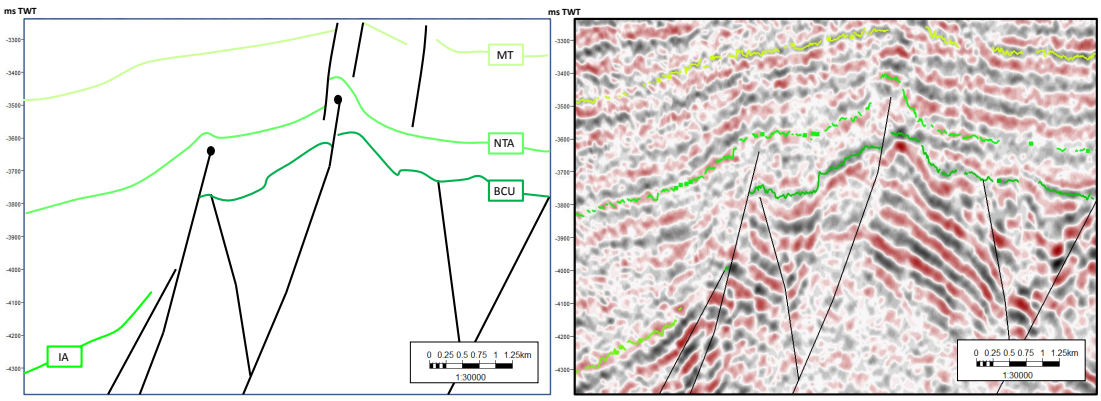

Figure 4.12: The Klakk Fault Complex might grow in late Albian time, the tip points of the faults made the Near Top Albian upwarp. Horizons Near Top Albian Intra Mid-Turonian are cut by the younger faults.

in the Late Cretaceous. These relative uniform successions are characterized by parallel reflections.

However, in Key profile VII (Figure 4.13), reflections show a contrast configuration in the deep Vøring Basin center (at the Helland-Hansen Arch area). Figure 4.13 illustrates that the the post-rift sequences K10-50 were still influenced by the basin topography of the late stage of the syn-rift. According to Gabrielsen et al. (2001), the earliest stage of the post-rift development invokes amalgamation of sub-basins and smoothening of the basin floor. These sequences, therefore, may have experienced the incipient (or middle) stage of post-rift. From sequence K60, it generally heralds the vanishing influence of the syn-rift structural pattern, which becomes drowned in a sediment package of increasing thickness. In sequences K70 and K80, the syn-rift structural pattern becomes leveled and it almost has no influence of the syn-rift structural pattern. According to Færseth and Lien (2002), this depositional pattern to reflect infilling of earlier rift topography during period which were characterized by relatively high sedimentation rate. This coincides with Prosser (1993) in the interpretation of parallel reflections in a late post-rift infill which reveal a more continuous nature than the early post-rift succession. Færseth and Lien (2002) interpreted that the reflections in the Early Cretaceous remained significant morphological escarpments on the basin floor and influenced sedimentation for a considerable time after the cessation of rifting subsidence due to the low rate of sedimentation. During the Early Cretaceous, the subsidence rate outpaced the sedimentation rate, at least at the distal part of the Early Cretaceous depositional system, as the thermal subsidence has highest rate during the first tens of million years and decreases asympotically with time (McKenzie, 1978). The reflections in the seismic section (Figure 4.13) shows that from Top Early Santonian (the accurate one is supposed to occur in sequence K60), the topographic relief was levelled as a result of the increased sediments supply outpacing the subsidence rate. Gabrielsen et al. (2001) postulated that the definition of mature stage of the post-rift basin development is reached when thermal equilibrium is obtained, and final shape will be that of a wide, saucer-shaped basin. Thus, it seems most likely

that in sequences K70 and K80, the sedimentary strata are characterized by the mature stage of the post-rift.

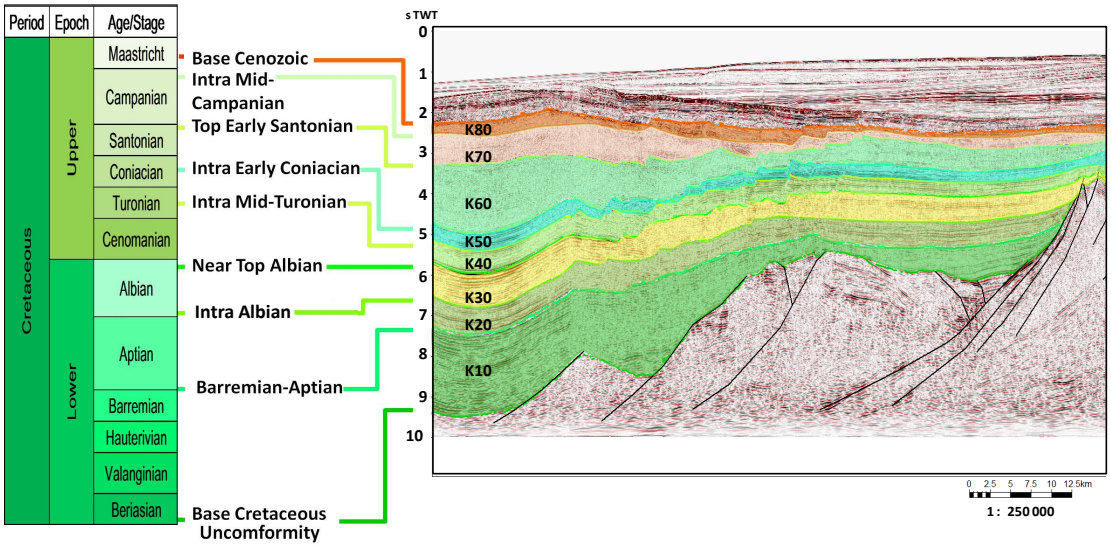

Figure 4.13: Lithostratigraphic column for the Cretaceous of the study area. The notations for the Cretaceous sequences (K10 to K80) as used in the present work are correlated to the formal stratigraphical nomenclature suggested by Færseth and Lien (2002).

At the onset of the Campanian rifting, the area between Norway and Greenland was an epicontinental sea covering a region in which the crust had been extensively attenuated by previous rift events (Tsikalas et al., 2005). This rift episode ended up in continental separation in the North Atlantic region and Norwegian Sea in earliest Eocene. However, in our study area, the Campanian rifting event is difficult to detect.

The most conspicuous structure associated with the event in Cenozoic is the contractional deformation which is visualized as the large anticlines and small local folds (Figure 4.14). Contractional structures have been reported from the Vøring Basin and northern Møre Basin of the mid-Norwegian continental shelf (Gabrielsen and Robinson, 1984; Brekke and Riis, 1987; Grunnaleite and Gabrielsen, 1995; Doré and Lundin, 1996). Although the mechanism of the arch is highly debated, contractional deformation is more reasonable in our case. Figure 4.14 demonstrates the anticlines at least formed after Cretaceous due to the upwarped Base Cenozoic horizon. Asymmetric folds appear between the pre-Cretaceous tilted fault blocks. Large anticlines formed Horizons in Cenozoic are not mapped in this study. Therefor, the accurate time in Cenozoic for initiating the inversion is unknown. According to Bøen et al. (1984) and Blystad et al. (1995), these anticlines (or domes in 3D view) in the Vøring Basin developed in the the compressional regime during Palaeocene-Eocene and Late Miocene.

We have drawn the relative symmetrical anticlines in the study area with the asymmetrical underlain ridge and high in the same polygon (Figure 4.15), and it shows that the Fles Fault Complex, Slettringen Ridge and Grip High are situated at the west of the anticlines, the anticlines are constrained by the Fles Fault Complex which is the west-

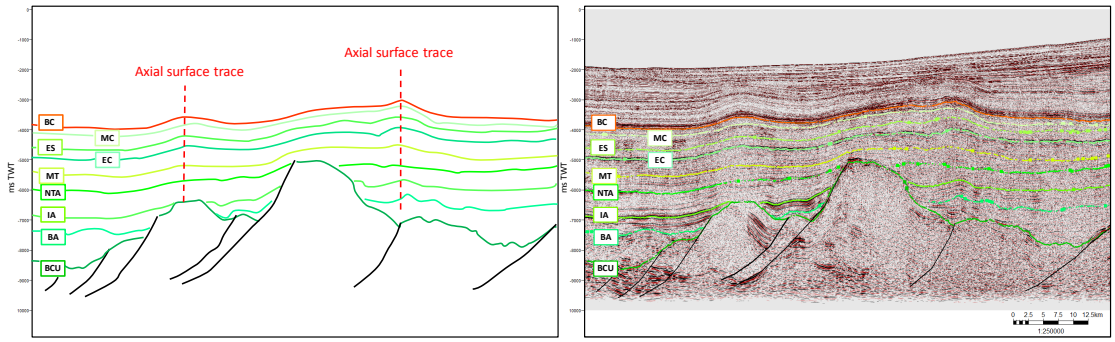

Figure 4.14: Seismic section illustrates the anticlines. Two anticlines are shown in the figure and their axial surface traces are marked in the red dash lines. The axial traces imply these anticline may generated in the same time interval.

bounding fault of the Slettringen Ridge in the north, and the southern anticline in the study area follows the same trend as Grip High in the northern part. This is stated by Vågnes et al. (1998) that the faults beneath the Helland-Hansen Arch are subordinate to the crustal-scale N-S trending Klakk Fault Complex which defines the eastern margin of the Vøring and Møre Basin. The inversion direction is only recorded in the southwestern Barents Sea in SE-directed compression (Gabrielsen et al., 1992, 1997), but it seems incompatible in our study area.

Based on the tectonic evolution in the study area, a new chronostratigraphy with the local tectonism can be constructed (Figure 4.16)

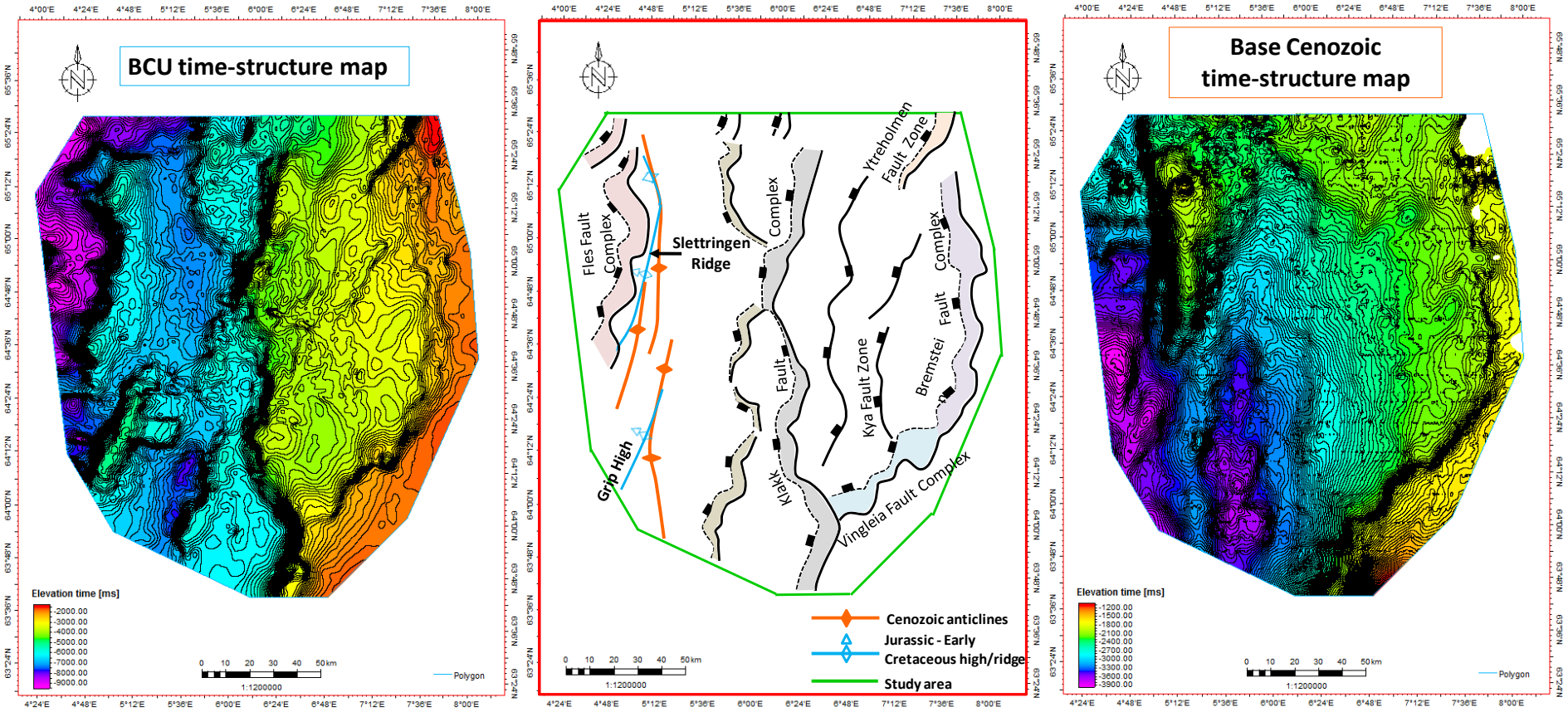

Figure 4.15: Based on the time-structure maps of the BCU and Base Cenozoic, the trend of the Slettringen Ridge, Grip High and the Helland-Hansen Arch are drawn with the faults polygon in the study area. The relationship between the Middle Jurassic-Early Cretaceous faults with the Late Cretaceous-Cenozoic anticline can be visualized. Discussion see text.

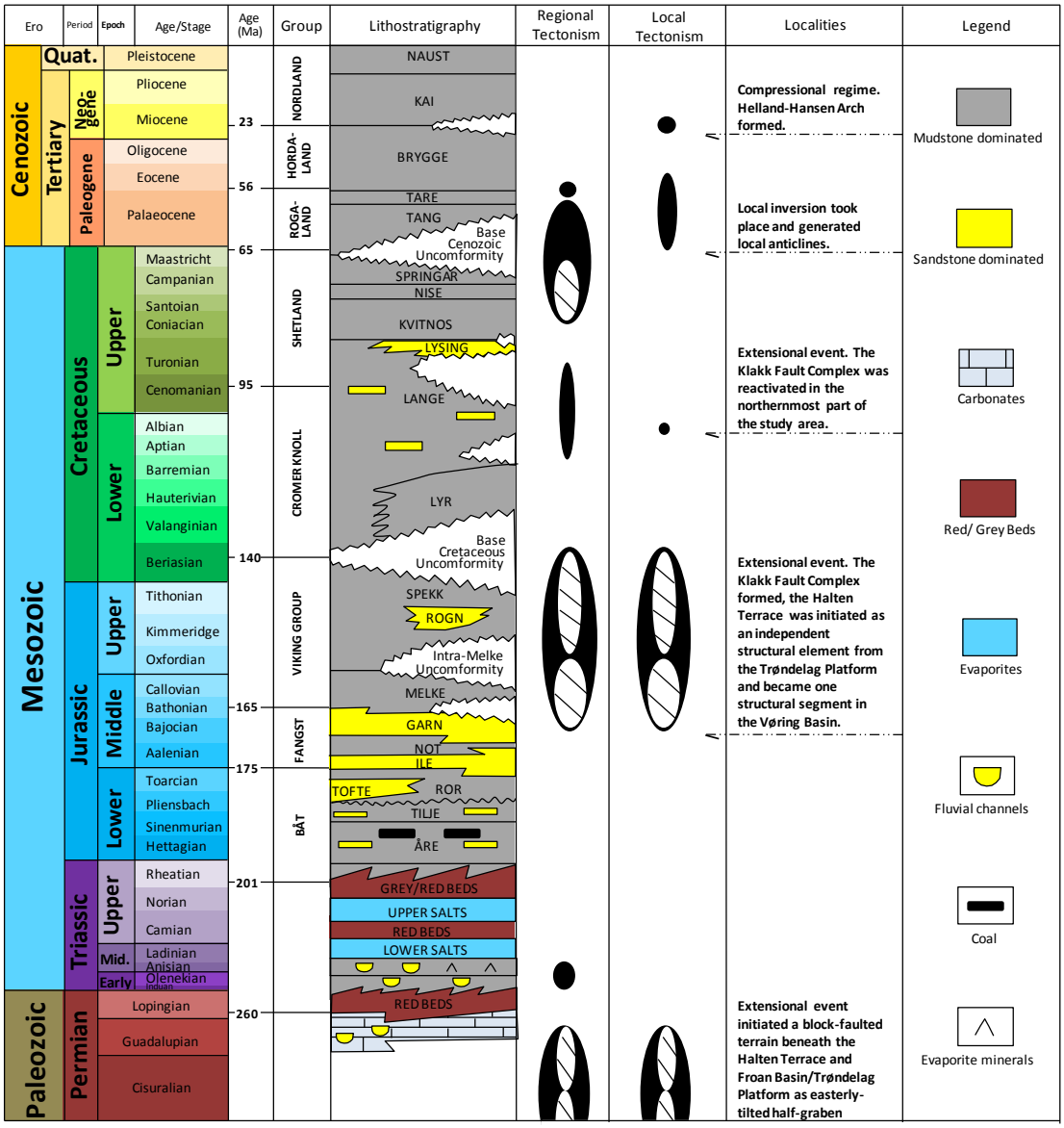

Figure 4.16: Chronostratigraphy with the local tectonism and the localities in the study area. Modified after Dalland et al. (1988); Tsikalas et al. (2005); Elliott et al. (2012); Tsikalas et al. (2012) and Bell et al. (2014).

Chapter 5

Conclusions

The approach of this study, mainly utilizing the seismic data, has limitations on interpreting the Klakk Fault Complex. The essential geometry, strikes and fault patterns, however, can be demonstrated in the seismic sections and BCU time-structure map. It has shown some discrepancies from the previous definitions of the Klakk Fault Complex, and the transition from the Halten Terrace to the Rås Basin has challenged some traditional maps. The Klakk Fault Complex strikes in two main orientations which are NE-SW and NW-SE. The N-S strike is not evident in our interpretation. The NE-SW orientation segments have the most significant displacement and lower dip angle, while the NW-SE orientation segments have smaller displacement and higher dip angle. The NE-SW-trending faults in the Klakk Fault Complex are portrayed by the outer listric normal faults and the relative more planar synthetic faults at their backs. All the faults with NE-SW strike have the same west-facing polarity. The transition from the Halten Terrace to the Rås Basin can be represented by the displaced fault planes. On the contrary, some of the faults in NW-SE strike have an east-facing polarity and are slightly tilted towards the basin side. The transition from the Halten Terrace to the Rås Basin in NW-SE-striking segments is based on the base Cretaceous level and its flexure. This reveals that the traditional maps illustrating the Rås Basin as the result of the down-to-the-basin faulting along the Klakk Fault Complex do not indicate the true nature.

The Klakk Fault Complex, integrated with the west-bounding faults of the rhomboidal-shaped sub-terraces, are all dominated by NE-SW and NW-SE trends. It is most likely to be the structural inheritance of the basement lineaments which have been influenced by the combined effect of Proterozoic shear zone in the basement and the NW-SE Devonian shear zones, as well as the NE-SW orientation related to Devonian extensional collapse structure and the post-Devonian fault activities. Therefore, the old definition of the Klakk Fault Complex characterized by a N-S trend dating back to the Permian can not

accurately reveal the structural inheritance of the basement grain set.

The Permian-Triassic extensional event can be observed underneath the Halten Terrace and the Froan Basin/Trøndelag Platform, which is characterized by an easterly-tilted block-faulted terrain. The Klakk Fault Complex was initiated during the late Middle Jurassic – Early Cretaceous rifting event on the mid-Norwegian margin, and the Halten Terrace was separated from the Trøndelag Platform as an individual structural element in the Vøring Basin. The recorded reactivation of the Klakk Fault Complex in Aptian-Albian times from the previous works is not widely detected in the study area, except in the northernmost part of the study area which may be attributed to the late Albian rifting event due to the blind faults beneath the Near Top Albian. The Campanian rifting event, which was prominent in western parts of the Vøring Basin, is not evident in our interpretation.

Bibliography

Basic Principle in Tectonics (2015). **URL:** http://homepage.ufp.pt/biblioteca/, [Accessed: May, 2015].

Bell, R., Jackson, C., Elliott, G., Gawthorpe, R., Sharp, I. R., Michelsen, L. et al. (2014). Insights into the development of major rift-related unconformities from geologically constrained subsidence modelling: Halten terrace, offshore mid Norway, *Basin Research* **26**(1): 203–224.

Blystad, P., Brekke, H., Færseth, R. B., Larsen, B. T., Skogseid, J. and Tørudbakken, B. (1995). *Elements of the Norwegian Continental Shelf : The Norweigan Sea Region*, Norwegian Petroleum Directorate.

Braathen, A. (1999). Kinematics of post-Caledonian polyphase brittle faulting in the Sunnfjord region, western Norway, *Tectonophysics* **302**(1): 99–121.

Braathen, A., Nordgulen, Ø., Osmundsen, P.-T., Andersen, T. B., Solli, A. and Roberts, D. (2000). Devonian, orogen-parallel, opposed extension in the Central Norwegian Caledonides, *Geology* **28**(7): 615–618.

Braathen, A., Osmundsen, P. T., Nordgulen, O., Roberts, D. and Meyer, G. B. (2002). Orogen-parallel extension of the Caledonides in northern Central Norway: an overview, *Norsk Geologisk Tidsskrift* **82**(4): 225–242.

Brekke, H. (2000). The tectonic evolution of the Norwegian Sea continental margin, with emphasis on the Vøring and Møre basins, *Special Publication-Geological Society of London* **167**: 327–378.

Brekke, H. and Riis, F. (1987). Tectonics and basin evolution of the norwegian shelf between 62 n and 72 n, *Norsk Geologisk Tidsskrift* **67**: 295–322.

Brekke, H., Sjulstad, H. I., Magnus, C. and Williams, R. W. (2001). Sedimentary environments offshore Norway – an overview, *in* O. J. Martinsen and T. Dreyer (eds), *Sedimentary Environments Offshore Norway – Palaeozoic to Recent Proceedings of the Norwegian Petroleum Society Conference*, Vol. 10 of *Norwegian Petroleum Society Special Publications*, Elsevier, pp. 7–37.

Bugge, T., Ringas, J., Leith, D., Mangerud, G., Weiss, H. and Leith, T. (2002). Upper Permian as a new play model on the mid-Norwegian continental shelf: Investigated by shallow stratigraphic drilling, *AAPG bulletin* **86**(1): 107–127.

Bukovics, C., Cartier, E., Shaw, N. and Ziegler, P. (1984). Structure and development of the mid-Norway continental margin, *Petroleum geology of the North European margin*, Springer, pp. 407–423.

Bütler, H. and Sørensen, T. (1935). *Some new investigations of the Devonian stratigraphy and tectonics of East Greenland*, Reitzel.

Bøen, F., Eggen, S. and Vollset, J. (1984). *Structures and basins of the margin from 62 to 69 N and their development*, Springer.

Caselli, F. (1987). Oblique-slip tectonics, mid-norway shelf, *Petroleum geology of north west Europe: London, Graham and Trotman* pp. 1049–1063.

Coward, M. (1993). The effect of Late Caledonian and Variscan continental escape tectonics on basement structure, Paleozoic basin kinematics and subsequent Mesozoic basin development in NW Europe, *Geological Society, London, Petroleum Geology Conference series*, Vol. 4, Geological Society of London, pp. 1095–1108.

Crowell, J. C. (1974). Origin of late cenozoic basins in southern california.

Dalland, A., Worsley, D. and Ofstad, K. (1988). *A Lithostratigraphic Scheme for the Mesozoic and Cenozoic and Succession Offshore Mid-and Northern Norway*, Oljedirektoratet.

Doré, A. G., Lundin, E. R., Fichler, C. and Olesen, O. (1997b). Patterns of basement structure and reactivation along the NE Atlantic margin, *Journal of the Geological Society* **154**: 85–92.

Doré, A. and Lundin, E. (1996). Cenozoic compressional structures on the NE Atlantic margin; nature, origin and potential significance for hydrocarbon exploration, *Petroleum Geoscience* **2**(4): 299–311.

Doré, A., Lundin, E., Jensen, L., Birkeland, Ø., Eliassen, P. and Fichler, C. (1999). Principal tectonic events in the evolution of the northwest European Atlantic margin, *in* A. J. Fleet and S. A. R. Boldy (eds), *Petroleum Geology of Northwest Europe: Proceedings of the 5th Conference*, Vol. 5, Geological Society of London, London, pp. 41–61.

Earle, M., Jankowski, E. and Vann, I. (1989). Structural and stratigraphic evolution of the Færoe-Shetland Channel and northern Rockall Trough, *Extensional Tectonics and Stratigraphy of the North Atlantic Margins. American Association of Petroleum Geologists Memoir* **46**: 461–469.

Eldholm, O., Tsikalas, F. and Faleide, J. (2002). Continental margin off Norway 62–75¡ N: Palaeogene tectono-magmatic segmentation and sedimentation, *Geological Society, London, Special Publications* **197**(1): 39–68.

Elliott, G. M., Wilson, P., Jackson, C. A.-L., Gawthorpe, R. L., Michelsen, L. and Sharp, I. R. (2012). The linkage between fault throw and footwall scarp erosion patterns: an example from the Bremstein Fault Complex, offshore Mid-Norway, *Basin Research* **24**(2): 180–197.

Factpages (2015). **URL:** factpages.npd.no/factpages/, [Accessed: March, 2015]. Factpages2015.

Faleide, J. I., Bjørlykke, K. and Gabrielsen, R. H. (2010). Geology of the Norwegian continental shelf, *in* K. Bjørlykke (ed.), *Petroleum Geoscience: From Sedimentary Environments to Rock Physics*, Springer, Berlin, chapter 22, pp. 467–499.

Faleide, J. I., Tsikalas, F., Breivik, A. J., Mjelde, R., Ritzmann, O., Engen, O., Wilson, J. and Eldholm, O. (2008). Structure and evolution of the continental margin of Norway and the Barents Sea, *Episodes* **31**(1): 82.

Færseth, R. B. and Lien, T. (2002). Cretaceous evolution in the Norwegian Sea a period characterized by tectonic quiescence, *Marine and Petroleum Geology* **19**(8): 1005–1027.

Gabrielsen, R., Grunnaleite, I. and Ottesen, S. (1992). Reactivation of fault complexes in the Loppa High area, southwestern Barents Sea, *Arctic Geology and Petroleum Potential*, Vol. 2, Elsevier Amsterdam, pp. 631–641.

Gabrielsen, R. H. (1986). Structural elements in graben systems and their influence on hydrocarbon trap types, *in* A. M. Spencer (ed.), *Habitat of Hydrocarbons on the Norwegian Continental Shelf*, Graham & Trotman, pp. 55–60.

Gabrielsen, R. H. (2010). The Structure and Hydrocarbon Traps of Sedimentary Basins, *in* K. Bjørlykke (ed.), *Petroleum Geoscience: From Sedimentary Environments to Rock Physics*, Springer, Berlin, chapter 12, pp. 299–327.

Gabrielsen, R. H. and Doré, A. G. (1995). History of tectonic models on the Norwegian continental shelf, *Norwegian Petroleum Society Special Publications* **4**: 333–368.

Gabrielsen, R. H., Foerseth, R., Hamar, G. and Rønnevik, H. (1984). Nomenclature of the main structural features on the Norwegian Continental Shelf north of the 62nd parallel, *Petroleum Geology of the North European Margin*, Springer, pp. 41–60.

Gabrielsen, R. H., Grunnaleite, I. and Rasmussen, E. (1997). Cretaceous and tertiary inversion in the Bjørnøyrenna Fault Complex, south-western Barents Sea, *Marine and Petroleum Geology* **14**(2): 165–178.

Gabrielsen, R. H., Kyrkjebø, R., Faleide, J. I., Fjeldskaar, W. and Kjennerud, T. (2001). The Cretaceous post-rift basin configuration of the northern North Sea, *Petroleum Geoscience* **7**: 137–154.

Gabrielsen, R. H. and Robinson, C. (1984). Tectonic inhomogeneities of the Kristiansund bodø Fault Complex, offshore mid-Norway, *Petroleum geology of the north European margin*, Springer, pp. 397–406.

Gabrielsen, R., Odinsen, T. and Grunnaleite, I. (1999). Structuring of the Northern Viking Graben and the Møre basin; the influence of basement structural grain, and the particular role of the Møre-Trøndelag fault complex, *Marine and Petroleum Geology* **16**(5): 443–465.

Gabrielsen, R. and Ramberg, I. (1979). Fracture patterns in Norway from Landsat imagery: results and potential use, *Proceedings, Norwegian Sea Symposium, Tromsø*, pp. 1–28.

Gernigon, L., Lucazeau, F., Brigaud, F., Ringenbach, J.-C., Planke, S. and Le Gall, B. (2006). A moderate melting model for the vøring margin (Norway) based on structural observations and a thermo-kinematical modelling: Implication for the meaning of the lower crustal bodies, *Tectonophysics* **412**(3): 255–278.

Gibson, J., Walsh, J. and Watterson, J. (1989). Modelling of bed contours and cross-sections adjacent to planar normal faults, *Journal of Structural Geology* **11**(3): 317–328.

Gómez, M., Vergés, J., Fernàndez, M., Torne, M., Ayala, C., Wheeler, W. and Karpuz, R. (2004). Extensional geometry of the Mid Norwegian Margin before Early Tertiary continental breakup, *Marine and petroleum geology* **21**(2): 177–194.

Graue, K. (1992). Extensional tectonics in the Northernmost North Sea: Rifting, uplift, erosion and footwall collapse in late jurassic to early cretaceous times, *Generation, accumulation and production of Europe s hydrocarbons II* pp. 23–34.

Grunnaleite, I. and Gabrielsen, R. H. (1995). Structure of the møre Basin, mid-Norway continental margin, *Tectonophysics* **252**(1): 221–251.

Henkel, H. and Eriksson, L. (1987). Regional aeromagnetic and gravity studies in Scandinavia, *Precambrian research* **35**: 169–180.

Herron, D. A. and Latimer, R. B. (2011). First Steps in Seismic Interpretation.

Hooper, R. J. and Walker, I. (2003). The Mesozoic and Early tertiary opening of the North Atlantic and its impact on the development of the Færoe–Shetland basin system, *6th Petroleum Geology Comference: North-West Europe and Global Perspectives, London, Abstracts* **43**.

Hopper, J. R., Dahl-Jensen, T., Holbrook, W. S., Larsen, H. C., Lizarralde, D., Korenaga, J., Kent, G. M. and Kelemen, P. B. (2003). Structure of the SE Greenland margin from seismic reflection and refraction data: Implications for nascent spreading center subsidence and asymmetric crustal accretion during North Atlantic opening, *Journal of Geophysical Research: Solid Earth (1978–2012)* **108**(B5).

Jongepier, K., Rui, J. and Grue, K. (1997). Triassic to early Cretaceous stratigraphic and structural development of the northeastern Møre Basin margin, off mid-Norway, *Oceanographic Literature Review* **7**(44): 703.

Kim, Y.-S. and Sanderson, D. J. (2005). The relationship between displacement and length of faults: a review, *Earth-Science Reviews* **68**(3): 317–334.

Knott, S. D. (1993). Fault seal analysis in the North Sea, *AAPG Bulletin* **77**(5): 778–792.

Krabbendam, M. and Dewey, J. F. (1998). Exhumation of UHP rocks by transtension in the Western Gneiss Region, Scandinavian Caledonides, *Geological Society, London, Special Publications* **135**(1): 159–181.

Kyrkjebø, R., Gabrielsen, R. H. and Faleide, J. I. (2004). Unconformities related to the Jurassic–Cretaceous synrift–post-rift transition of the northern North Sea, *Journal of the Geological Society* **161**(1): 1–17.

Lundin, E. R. and Doré, A. G. (1997). A tectonic model for the Norwegian passive margin with implications for the NE Atlantic: Early Cretaceous to break-up, *Journal of the Geological Society* **154**(3): 545–550.

McKenzie, D. (1978). Some remarks on the development of sedimentary basins, *Earth and Planetary Science Letters* **40**(1): 25–32.

Morley, C. (1988). Variable extension in lake Tanganyika, *Tectonics* **7**(4): 785–801.

Morley, C., Nelson, R., Patton, T. and Munn, S. (1990). Transfer zones in the East African rift system and their relevance to hydrocarbon exploration in rifts (1), *AAPG Bulletin* **74**(8): 1234–1253.

Nøttvedt, A., Gabrielsen, R. H. and Steel, R. J. (1995). Tectonostratigraphy and sedimentary architecture of rift basins, with reference to the northern North Sea, *Marine and Petroleum Geology* **12**(8): 881–901.

Olafsson, I., Sundvor, E., Eldholm, O. and Grue, K. (1992). Møre margin: crustal structure from analysis of expanded spread profiles, *Marine Geophysical Researches* **14**(2): 137–162.

Olesen, O., Lundin, E., Nordgulen, O., Osmundsen, P. T., Skilbrei, J. R., Smethurst, M. A., Solli, A., Bugge, T. and Fichler, C. (2002). Bridging the gap between the onshore and offshore geology in Nordland, northern Norway, *Norsk Geologisk Tidsskrift* **82**(4): 243–262.

Olesen, O., Skilbrei, J., Osmundsen, P. and Hartz, E. (2004). Is the segmentation of the rifting in the Norwegian-Greenland Sea controlled by Late Caledonian detachment structures, *The 26th Nordic Geological Winter Meeting, Uppsala, Abstracts*, pp. 82–83.

Osmundsen, P., Andersen, T. and Markussen, S. (1998). Tectonics and sedimentation in the hangingwall of a major extensional detachment: the Devonian Kvamshesten Basin, western Norway, *Basin Research* **10**(2): 213–234.

Osmundsen, P., Braathen, A., Nordgulen, Ø., Roberts, D., Meyer, G. and Eide, E. (2003). The Devonian Nesna shear zone and adjacent gneiss-cored culminations, North–Central Norwegian Caledonides, *Journal of the Geological Society* **160**(1): 137–150.

Osmundsen, P. and Ebbing, J. (2008). Styles of extension offshore mid-Norway and implications for mechanisms of crustal thinning at passive margins, *Tectonics* **27**(6).

Osmundsen, P. T., Sommaruga, A., Skilbrei, J. and Olesen, O. (2002). Deep structure of the Mid Norway rifted margin, *Norwegian Journal of Geology* **82**: 205–224.

Pascal, C. and Gabrielsen, R. H. (2001). Numerical modeling of Cenozoic stress patterns in the mid-Norwegian margin and the northern North Sea, *Tectonics* **20**(4): 585–599.

Pascoe, R., Hooper, R., Storhaug, K. and Harper, H. (1999). Evolution of extensional styles at the southern termination of the Nordland Ridge, Mid-Norway: a response to variations in coupling above Triassic salt, *Geological Society, London, Petroleum Geology Conference series*, Vol. 5, Geological Society of London, pp. 83–90.

Prosser, S. (1993). Rift-related linked depositional systems and their seismic expression, *in* G. D. Williams and A. Dobb (eds), *Tectonics and Seismic Sequence Stratigraphy*, Vol. 71, Geological Society of London, pp. 35–66.

Rattey, R. P. and Hayward, A. B. (1993). Sequence stratigraphy of a failed rift system: the Middle Jurassic to Early Cretaceous basin evolution of the Central and Northern North Sea, *Petroleum Geology Conference series*, Vol. 4, Geological Society of London, pp. 215–249.

Reemst, P. and Cloetingh, S. (2000). Polyphase rift evolution of the Vøring margin (mid-Norway): Constraints from forward tectonostratigraphic modeling, *Tectonics* **19**(2): 225–240.

Ren, S., Faleide, J. I., Eldholm, O., Skogseid, J. and Gradstein, F. (2003). Late Cretaceous–Paleocene tectonic development of the NW Vøring basin, *Marine and Petroleum Geology* **20**(2): 177–206.

Roberts, D. (1983). Devonian tectonic deformation in the Norwegian Caledonides and its regional perspectives, *Nor. geol. unders* **380**: 85–96.

Roberts, D., Thompson, M., Mitchener, B., Hossack, J., Carmichael, S. and Bjørnseth, H.-M. (1999). Palaeozoic to Tertiary rift and basin dynamics: mid-Norway to the Bay of Biscay–a new context for hydrocarbon prospectivity in the deep water frontier, *Geological Society, London, Petroleum Geology Conference series*, Vol. 5, Geological Society of London, pp. 7–40.

Romer, R. L. and Bax, G. (1992). The rhombohedral framework of the Scandinavian Caledonides and their foreland, *Geologische Rundschau* **81**(2): 391–401.

Rosendahl, B. R. (1987). Architecture of continental rifts with special reference to East Africa, *Annual Review of Earth and Planetary Sciences* **15**: 445.

Rosendahl, B., Reynolds, D., Lorber, P., Burgess, C., McGill, J., Scott, D., Lambiase, J. and Derksen, S. (1986). Structural expressions of rifting: lessons from Lake Tanganyika, Africa, *Geological Society, London, Special Publications* **25**(1): 29–43.

Rønnevik, H., Eggen, S. and Vollset, J. (1983). Exploration of the Norwegian shelf, *Geological Society, London, Special Publications* **12**(1): 71–93.

Schmidt, W. (1992a). Structure for the Mid-Norway Heidrun Field and its regional implications, *Structural and Tectonic Modelling and its Applications to Petroleum Geology, Norwegian Petroleum Society Spec. Publ* **1**: 381–395.

Schmidt, W. (1992b). Structure for the Mid-Norway Heidrun Field and its regional implications, *Structural and Tectonic Modelling and its Applications to Petroleum Geology, Norwegian Petroleum Society Spec. Publ* **1**: 381–395.

Scott, D. L. and Rosendahl, B. R. (1989). North Viking graben: an east African perspective, *AAPG Bulletin* **73**(2): 155–165.

Skilbrei, J. R. and Olesen, O. (2005). Deep structure of the Mid-Norwegian shelf and onshore-offshore correlations: Insight from potential field data, *Norwegian Petroleum Society Special Publications* **12**: 43–68.

Skilbrei, J. R., Olesen, O., Osmundsen, P. T., Kihle, O., Aaro, S. and Fjellanger, E. (2002). A study of basement structures and onshore-offshore correlations in Central Norway, *Norsk Geologisk Tidsskrift* **82**(4): 263–280.

Skogseid, J. (1994). Dimensions of the late Cretaceous-Paleocene northeast Atlantic rift derived from Cenozoic subsidence, *Tectonophysics* **240**(1): 225–247.

Skogseid, J. and Eldholm, O. (1989). Vøring Plateau continental margin: seismic interpretation, stratigraphy and vertical movements, *Proceedings of the Ocean Drilling Program, Scientific Results*, Vol. 104, (Ocean Drilling Program) College Station, TX, pp. 993–1030.

Skogseid, J., Pedersen, T. and Larsen, V. (1992). Vøring Basin: subsidence and tectonic evolution, *Structural and Tectonic Modelling and Its Application to Petroleum Geology, NPF Spec. Publ* **1**: 55–82.

Skogseid, J., Planke, S., Faleide, J. I., Pedersen, T., Eldholm, O. and Neverdal, F. (2000). Ne atlantic continental rifting and volcanic margin formation, *in* A. Nøttvedt (ed.), *Dynamics of the Norwegian margin*, Vol. 167, Geological Society of London, pp. 295–326.

Strömberg, A. G. (1978). Early tectonic zones in the Baltic Shield, *Precambrian Research* **6**(2): 217–222.

Surlyk, F. (1990). Timing, style and sedimentary evolution of Late Palaeozoic-Mesozoic extensional basins of East Greenland, *Geological Society, London, Special Publications* **55**(1): 107–125.

Surlyk, F., Clemmensen, L. B. and Larsen, H. (1981). Post-Paleozoic evolution of the East Greenland continental margin.

Surlyk, F., Piasecki, S., Rolle, F., Stemmerik, L., Thomsen, E. and Wrang, P. (1984). The Permian base of East Greenland, *Petroleum geology of the North European margin*, Springer, pp. 303–315.

Swiecicki, T., Gibbs, P., Farrow, G. and Coward, M. (1998). A tectonostratigraphic framework for the Mid-Norway region, *Marine and Petroleum Geology* **15**(3): 245–276.

Tsikalas, F., Eldholm, O. and Faleide, J. I. (2002). Early Eocene sea floor spreading and continent-ocean boundary between Jan Mayen and Senja fracture zones in the Norwegian-Greenland sea, *Marine Geophysical Researches* **23**(3): 247–270.

Tsikalas, F., Faleide, J., Eldholm, O. and Wilson, J. (2005). Late Mesozoic-Cenozoic structural and stratigraphic correlations between the conjugate mid-Norway and NE greenland continental margins, *Petroleum Geology: North-West Europe and Global Perspectives Proceedings of the 6th Petroleum Geology Conference: Geological Society, London*, pp. 785–801.

Tsikalas, F., Faleide, J. I. and Eldholm, O. (2001). Lateral variations in tectono-magmatic style along the Lofoten–Vesterålen volcanic margin off Norway, *Marine and Petroleum Geology* **18**(7): 807–832.

Tsikalas, F., Faleide, J. I., Eldholm, O. and Blaich, O. A. (2012). The NE Atlantic conjugate margins, *Phanerozoic Passive Margins, Cratonic Basins and Global Tectonic Maps. Elsevier* pp. 141–201.

Van Balen, R. and Skar, T. (2000). The influence of faults and intraplate stresses on the overpressure evolution of the Halten Terrace, mid-Norwegian margin, *Tectonophysics* **320**(3): 331–345.

Vågnes, E., Gabrielsen, R. and Haremo, P. (1998). Late Cretaceous–Cenozoic intraplate contractional deformation at the Norwegian continental shelf: timing, magnitude and regional implications, *Tectonophysics* **300**(1): 29–46.

Whitham, A., Price, S., Koraini, A. and Kelly, S. (1999). Cretaceous (post-Valanginian) sedimentation and rift events in NE Greenland (71–77 N), *Geological Society, London, Petroleum Geology Conference series*, Vol. 5, Geological Society of London, pp. 325–336.

Withjack, M. O. and Callaway, S. (2000). Active normal faulting beneath a salt layer: an experimental study of deformation patterns in the cover sequence, *AAPG bulletin* **84**(5): 627–651.

Zastrozhnov, D., Faleide, J., Theissen-Krah, S., Abdelmalak, M. and Planke, S. (n.d.). Structure and tectonic evolution of the V/oring Margin.

Ziegler, P. A. (1988a). Evolution of the Arctic-North Atlantic and the western Tethys–a visual presentation of a series of Paleogeographic-Paleotectonic maps*, *AAPG memoir* **43**: 164–196.

Ziegler, P. A. (1988b). Laurussia – The Old Red Continent, *Devonian of the World: Proceedings of the 2nd International Symposium on the Devonian System*, Vol. 1 of *Memoir 14*, CSPG Special Publications, pp. 15–48.

Ziegler, P. A. (1992). European Cenozoic rift system, *Tectonophysics* **208**(1): 91–111.